



PHD

Increasing the thermal stability of a xylanase by directed evolution and rational design

Briggs, Teresa

Award date:
2002

Awarding institution:
University of Bath

[Link to publication](#)

Alternative formats

If you require this document in an alternative format, please contact:
openaccess@bath.ac.uk

Copyright of this thesis rests with the author. Access is subject to the above licence, if given. If no licence is specified above, original content in this thesis is licensed under the terms of the Creative Commons Attribution-NonCommercial 4.0 International (CC BY-NC-ND 4.0) Licence (<https://creativecommons.org/licenses/by-nc-nd/4.0/>). Any third-party copyright material present remains the property of its respective owner(s) and is licensed under its existing terms.

Take down policy

If you consider content within Bath's Research Portal to be in breach of UK law, please contact: openaccess@bath.ac.uk with the details. Your claim will be investigated and, where appropriate, the item will be removed from public view as soon as possible.

**INCREASING THE THERMAL STABILITY OF A XYLANASE BY DIRECTED
EVOLUTION AND RATIONAL DESIGN**

Submitted by Teresa Briggs

For the degree of PhD

Of the University of Bath

2002

COPYRIGHT

Attention is drawn to the fact that copyright of this thesis rests with its author.

This copy of the thesis has been supplied on condition that anyone who consults it is understood to recognise that its copyright rests with its author and that no quotation from the thesis and no information derived from it may be published without prior written consent of the author.

A handwritten signature in black ink, reading 'Teresa Briggs', with a stylized flourish at the end.

This thesis may be made available for consultation within the University Library and may be photocopied or lent to other libraries for the purpose of consultation.

UMI Number: U601459

All rights reserved

INFORMATION TO ALL USERS

The quality of this reproduction is dependent upon the quality of the copy submitted.

In the unlikely event that the author did not send a complete manuscript and there are missing pages, these will be noted. Also, if material had to be removed, a note will indicate the deletion.



UMI U601459

Published by ProQuest LLC 2013. Copyright in the Dissertation held by the Author.
Microform Edition © ProQuest LLC.

All rights reserved. This work is protected against
unauthorized copying under Title 17, United States Code.



ProQuest LLC
789 East Eisenhower Parkway
P.O. Box 1346
Ann Arbor, MI 48106-1346

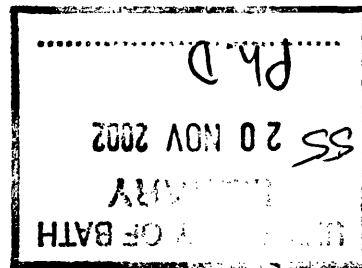


TABLE OF CONTENTS

TABLE OF CONTENTS	I
LIST OF FIGURES	IX
LIST OF TABLES	XII
ABBREVIATIONS	XIII
ACKNOWLEDGEMENTS	XV
ABSTRACT	XVI
Chapter 1	1
INTRODUCTION	1
1.1 RATIONALE AND AIMS OF PROJECT	1
1.2 XYLANASE IN INDUSTRY	2
1.2.1 Xylanase in the animal feed industry	3
1.3 XYLAN AND XYLANASE	5
1.3.1 Mechanism of catalysis	7
1.3.2 Xylanase assay methods	10
1.3.3 Molecular architecture of xylanases	12
1.3.3.1 Catalytic domains	13
1.3.3.2 Substrate binding domains	13
1.3.3.3 Thermostabilising domains	13
1.3.3.4 Cellulosome docking domains	14
1.3.4 Neocallimastix patriciarum Xylanase A	15
1.4 PROTEIN STABILITY	17
1.4.1 Factors contributing to thermal stability	19
1.4.1.1 Examples of non-covalent interactions involved in thermostabilisation	20
1.4.1.2 Examples of covalent interactions involved in thermostabilisation	21
1.5 ENGINEERING STABILITY	22
1.5.1 Rational design	23
1.5.2 Random mutagenesis	25
1.5.2.1 Directed evolution	26

1.5.2.2	DNA shuffling	28
1.5.3	Successful examples of protein engineering in xylanases	30
1.5.4	Alternatives to protein engineering	31
1.6	OBJECTIVES	31
Chapter 2		33
MATERIALS AND METHODS		33
2.1	MOLECULAR BIOLOGY MATERIALS AND METHODS	33
2.1.1	Materials	33
2.1.2	Agarose gel electrophoresis	33
2.1.3	Polymerase chain reaction	34
2.1.4	Purification of PCR products	35
2.1.4.1	Gel purification	35
2.1.4.2	Column purification	35
2.1.5	Restriction digestion of DNA	35
2.1.6	Ligation	35
2.1.7	Transformation of DNA into <i>E. coli</i> - heat shock method	35
2.1.8	Preparation of plasmid DNA	36
2.1.9	DNA sequencing	36
2.2	PROTEIN MATERIALS AND METHODS	36
2.2.1	Materials	36
2.2.2	Bradford protein estimation assay	37
2.2.3	Sodium dodecyl sulphate-polyacrylamide gel electrophoresis	37
2.2.4	Zymogram analysis	38
2.2.5	Purification of XylA.cd2	38
2.2.5.1	Preparation of cell extract	38
2.2.5.2	Anion exchange chromatography	39
2.2.5.3	Concentration of purified protein	39
2.3	ASSAY MATERIALS AND METHODS	39
2.3.1	Materials	39
2.3.2	Dinitrosalicylic acid (DNS) assay	40
2.3.2.1	Preparation of soluble xylan	40

2.3.3	Congo Red overlay assay	40
Chapter 3		42
CLONING, EXPRESSION, PURIFICATION AND CHARACTERISATION OF RECOMBINANT <i>N. PATRICIARUM</i> XYLANASE A SECOND CATALYTIC DOMAIN		42
3.1	INTRODUCTION	42
3.2	MATERIALS AND METHODS	43
3.2.1	Materials	43
3.2.2	PCR amplification of the xylA.cd2 fragment and ligation into pUC18	43
3.2.3	Expression of recombinant xylA.cd2 in <i>E. coli</i>	43
3.2.4	Purification of recombinant xylA.cd2 from <i>E. coli</i>	43
3.2.5	Determination of specific activity	44
3.2.6	Determination of temperature optimum for activity	44
3.2.7	Thermal inactivation of xylA.cd2	44
3.3	RESULTS	45
3.3.1	Construction of the pUC18.cd2 clone	45
3.3.1.1	PCR amplification of xylanase A second catalytic domain	47
3.3.1.2	Identification of clones with correctly oriented xylA.cd2 insert	49
3.3.1.3	Sequencing of the PCR insert	50
3.3.2	XylA.cd2 purification	50
3.3.3	XylA.cd2 characterisation	54
3.3.3.1	Determination of appropriate enzyme dilution and specific activity	54
3.3.3.2	Temperature optimum for activity	55
3.3.3.3	Thermal Inactivation	55
3.4	DISCUSSION	59
3.4.1	Cloning and expression	59
3.4.2	Recombinant xylA.cd2 purification	59
3.4.3	Temperature activity and thermal stability	60
Chapter 4		62
STRUCTURAL STUDIES OF <i>NEOCALLIMASTIX PATRICIARUM</i> XYLANASE A SECOND CATALYTIC DOMAIN		62

4.1	INTRODUCTION	62
4.2	METHODS	63
4.2.1	Sequence manipulation	63
4.2.2	Molecular modelling	63
4.2.3	Preliminary analysis of side-chain positions	63
4.2.4	Detailed analysis of the structural model	64
4.3	RESULTS	65
4.3.1	Sequence homology	65
4.3.2	Model analysis	65
4.4	FEATURES OF MODEL	69
4.4.1	Conserved sequences and their functional properties	69
4.4.1.1	Structural features	69
4.4.1.2	Binding activity	69
4.4.1.3	Catalytic activity	70
4.4.2	Non-conserved sequences	70
4.5	IMPROVEMENT OF THERMOSTABILITY	71
4.5.1	Disulphide bonds	71
4.5.2	Ionic interactions	73
4.5.3	Aromatic residues	73
4.5.4	Other engineering possibilities	74
4.6	CONCLUSIONS	76
Chapter 5		77
	CONSTRUCTION AND CHARACTERISATION OF A SITE-DIRECTED MUTANT OF THE SECOND CATALYTIC DOMAIN OF <i>N. PATRICIARUM</i> XYLANASE A	77
5.1	INTRODUCTION	77
5.2	MATERIALS AND METHODS	78
5.2.1	Materials	78
5.2.2	Construction of disulphide bond mutant xylA.cd2	78
5.2.3	Expression of recombinant mutant xylA.cd2 in <i>E. coli</i>	81
5.2.4	Purification of mutant xylA.cd2 from <i>E. coli</i>	81

5.2.5	Identification of disulphide bond	81
5.2.6	Characterisation of mutant xylA.cd2	83
5.3	RESULTS	84
5.3.1	Construction of mutant xylA.cd2 clone	84
5.3.1.1	PCR amplification and introduction of site-directed mutations	84
5.3.1.2	Identification of clones with correctly oriented mutant insert	87
5.3.1.3	Sequencing of the mutant xylA.cd2 PCR insert	88
5.3.2	Mutant xylA.cd2 purification	88
5.3.3	Mutant xylA.cd2 characterisation	92
5.3.3.1	Identification of disulphide bond	92
5.3.3.2	Determination of appropriate enzyme dilution and specific activity	93
5.3.3.3	Temperature optimum for activity	93
5.3.3.4	Thermal inactivation	94
5.3	DISCUSSION	98
5.3.1	Construction of a site-directed mutant xylA.cd2 enzyme and confirmation of the introduction of a disulphide bond	98
5.3.2	Comparison of mutant to original xylA.cd2 enzyme	99
5.4	CONCLUSIONS	103
Chapter 6		104
CONSTRUCTION OF A RANDOM MUTANT LIBRARY AND INITIAL SCREENING		104
6.1	INTRODUCTION	104
6.2	MATERIALS AND METHODS	106
6.2.1	Materials	106
6.2.2	Random mutagenesis technique: Error-prone PCR	106
6.2.3	Construction of the random mutant library and transformation into <i>E. coli</i>	108
6.2.4	Agar plate screen: Heat inactivation and RBB-xylan overlay assay	108
6.2.5	Further characterisation of improved mutants	109
6.2.6	Expression and partial purification of mutant xylA.cd2 enzymes	109
6.2.7	Characterisation of mutant xylA.cd2 enzymes	109

6.3	RESULTS	110
6.3.1	Construction of the random mutant library	110
6.3.1.1	Amplification of xylA.cd2 by EP-PCR	110
6.3.1.2	Estimation of library size and number of active clones	110
6.3.2	Selection criteria for agar plate screen	111
6.3.3	Identification of stable mutants	111
6.3.4	Sequencing of mutants 3, 4, 5 & 12	113
6.3.5	Characterisation of mutants 3, 4, 5 & 12	113
6.3.5.1	Specific activities	113
6.3.5.2	Temperature optima for activity	113
6.3.5.3	Thermal stability at 60°C	114
6.4	DISCUSSION	117
6.4.1	Random mutant library construction	117
6.4.2	Library screening and identification of improved mutants	117
6.4.3	Expression and partial purification of improved mutants	118
6.4.4	Comparison of improved mutants to original xylA.cd2	119
6.5	CONCLUSIONS	120
Chapter 7		121
DEVELOPMENT OF A SYSTEM FOR RANDOM MUTANT LIBRARY		
SCREENING		121
7.1	INTRODUCTION	121
7.2	MATERIALS AND EQUIPMENT	123
7.2.1	Materials	123
7.2.2	Equipment	123
7.3	CELL GROWTH	124
7.3.1	Aim	124
7.3.2	Method	124
7.3.3	Results and discussion	124
7.4	LYSIS OF CELL CULTURES	126
7.4.1	Aim	126
7.4.2	Method	126

7.4.3	Assessment of results	127
7.4.4	Optimisation of lysis using lysozyme	129
7.4.5	Assessment of results	129
7.4.6	Final culture lysis conditions	130
7.5	OPTIMISATION OF XYLANASE ACTIVITY ASSAY	131
7.5.1	Aim	131
7.5.2	Standard Curve	131
7.5.3	Lysate volume, amount of substrate and assay incubation time	132
7.5.3.1	Undiluted lysate	133
7.5.3.2	Diluted lysate	133
7.5.3.3	100-fold lysate dilution: assay incubation time study	135
7.5.3.4	Varying substrate amount	136
7.5.3.5	Assay incubation time study: 0.6% soluble xylan, 100-fold lysate dilution	139
7.5.3.6	Lysate volume study: 100-fold lysate dilution, 0.6% soluble xylan substrate, 15-minute assay	140
7.5.3.7	Final assay incubation time study: 250-fold lysate dilution, 0.6% soluble xylan substrate	141
7.6	ASSESSMENT OF THERMAL STABILITY	143
7.6.1	Aim	143
7.6.2	Heat Inactivation: 65°C, micro-plate heater	144
7.6.3	Problems with micro-plate heater	145
7.6.4	Heat inactivation: 65°C, 96-well thermal cycler	147
7.6.5	Heat inactivation: 60°C, 96-well thermal cycler	147
7.6.6	Heat inactivation: 60°C, 96-well thermal cycler, inactivating assay volume only	148
7.6.7	Final heat inactivation study: 60°C time-course study with 20µl of diluted lysate only	149
7.7	FINAL TEST: USING OPTIMISED CONDITIONS IN AN ASSAY SITUATION	150
7.8	SUMMARY: OPTIMISED PROTOCOL AND SELECTION CRITERIA	152

Chapter 8	154
RANDOM MUTANT LIBRARY SCREENING USING 96-WELL PLATE SYSTEM	154
8.1 INTRODUCTION	154
8.2 MATERIALS AND METHODS	155
8.2.1 Materials	155
8.2.2 Random mutant library screening	155
8.2.3 Further characterisation of improved mutants	155
8.2.4 Expression and partial purification of mutant xylA.cd2 enzymes	155
8.2.5 Characterisation of mutant xylA.cd2 enzymes	156
8.3 RESULTS	157
8.3.1 Initial random mutant selection	157
8.3.2 Identification of stable mutants and further study	157
8.3.3 Sequencing of mutants 1-A10, 1-B6 & 2-C10	160
8.4.1 Characterisation of mutants 1-A10, 1-B6 & 2-C10	160
8.4.1.1 Specific activities	161
8.4.1.2 Temperature optima for activity	161
8.4.1.3 Thermal stability at 64°C	161
8.4 DISCUSSION	164
8.4.1 Library screening and identification of improved mutants	164
8.4.2 Characterisation of improved mutants	164
8.4.2.1 Sequence comparison	164
8.4.2.2 Thermoactivity and thermostability	166
8.5 CONCLUSIONS	168
Chapter 9	169
FINAL CONCLUSIONS AND FUTURE WORK	169
9.1 FINAL CONCLUSIONS	169
9.2 FUTURE WORK	171
APPENDIX	173
REFERENCES	174

LIST OF FIGURES

Figure 1.1	Generalised structure of a xylan polymer	7
Figure 1.2	Reaction mechanism of retaining glycosyl hydrolases	9
Figure 1.3	The 'open cleft' active site structure	10
Figure 1.4	Mechanism of dinitrosalicylic acid assay	11
Figure 1.5	Molecular architecture of <i>Neocallimastix patriciarum</i> xylanase A	16
Figure 3.1	<i>N. patriciarum</i> xylanase A gene sequence	46
Figure 3.2	Identification of xylA.cd2 PCR product by agarose gel electrophoresis	48
Figure 3.3	BamHI digested pUC18.cd2, to confirm the cloning of xylA.cd2 insert into pUC18 plasmid	48
Figure 3.4	Congo Red assay confirming xylanase activity of pUC18.cd2 clones	49
Figure 3.5	Sequence of xylA.cd2	52
Figure 3.6	SDS-PAGE analysis of the purification stages of xylA.cd2	53
Figure 3.7	Zymogram of purification stages of xylA.cd2	54
Figure 3.8	XylA.cd2 activity against volume of a 1/250 enzyme dilution	56
Figure 3.9	Temperature activity curve for xylA.cd2	56
Figure 3.10	Thermal inactivation of xylA.cd2	57
Figure 3.11	Arrhenius plot for xylA.cd2 thermal inactivation data	58
Figure 4.1	Sequence alignment of <i>N. patriciarum</i> xylA.cd2 with template and thermostable xylanases only	66
Figure 4.2	Final Ramachandran plot for xylA.cd2 model	67
Figure 4.3	Final model of <i>Neocallimastix patriciarum</i> xylanase A second catalytic domain	68
Figure 4.4	Model structure of <i>N. patriciarum</i> xylA.cd2	72
Figure 5.1	Schematic diagram representing the PCR strategy for construction of the site-directed xylA.cd2 mutant	80
Figure 5.2	Schematic diagram demonstrating the reaction of DTNB with a protein thiol group	82
Figure 5.3	Identification of PCR reaction 1 product (megaprimer 1) by agarose gel electrophoresis	85

Figure 5.4	Identification of PCR reaction 2 product (megaprimer 2) by agarose gel electrophoresis	85
Figure 5.5	Identification of final mutant xylA.cd2 PCR product by agarose gel electrophoresis	86
Figure 5.6	BamHI digested pUC18.mutant.cd2, to confirm the cloning of mutant xylA.cd2 insert into pUC18 plasmid	86
Figure 5.7	Congo Red assay confirming xylanase activity of pUC18.mutant.cd2 clones	87
Figure 5.8	Sequence of mutant xylA.cd2	90
Figure 5.9	SDS-PAGE analysis of the purification stages of mutant xylA.cd2	91
Figure 5.10	Zymogram of purification stages of mutant xylA.cd2	92
Figure 5.11	Mutant xylA.cd2 activity against volume of a 1/250 enzyme dilution	94
Figure 5.12	Temperature activity curve for xylA.cd2	95
Figure 5.13	Thermal inactivation of mutant xylA.cd2	96
Figure 5.14	Arrhenius plot for mutant xylA.cd2 thermal inactivation data	97
Figure 5.15	Comparison of temperature activity profiles for original and mutant xylA.cd2	100
Figure 5.16	Comparison of thermal inactivation data from original & mutant xylA.cd2	101
Figure 5.17	Comparison of Arrhenius plots for original and mutant xylA.cd2 thermal inactivation data	102
Figure 6.1	Identification of EP-PCR products by agarose gel electrophoresis	112
Figure 6.2	Temperature activity curves for original and 4 mutant xylA.cd2 enzymes	115
Figure 6.3	Thermal inactivation at 60°C of original and 4 mutant xylA.cd2 enzymes	116
Figure 7.1	A typical standard curve obtained using 96-well plate assay format	132
Figure 7.2	Study of xylA.cd2 activity against lysate volume for a 20-fold dilution of cell lysate	134
Figure 7.3	Study of xylA.cd2 activity against lysate volume for different cell lysate dilutions	135

Figure 7.4	Study of xylA.cd2 activity against time for 10µl of a 100-fold dilution of culture lysate	136
Figure 7.5	Study of xylA.cd2 activity against percentage of soluble xylan substrate for an 8-minute assay	138
Figure 7.6	Study of xylA.cd2 activity against percentage of soluble xylan substrate for a 15-minute assay	138
Figure 7.7	Study of xylA.cd2 activity against time	139
Figure 7.8	Study of xylA.cd2 activity (shown as absorbance at 575nm) against 100-fold diluted lysate volume	141
Figure 7.9	Study of xylA.cd2 activity (shown as absorbance at 575nm) against time	142
Figure 7.10	Heat inactivation study at 65°C using a micro-plate heater	145
Figure 7.11	Heat inactivation study at 60°C using a 96-well thermal cycler	147
Figure 7.12	Heat inactivation study at 60°C using a 96-well thermal cycler and 20µl of diluted culture lysate only	149
Figure 7.13	Graph showing stability against initial activity for 96 individual xylA.cd2 cultures	151
Figure 8.1	Stability versus initial activity plot for the 960 random mutants screened for activity after 3 minutes at 60°C	158
Figure 8.2	Stability versus initial activity plot for the 135 random mutants screened for activity after 3 and 5 minutes at 60°C	159
Figure 8.3	Temperature activity curves for 3 mutant xylA.cd2 enzymes	162
Figure 8.4	Thermal inactivation at 64°C of 3 mutant xylA.cd2 enzymes	163

LIST OF TABLES

Table 1.1	Examples of enzyme properties improved by directed evolution	27
Table 3.1	Summary of purification of xylA.cd2 from <i>E. coli</i> strain JM109	53
Table 5.1	Reagents and amounts used in DTNB assay	83
Table 5.2	Summary of purification of mutant xylA.cd2 from <i>E. coli</i> strain JM109	91
Table 5.3	Comparison of temperature optimum and thermal stability data for original and mutant xylA.cd2 enzymes	102
Table 6.1	Summary of concentrations of deoxynucleoside triphosphates and MgCl ₂ used in EP-PCR reactions	107
Table 6.2	Summary of mutations identified in the xylA.cd2 coding region of the random mutant clones	114
Table 6.3	Summary of original and mutant xylA.cd2 enzyme specific activities	115
Table 6.4	Comparison of half-lives at 60°C of original and mutant xylA.cd2 enzymes	116
Table 7.1	Comparison of xylanase activity after the various lysis methods tested	127
Table 7.2	Comparison of xylanase activity after lysis of cell cultures with lysozyme for varying times and at varying temperatures	129
Table 7.3	Summary of the activity values obtained from the final test of the 96-well plate random mutant library screening system	150
Table 8.1	Summary of mutations identified in the xylA.cd2 coding region of the 3 random mutant clones	160
Table 8.2	Summary of original and mutant xylA.cd2 enzyme specific activities	161
Table 8.3	Comparison of half-lives at 64°C of original and mutant xylA.cd2 enzymes	163

ABBREVIATIONS

Alanine Ala A	Arginine Arg R	Asparagine Asn N	Aspartic acid Asp D	Cysteine Cys C
Glutamic Acid Glu E	Glutamine Gln Q	Glycine Gly G	Histidine His H	Isoleucine Ile I
Leucine Leu L	Lysine Lys K	Methionine Met M	Phenylalanine Phe F	Proline Pro P
Serine Ser S	Threonine Thr T	Tryptophan Trp W	Tyrosine Tyr Y	Valine Val V

Å	Angstrom
A575	absorbance at 575nm
APS	ammonium persulphate
bp	base pairs
BSA	bovine serum albumin
Da	daltons
DNA	deoxyribonucleic acid
DNS	3,5-dinitrosalicylic acid
dNTP	deoxynucleotide triphosphate
DTNB	5, 5'-dithiobis-(2-nitrobenzoic acid)
EDTA	(di sodium) ethylenediamine tetraacetate
EP-PCR	error-prone polymerase chain reaction
FPLC	fast performance liquid chromatography
g	gravity

kb	kilo-base pairs
kDa	kilo-daltons
LB	Luria-Bertani (medium)
mA	milli-ampules
Mr	relative molecular mass
PAGE	polyacrylamide gel electrophoresis
PC buffer	phosphate-citrate buffer
PCR	polymerase chain reaction
RBB-xylan	4-O-methyl-D-glucurono-D-xylan-remazol brilliant blue R
rDNA	recombinant DNA
RNA	ribonucleic acid
SDS	sodium dodecyl sulphate
TAE	tris-acetate, EDTA (buffer)
<i>Taq</i>	<i>Thermus aquaticus</i>
TEMED	N, N, N', N' tetramethylethylene diamine
Tris	tris-(hydroxymethyl)-methylamine
TNB	5-thio-2-nitrobenzoate
UV	ultraviolet
V	volts
(v/v)	volume to volume ratio
(w/v)	weight to volume ratio
X-gal	5-bromo-4-chloro-3-indoyl- β -D-galactoside
xylA	<i>Neocallimastix patriciarum</i> xylanase A
xylA.cd2	<i>Neocallimastix patriciarum</i> xylanase A second catalytic domain

ACKNOWLEDGEMENTS

I would firstly like to thank my supervisors, Dr David Hough and Professor Mike Danson, for guiding me through the 3 years I have spent working in the Centre for Extremophile Research. Their support, suggestions and encouragement were always appreciated, even after the hundredth assay of the day! Many thanks are also due to Dr Susan Crennell and Robert Williams for their invaluable contribution to the structural work presented in chapter 4. Thanks go to Dr Geoff Hazlewood, Dr Peter Street and Dr Heidi Burrows at Finnfeeds International for their helpful discussions, suggestions and information on the animal feed industry. My project was funded by Danisco-Cultor and I would like to thank them for giving me the opportunity to spend time in the lab of Professor Harry Gilbert, and to present my work to ‘the group’ in Finland.

Numerous thanks are due for help with practical techniques: Prof. Harry Gilbert and Dr Simon Andrews at the University of Newcastle for guidance on the error-prone PCR technique; Tom Nightingale for developing the novel zymogram technique; Paul Jones for carrying out all sequencing reactions. A huge thank-you must go to all the past and present members of lab 1.33, Frankie, Eva, Ursula, Becky, Tina, Amie, Mikki, Cat & Nina for making my time in (and out of) the lab so enjoyable, and for keeping me smiling through the haze of 96-well plates and multi-channel pipettes! An extra huge thank-you must go to Dr Carl Thompson for his never ending patience and knowledge.

Finally I’d like to thank my family. To Mum, Dad and Becky for always being there, and to Matt for sharing my life: I dedicate this thesis to you.

ABSTRACT

The use of biological catalysts is common in many of today's industrial processes. Interest in enzymes capable of working under harsh industrial conditions has heightened over recent years with the identification and characterisation of enzymes from extremophilic organisms. In addition, advancements in laboratory techniques suited to the modification of proteins mean that it is now possible to design and engineer an enzyme to suit specific needs within the laboratory environment.

The aim of this project is to enhance the thermal stability of xylanase A from the anaerobic ruminal fungus *Neocallimastix patriciarum*, whilst retaining its high levels of activity at lower temperatures. Xylanase A has a potential application in the animal feed industry, and this forms the basis for this project.

Two separate techniques have been applied in order to fulfil the aims of this project. Using a generated three-dimensional model of the second catalytic domain of xylanase A (xylA.cd2), mutations predicted to increase the thermal stability of the enzyme were introduced by site-directed mutagenesis. Two cysteine residues were introduced with the aim of forming a disulphide bond. The mutant enzyme was as active as the original enzyme, yet displayed at least 2.5 times greater stability at the temperatures assayed.

The second approach was to use directed evolution in attempts to increase the thermal stability of xylA.cd2. A library of xylA.cd2 random mutants was generated, and after initial unsuccessful attempts to screen the mutants for those with greater thermal stability a screening system based on 96-well plate format was developed. This screen was used to identify 12 mutants retaining high levels of activity after incubation at 65°C. The three of these 12 mutants that were characterised in detail all demonstrate improvements in thermal stability over the original enzyme while retaining similar temperature optima. The most stable mutant of the three characterised demonstrates a half-life at 64°C 36 times greater than that of xylA.cd2.

Chapter 1

INTRODUCTION

1.1 RATIONALE AND AIMS OF PROJECT

The rationale behind this project comes from a problem faced by many industrial companies. The use of enzymes to aid and improve existing processes is increasingly common in today's industrial market place, and many companies are now seeking to acquire enzymes capable of carrying out processes in more demanding situations, for example in conditions of extreme pH or temperature. While, through the use of enzymes from 'extremophilic' organisms, it is possible to find natural enzymes capable of working in extreme conditions, there are some applications where enzymes with 'non-natural' properties would be more suited to the task. This problem forms the basis for this project, as outlined by its industrial sponsors. One of their main interests is in the use of enzymes as additives in animal feeds. Some of the stages of feed processing involve high temperature steps, and the mesophilic enzymes currently added to the feed cannot fully withstand these temperatures. As a result much of the added enzyme is rendered inactive, and in attempts to overcome this problem higher quantities of the enzyme are added to the feed prior to processing, an option that is economically unfavourable. There are a couple of obvious solutions to this problem: one would be to add the enzyme to the feed after processing, and the other would be to substitute the current mesophilic enzyme for a thermophilic one. It is possible to add enzyme to the feed following processing, and this is achieved by spraying it over the feed in a liquid form. There are disadvantages associated with this option though, and they include non-uniform coverage of the feed and the necessity for specialised equipment to carry out this process. Substituting the current mesophilic enzyme for a thermophilic one would solve the problem of inactivation at high temperatures, but the fact that thermophilic enzymes often demonstrate a decreased activity at lower temperatures means that this option is not practical as the enzyme additive needs to demonstrate high levels of activity at normal, physiological temperatures. An ideal animal feed enzyme additive should be both stable at elevated temperatures and highly active at lower temperatures.

The enzyme of interest in this study is a xylanase, and the problems outlined above form the basis for the aims of the project. Using a variety of techniques, attempts will be made to increase the thermal stability of a mesophilic xylanase whilst retaining its high levels of activity at lower temperatures.

1.2 XYLANASE IN INDUSTRY

In 2000 the global industrial enzyme market was estimated to be worth US\$2 billion (Diversa Corporation), and US demand alone is projected to exceed \$2.6 billion by 2004 (The-infoshop.com). Enzymes including cellulases, xylanases, proteases, lipases, amylases, pectinases and phosphatases are widely used in the pulp and paper, textiles, detergent, and food and beverage industries. Xylanases in particular, the focus of this project, have numerous biotechnological applications. Many industrial processes utilise xylanases to enhance and improve existing systems, resulting in more economically sound and environmentally friendly processes. Xylanases are already produced on an industrial scale and used in bakeries to improve the texture of bread dough, which in turn improves the loaf volume, texture and shelf life of the bread (Maat *et al.*, 1992). Another area where the use of xylanases, and in particular thermostable xylanases, is becoming increasingly common is in the pulp and paper industry. Traditionally, paper pulp is bleached using chlorine and hypochlorite. This bleaching process is essentially to remove lignin from the pulp, and it is estimated that over 2×10^6 tonnes of chlorine and chlorine derivatives are used annually in the United States for this purpose. The chlorinated derivatives generated by this process constitute a major environmental problem (McDonough, 1992), and public demand and environmental regulations have now put restrictions on the use of chlorine in the bleaching process of the pulp and paper industry, particularly in Western Europe and North America (Chauvt *et al.*, 1987). Recent studies have demonstrated the feasibility of enzymatic treatment as an alternative to chlorine bleaching for the removal of lignin from pulp (Viikari *et al.* 1994). Treatment of pulp with xylanase leads to the release of xylan and lignin without unnecessary loss of other pulp components. Performing this enzymatic bleaching at elevated temperatures opens up the cell wall structure of the pulp and facilitates lignin removal in subsequent stages, and it is for this reason that industrial interest for this application concentrates on

thermostable xylanases. Other industrial applications of xylanases include the clarification of wine and juices and the extraction of flavours, spices, oils and pigments (Biely, 1985). Another major use of xylanases is in the animal feed industry, and the remainder of this section shall focus on this application.

1.2.1 Xylanase in the animal feed industry

In today's animal feed market the use of exogenous enzymes in the diets of non-ruminant animals is common. Their use has allowed an increase in the utilisation of lower quality feedstuffs, along with an improvement in animal performance due to the increased absorption of nutrients. Non-ruminant animals such as pigs and poultry lack the digestive advantages possessed by ruminant animals. Ruminants have an extensive array of microbial enzymes, produced and secreted by rumen inhabitants, that play an important role in their digestive process. These enzymes aid in the digestion of fibre and other plant cell wall polymers, and allow the animal to obtain nutritional value from otherwise indigestible feed. Non-ruminant animals, which are also referred to as monogastric, do not have the benefit of such advantageous symbiotic relationships and as a result are not capable of releasing the full potential of nutrients from their feed. The presence of exogenous enzymes in non-ruminant feed aids the animal in obtaining greater nutritional value from the normally indigestible feed fraction.

Common feedstuff ingredients include wheat, barley, oats, rye and maize. These all contain anti-nutritional factors (ANFs), that is, they all contain elements that limit animal performance by affecting the way in which an animal can obtain nutrients from its feed. The most common ANFs are non-starch polysaccharides (NSPs), including cellulose, arabinoxylans, β -glucans, galactomannans and pectin, which are primarily derived from plant cell walls. Non-ruminants do not possess all the necessary enzymes to completely digest the carbohydrate portion of their feed. Whilst they produce enzymes such as amylases and disaccharidases to ensure the hydrolysis of starch, sucrose and lactose, they lack the enzymes necessary to digest NSPs. NSPs interfere with the digestibility, absorption and utilisation of nutrients and the main problem that arises as a result of this is increased intestinal digesta viscosity. Increased digesta

viscosity effectively slows down the gastrointestinal passage rate (van der Klis *et al.*, 1993; Sudendey & Kamphues, 1995) and reduces the diffusion of digestive enzymes, and their substrates and products (Bedford & Morgan, 1996; Ellis *et al.*, 1996). These factors have a direct impact on animal performance, particularly in poultry, and it is for this reason that NSPs are the major target substrates when exogenous enzymes are used as animal feed additives.

NSP-degrading enzymes can affect the nutritional value of feedstuffs in several ways. By breaking down cell walls they allow digestive enzymes to access normally unavailable nutrients. By hydrolysing the actual NSPs they can help to produce absorbable nutrients or to yield a more digestible substrate. Finally, by breaking down the NSPs they can decrease intestinal viscosity, which has the knock-on effect of increasing nutrient uptake. The most common NSP-degrading enzymes used as feed additives are xylanases and β -glucanases.

The enzymes in current commercial use are commonly isolated from the bacterial genera *Bacillus*, or from fungal strains of *Aspergillus*, *Trichoderma*, *Penicillium* or *Humicola* (Official Journal of the European Communities, 1996). A major consideration in the selection of appropriate enzymes for use as additives is their stability. The feed pelleting process involves subjecting the feed to moist heat (often 70-90°C), followed by mechanical pressing. Exogenous enzymes added to feed prior to pelleting are susceptible to heat inactivation (Inborr & Bedford, 1994), and whilst this problem can be overcome by application of the enzyme post-processing, it is economically desirable to include the enzyme before processing. The development of a more thermostable enzyme that retains good activity at 37°C in the digestive tract would overcome this problem. Thermal stability is not the only factor that requires consideration when selecting appropriate feed enzymes: pH and proteolytic stability are also of importance. An enzyme must be sufficiently stable to withstand the low pH, proteolytic environment of the stomach. These above considerations are all of considerable importance when selecting an enzyme that will function well as a feed additive.

Current research into potential animal feed enzyme additives is focusing on the identification of new enzymes, or the development of existing ones, that are more suitable for inclusion in animal feeds (by fulfilling the stability criteria discussed above). Techniques such as protein engineering and directed evolution have significant potential for 'customising' existing enzymes, and have already been employed with success in other areas of industry. Both of these techniques will be discussed in detail in subsequent sections of this chapter.

1.3 XYLAN AND XYLANASE

Plant cell walls have three major polymeric constituents: cellulose, hemicellulose and lignin. Xylan, a heteropolysaccharide based on a backbone structure of β -1,4-linked D-xylose residues, is the major constituent of hemicellulose and can be found in the cell walls of all land plants and in almost all plant parts (Whistler & Richards, 1970). Xylan is a heteropolysaccharide as its backbone structure is branched with side chains, the most common of which include acetyl and arabinofuranosyl groups, and glucuronic acid (Figure 1.1). Xylan chains can also be polymerised, and both the degree of polymerisation and the composition of the branched side chains are dependent on their biological source. β -1,4-xylans are mainly found in secondary cell walls, the major component of mature cell walls in woody tissue, and are characteristic of hardwoods, softwoods and grasses (Timell, 1967). There are differences in the composition of side chains between hardwood and softwood xylans, with hardwood xylan being mainly acetylated and softwood being substituted with arabinofuranosyl groups. Approximately one in ten xylose backbone residues are substituted with a glucuronic acid residue at carbon position 2 (C2) in hardwood xylan, and 70% are substituted with acetyl groups at C2 or C3 (Puls & Schuseil, 1993). In contrast, softwood xylan is not acetylated, but instead 20% of its xylose backbone residues are substituted at C2 with glucuronic acid residues and 13% are substituted at C3 with arabinofuranosyl residues (Puls & Schuseil, 1993). The xylan of grasses contains fewer glucuronic acid residues than hardwood xylan but has a large number of arabinofuranosyl residues (Puls & Schuseil, 1993). In grass xylan, in addition to the xylose backbone residues being substituted, the arabinofuranosyl residues are also branched: 6% are substituted with feruloyl groups and

3% with p-coumaroyl residues (Coughlan & Hazlewood, 1993; Mueller-Harvey *et al.*, 1996).

Given the widespread abundance and complexity of polysaccharides in nature, it is not surprising that their degradation entails diverse enzymes with differing specificities and modes of action. Glycosyl hydrolases (EC 3.2.1.x) are the major group of enzymes involved in polysaccharide hydrolysis, and they achieve this by breaking the glycosidic bond either between carbohydrate molecules, or between a carbohydrate and a non-carbohydrate moiety. In addition to classification by the International Union of Biochemistry (IUB) nomenclature of enzymes, glycosyl hydrolases have also been classified into families based on hydrophobic cluster analysis and amino acid sequence similarities of enzyme catalytic domains (Henrissat, 1991; Henrissat & Bairoch, 1993). This additional classification system, of which there are 85 families to date (Coutinho & Henrissat, 1999), is based on the direct relationship between sequence and folding similarities, and was designed both to reflect common structural features and to reveal evolutionary relationships between enzymes. The classification also provides a convenient tool for deriving mechanistic information (Coutinho & Henrissat, 1999) about lesser-known enzymes. Xylanases have been classified into glycosyl hydrolase families 10 and 11. Members of family 10 include xylanases and cellulases, while family 11 contains only xylanases. The fact that xylanases catalyse the same reaction, yet can be grouped into two distinct families, indicates obvious differences at the amino acid sequence level. A major difference between family 10 and 11 xylanases is their three-dimensional structure. Family 10 xylanases adopt an 8-fold β/α -barrel structure, whereas family 11 xylanases have a β -sandwich structure (2 twisted β -sheets and an α -helix), also referred to as a β -jelly roll. The enzymes from both families catalyse the hydrolysis of the glycosidic bond via the same mechanism, and this will be discussed in more detail later in the subsequent section.

As the major constituent of hemicellulose, xylan is an abundant natural, renewable resource, and the enzymes that bring about its degradation play an enormous role in the maintenance of carbon flow through the carbon cycle. The hydrolysis of the β -1,4-

linked D-xylose backbone that is characteristic of xylans involves xylanases (β -1,4-D-xylan xylanohydrolase; EC 3.2.1.8) and xylosidases (β -1,4-D-xyloside xylohydrolase; EC 3.2.1.37). Generally, the xylanases hydrolyse internal xylosidic bonds on the backbone chain, and the β -xylosidases release xylose residues by hydrolysing from the ends of xylooligosaccharides formed by the action of the xylanases. Other enzymes are necessary for the complete degradation of xylan into its substituent units as xylanases and β -xylosidases cannot remove branched side chains. Esterases, arabinofuranosidases and glucuronidases are all involved in the degradation of the side chain branches.

Xylanases are produced by a multitude of organisms, including bacteria, algae, fungi, protozoa, gastropods and arthropods (Dekker & Richards, 1976). Most of the bacteria and fungi secrete xylanases into their extracellular surroundings, allowing them to live heterotrophically on the liberated xylose. Ruminant microorganisms in particular are known to be powerful producers of xylanolytic enzymes, presumably due to the high hemicellulose content of animal feed, and as discussed previously this is of benefit to the animal by allowing them to obtain greater nutritional value from their feed.

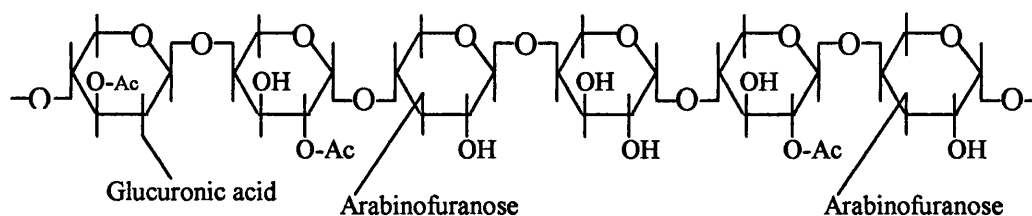


Figure 1.1 Generalised structure of a xylan polymer

Adapted from Coughlan & Hazlewood (1993). Ac represents acetyl group.

1.3.1 Mechanism of catalysis

The reaction that brings about hydrolysis of a glycosidic bond is formally a nucleophilic substitution at the saturated carbon of the anomeric centre (Sinnott, 1990). Glycosyl hydrolases can be classified according to the mechanism by which they hydrolyse glycosidic bonds. There are two classes of glycosyl hydrolases: the inverting enzymes and the retaining enzymes. These classifications correspond to the stereochemical

outcome of glycosidic bond hydrolysis, and refer to the overall inversion or retention of anomeric configuration during catalysis (Koshland, 1953; Sinnott, 1990). Mutagenesis studies and the availability of crystal structures have aided in the elucidation of accurate catalytic mechanisms for each class of glycosyl hydrolase. The xylanase of interest in this study is a member of glycosyl hydrolase family 11. Family 11 xylanases are known to retain the anomeric configuration during catalysis. Retaining enzymes are proposed to proceed via a double-displacement mechanism involving the production of a covalent glycosyl-enzyme intermediate (Koshland, 1953; Sinnott, 1990). The formation and hydrolysis of this covalent intermediate occurs via oxocarbenium ion-like transition states, aided by two active site residues. In family 11 xylanases the two active site catalytic residues have been identified as glutamic acids: one acts as a nucleophile and the other as an acid/base catalyst (Miao *et al.*, 1994; Torronen *et al.*, 1994; Wakarchuk *et al.*, 1994). The mechanism is summarised in Figure 1.2, and proceeds as follows: the first step involves the nucleophile attacking the anomeric carbon, displacing the leaving group and forming a covalent glycosyl intermediate, and the acid/base catalyst assisting in the formation of the intermediate by protonating the leaving group to allow bond cleavage. The second step involves deprotonation of an incoming water molecule, which attacks at the anomeric carbon and leads to displacement of the sugar. The distance between the two catalytic active site residues is approximately 5.5Å (McCarter & Withers, 1994), which allows the proton donor to be within hydrogen-bonding distance of the glycosidic oxygen and the nucleophile to be close to the anomeric carbon of the sugar.

The active site of family 11 xylanases has a cleft structure (Figure 1.3). This ‘open’ structure permits the xylan polymer to lie along the cleft, where several of its xylose units are bound by interactions with amino acid residues. Aromatic residues within the active site cleft are involved in stabilising the xylan backbone chain by packing against individual xylose units. Additionally, other residues along the active site cleft help to stabilise the xylan by forming hydrogen bonds with substrate hydroxyl groups.

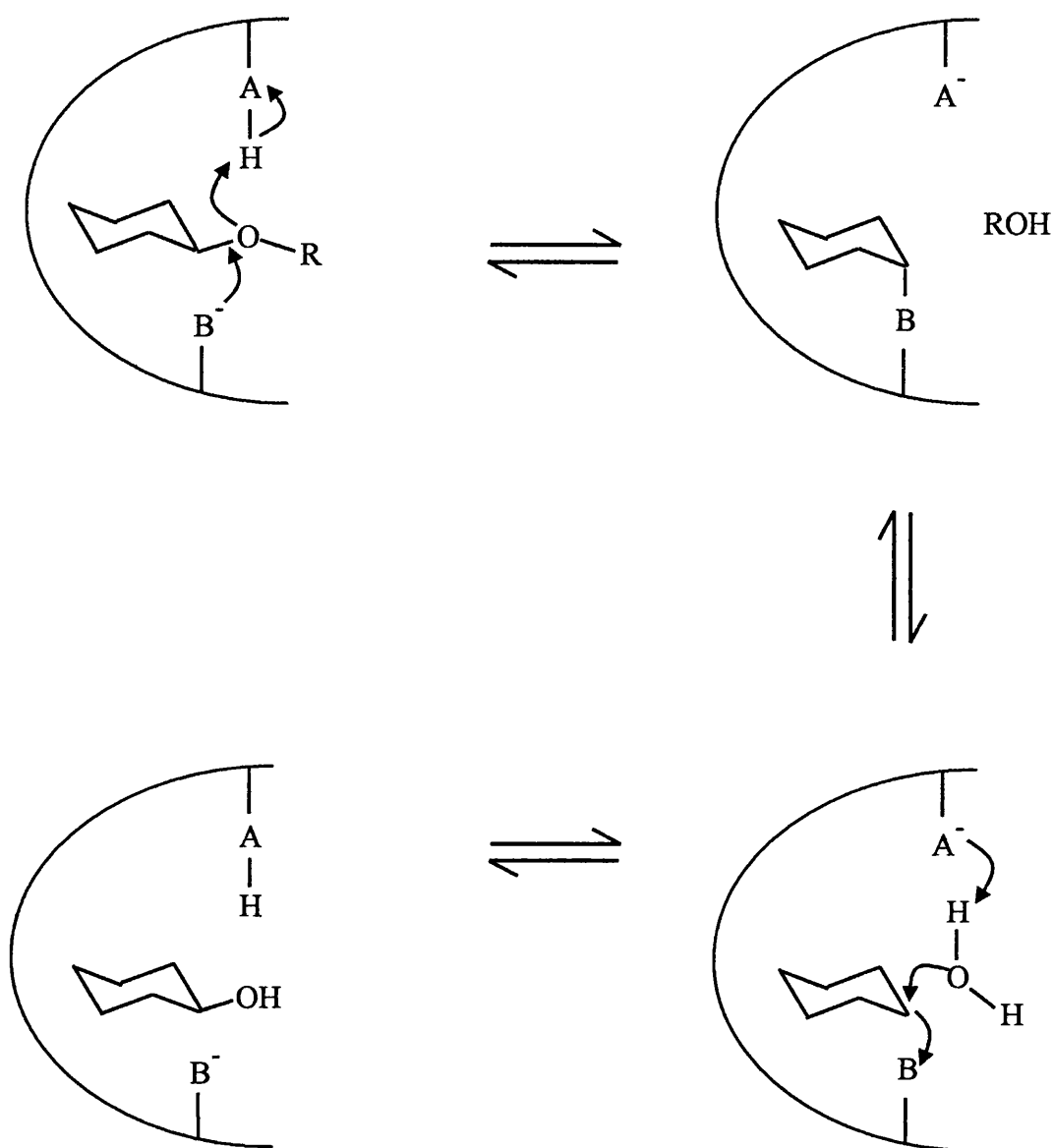


Figure 1.2 Reaction mechanism of retaining glycosyl hydrolases

Adapted from Davies & Henrissat (1995). Figure represents the stages of catalysis occurring in the active site cleft of retaining glycosyl hydrolases. A represents the acid/base catalyst, which assists in the formation of a glycosyl intermediate by protonating the leaving group (RO). B represents the nucleophile, which attacks the anomeric carbon and displaces the leaving group forming the covalent intermediate. In the second stage of the reaction an incoming water molecule is deprotonated by group A, leading to attack of the anomeric carbon and displacement of the sugar.

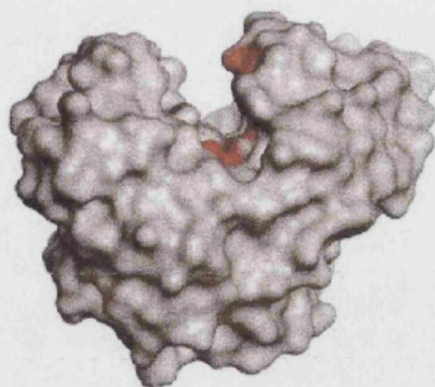


Figure 1.3 The 'open cleft' active site structure

Reproduced from Davies & Henrissat (1995). Image is of the three-dimensional structure of endoglucanase E2 from *Trichoderma reesei*. Red shaded areas correspond to the two active site catalytic residues.

These substrate binding sites within the active site cleft are known as subsites, and are labelled as -2, -1, +1, +2 and +3 (where positive numbers represent the reducing end of the substrate chain, and negative numbers the non-reducing end) (Bray & Clarke, 1992; Torronen & Rouvinen, 1995). Cleavage of the xylan backbone chain is thought to occur between subsites -1 and +1. Subsites -2 and -1 are well characterised by studies on a *Bacillus circulans* xylanase (Wakarchuck *et al.*, 1994) and xylanase II from *Trichoderma reesei* (Havukainen *et al.*, 1996), but characterisation of the reducing end subsites is based on modelling studies only.

1.3.2 Xylanase assay methods

There are numerous assay methods available to detect xylanase activity, including methods to detect activity on a solid support (for example, activity of a xylanase expressed in a microorganism that has been cultured on an agar plate) as well as in solution. The most common assay method used to detect xylanase activity in solution is the dinitrosalicylic acid (DNS) method, which was originally described by Miller (1959). It follows hydrolysis of a xylan substrate by determining the release of reducing

sugar. An interlaboratory evaluation of the various xylanase assays in use determined that when the DNS assay is standardised in terms of substrate and assay procedure it is capable of generating reproducible results that facilitate comparison of data between different laboratories (Bailey *et al.*, 1992). The DNS assay reagent comprises 3,5-dinitrosalicylic acid, sodium hydroxide, phenol and sodium sulphite and is used to detect the presence of free carbonyl groups in reducing sugars following incubation of a xylan substrate with a xylanase. Under alkaline conditions the aldehyde group present in reducing sugars is oxidised to a carboxyl group, while simultaneously the 3,5-dinitrosalicylic acid (DNS) is reduced to 3-amino-5-nitrosalicylic acid (Figure 1.4). Sulphite (in the form of sodium sulphite) is included in the reagent to absorb dissolved oxygen, as this may interfere with oxidation of the reducing sugar. By including phenol in the reagent the sensitivity of the assay can be increased. Xylanase activity is determined by comparison to a xylose standard curve, where the enzyme and substrate portion of the reaction are substituted for a selection of xylose solutions of known concentration. The xylanase activity is expressed as xylose equivalents.

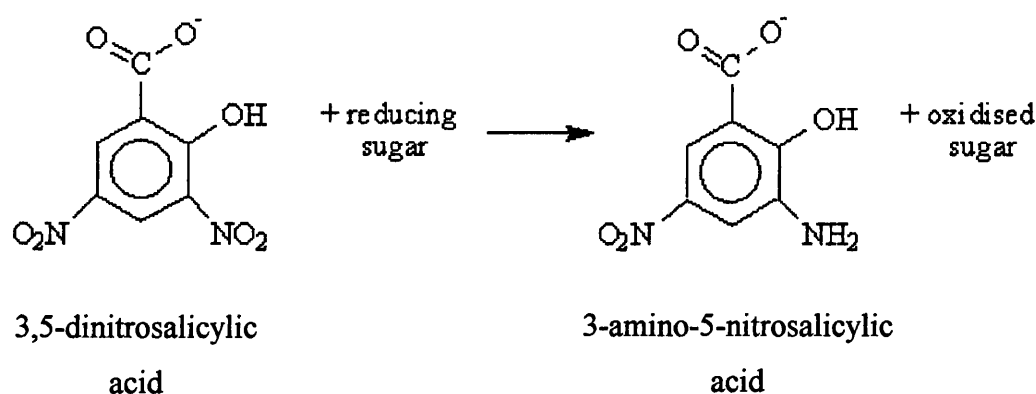


Figure 1.4 Mechanism of dinitrosalicylic acid assay

In situations where simply the presence or absence of xylanase activity needs to be determined, for example in determining whether a bacterial colony is expressing an active xylanase clone, there are two assay methods that can be used. Both are performed as 'solid-phase' assays, and involve dyes to highlight areas of substrate hydrolysis. The first method uses the dye Congo Red to indicate areas where the xylan substrate remains intact (Teather & Wood, 1982). Using the example above, a bacterial colony expressing a xylanase clone could be either grown on an agar plate containing a xylan substrate, or it could be grown on a regular LB-agar plate and overlaid with an agar containing xylan. After a suitable incubation time the agar plate is flooded with a 1% solution of Congo Red and unbound dye is washed away with 1M sodium chloride solution. Congo Red makes strong interactions with polysaccharides containing β -1,4-linked glycosidic bonds, and as such in areas where xylanase activity has hydrolysed the polymeric xylan into smaller units the dye does not bind and so a clearing zone, or 'halo', is seen around the area of xylanase activity.

An alternative method of detecting xylanase activity is to use a xylan substrate that has been tagged with a dye. A common dye in use is Remazol brilliant blue R (RBB), and RBB-xylan can be included in the agar plates on which bacterial colonies expressing xylanase clones are grown. In a similar way to the Congo Red assay, areas of xylanase activity are visible by the clearing zone present around them. Here, as the xylanase hydrolyses the polymeric xylan the dye is released and is free to diffuse away from the area leaving a clearing zone behind it.

1.3.3 Molecular architecture of xylanases

At the molecular level xylanase proteins are known to comprise individual modules, or domains. These domains can be catalytic or non-catalytic and are usually joined together by linker sequences that are rich in proline and hydroxy-amino acids. Observed domains include catalytic, substrate binding, thermostabilising and docking domains. On the basis of structural similarities between domains it has been suggested that xylanases (and cellulases) have evolved by domain shuffling, followed by subsequent domain modification (Gilkes *et al.*, 1991).

1.3.3.1 Catalytic domains

The catalytic domains of xylanases are individual modules that comprise the active site. As previously discussed, sequence similarity between catalytic domains is a major factor in the classification of glycosyl hydrolase enzyme families. Generally, xylanases consist of a single catalytic domain only, although there are examples of enzymes that possess more than one. Evidence for the ability of catalytic domains to function independently comes from deletion studies involving the removal of other, non-catalytic, domains in several xylanases (Ferreira *et al.*, 1990). The results of these studies suggest that the other domains do not necessarily play an important role in catalysis, as truncated enzymes, consisting of the catalytic domain only, retain almost full xylanase activity.

1.3.3.2 Substrate binding domains

Many xylanases are known to contain substrate binding domains in addition to their catalytic domains. The most common substrate binding domains identified in glycosyl hydrolases in general are cellulose binding domains (CBDs) and there are two commonly used explanations to suggest why CBDs are found in polysaccharide hydrolases other than cellulases. The first proposes that both the abundance and the ordered, invariant chemical structure of cellulose make it an ideal anchor for hydrolysing enzymes to attach to the plant cell wall; the second suggests that CBDs help to increase the synergism known to exist between plant cell-wall hydrolases by bringing an assortment of hydrolysing enzymes into close contact with the plant cell wall (Black *et al.*, 1995). Through amino acid sequence similarities, cellulose binding domains have been classified into unique families (called CBD families), in a similar way to the classification of glycosyl hydrolase catalytic domains (Tomme *et al.*, 1995). In addition to the CBDs originally classified there are now known to be xylan-specific binding domains (XBDs) and these have been identified in both family 10 and family 11 xylanases (Simpson *et al.*, 1999; Sunna *et al.*, 2000a).

1.3.3.3 Thermostabilising domains

Thermostabilising domains (TSDs) were originally identified in xylanases from thermophilic bacteria (Lee *et al.*, 1993; Fontes *et al.*, 1995; Winterhalten *et al.*, 1995)

and their role as thermostabilising domains was inferred by the decrease in enzyme stability observed when the domains were removed. TSDs are now also known to be present in xylanases from mesophilic organisms (identified by sequence homology to the original TSDs), and while the exact reason for conveying thermostability to a mesophilic enzyme is uncertain it has been suggested that TSDs may also confer additional stability against other detrimental factors including proteolytic attack and extremes of pH (Clarke *et al.*, 1996). Whilst TSDs have been shown to enhance the stability of thermostable xylanases their presence is not a prerequisite for thermal stability. There are several xylanases isolated from thermophiles that are single domain enzymes consisting of a catalytic domain only, and yet their stability at elevated temperatures is equal to, or in some cases greater than, those enzymes possessing a TSD (Gibbs *et al.*, 1995; Saul *et al.*, 1995). Recent studies have shown that some of the previously identified TSDs are actually xylan binding domains, and have suggested that the decreased thermal stability observed with removal of the domains is due to disruption of structure and exposure of previously buried residues, rather than the removal of a domain responsible for imparting thermostability (Charnock *et al.*, 2000; Sunna *et al.*, 2000b).

1.3.3.4 Cellulosome docking domains

The idea that cellulolytic enzymes can be organised into functional, high molecular mass complexes was first proposed in 1983 (Lamed *et al.*, 1983). These complexes, termed cellulosomes, are now known to contain not only cellulolytic enzymes but also hemicellulolytic enzymes. In contrast to aerobic organisms, whose enzymes do not appear to associate, anaerobic microorganisms often synthesise multienzyme cellulase-hemicellulase complexes (Gilbert & Hazlewood, 1993). Early research on the cellulosome was carried out on extracts from the anaerobic bacterium *Clostridium thermocellum*, and its cellulosome complex was shown to be composed of 18 individual proteins (Hazlewood *et al.*, 1988). Characterisation of some of these enzymes revealed a non-catalytic domain containing a 22-residue repeated sequence that was often present at the C-terminus of the protein. During this early cellulosome work an additional multifunctional, non-catalytic subunit, originally termed S1, was noted (Lamed *et al.*, 1983; Bayer *et al.*, 1985). This subunit was thought to be involved in both bringing

together the other subunits of the cellulosome, and in the attachment of the cellulosome to its substrate. Subsequent studies on this subunit from *C. thermocellum*, now renamed scaffoldin, have shown that it has a single cellulose binding domain and nine distinct but closely related domains called cohesins (Gerngross *et al.*, 1993). The cohesin domains have been shown to interact with the other catalytic subunits of the cellulosome complex to form a cohesive multienzyme complex (Yaron *et al.*, 1995). The interaction between cohesin domains and catalytically active cellulosome subunits occurs via a domain within each individual enzyme that contains the 22-residue repeated sequence described above. This domain, now termed a dockerin domain, serves to bond each individual enzyme to the scaffoldin protein and hence mediate their integration into the cellulosome complex. Dockerin domains have been identified in enzymes from both bacterial and fungal sources. A study of fungal cellulosome complexes identified a 100kDa polypeptide that was proposed to be the scaffoldin protein, and determined that fungal cellulosome complexes have a mass of about 700kDa (Fanutti *et al.*, 1995). This is in comparison to bacterial cellulosomes, which are known to be approximately 2×10^6 Da.

1.3.4 *Neocallimastix patriciarum* Xylanase A

The xylanase of interest in this study is xylanase A from the anaerobic fungus *Neocallimastix patriciarum*. *N. patriciarum* was originally isolated from the rumen of a sheep (Orpin & Munn, 1986) and its ability to degrade xylan was first noted by Williams and Orpin in 1987. The first characterisation of a xylanolytic enzyme from *N. patriciarum* came when Gilbert *et al.* (1992) used rDNA methodology to clone the cDNA encoding a xylanase into a plasmid vector and expressed the enzyme in *E. coli*. This enzyme was designated xylanase A, and subsequent studies have revealed a further two *N. patriciarum* xylanase enzymes, which have been designated xylanase B and C (Black *et al.*, 1995; Liu *et al.*, 1999).

The original characterisation studies by Gilbert *et al.* (1992) showed xylanase A to be a 66kDa protein, encoded by an 1821 base-pair gene. In common with other xylanases, xylanase A is a modular enzyme and consists of a signal peptide, a 225-amino acid

repeated sequence at the N-terminus and a 40-amino acid repeated sequence at the C-terminus. As with other modular glycosyl hydrolases, the modules are separated by linker sequences rich in proline and hydroxyamino acids. (Figure 1.5). The 225-amino acid repeats are highly analogous (91.6% identical and 95.6% similar), and have been shown by sequence homology to other known xylanases to be glycosyl hydrolase family 11 catalytic domains. Xylanase A is one of the few xylanases that contains two distinct catalytic domains, and the fact that the DNA encoding these two repeated domains demonstrates 92.7% identity suggests that *xynA* is a result of tandem duplication of an ancestral gene. The catalytic domains also show high homology to ruminal xylanases from bacterial sources, and Gilbert *et al.* (1992) concluded that this provides evidence for a common evolutionary origin. They proposed that gene transfer may have occurred between the rumen prokaryotic and lower eukaryotic organisms either within the rumen or prior to their colonisation of the rumen. Characterisation of the duplicated catalytic domains by deletion analysis showed that both domains can function independently of the other, and that they both cleave xylan only, producing both xylobiose and xylose in approximately equal amounts. One important observation made during this study was that the plasmid coding for a single catalytic domain expressed 15 times more recombinant xylanase protein in *E. coli* than the plasmid encoding the full-length enzyme. This was presumed to be a result of the utilisation of an *E. coli* translation initiation sequence by the plasmid coding for the truncated xylanase A catalytic domain protein (in comparison to the weak fungal translation initiation sequence utilised in the full-length enzyme).

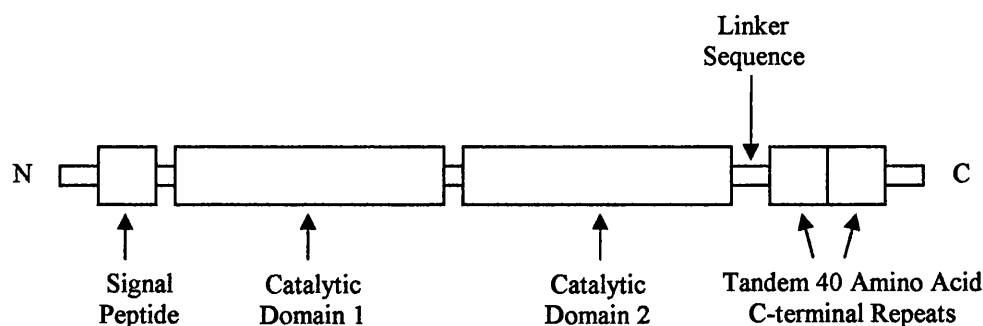


Figure 1.5 Molecular architecture of *Neocallimastix patriciarum* xylanase A

While in the original characterisation studies the function of the repeated 40-amino acid C-terminal domains remained unknown, they were shown by deletion analysis not to be necessary for catalysis. It has since been suggested that these repeated domains, which also demonstrate high homology (82.9% identical and 90.8% similar), are involved in cellulosome formation. A study by Fannutti *et al* (1995) on xylanase A and mannanase A from the anaerobic fungus *Piromyces* showed that both these enzymes possess a 40-amino acid repeated sequence homologous to that in the *N. patriciarum* xylanase A. They showed that the repeated sequence from both these enzymes bound to a protein found within the multi-enzyme cellulose-binding complex of both *Piromyces* and *N. patriciarum* that they proposed to be the scaffoldin protein. By sequence homology they suggested that the 40-amino acid repeats in *N. patriciarum* xylanase A would also be able to bind this proposed scaffoldin protein, and as such they classified the repeats as cellulosome docking domains.

1.4 PROTEIN STABILITY

The folded conformation of a protein is the conformation, as dictated by its primary sequence, in which the protein is able to carry out its biological function. This specific three-dimensional structure is maintained and stabilised by a variety of interactions. The most significant stabilising forces are known to be weak, non-covalent ones, although covalent disulphide bonds do contribute to protein stability. Entropy is known to be the main factor opposing the maintenance of a protein in its folded state, and given that the folded, active conformation of a protein is only marginally more thermodynamically stable than the unfolded, inactive conformation, these weak interactions play an important role in preserving the structure and, as a result, function of the protein.

Non-covalent interactions that contribute to the overall stability of a protein include ionic interactions, van der Waals interactions, hydrogen bonding and hydrophobic interactions. Ionic interactions, or the formation of an ionic bond, occur as a result of the association between two oppositely charged ionic groups within close proximity (up to 6 Å) in a protein molecule. Van der Waals interactions are the associations between electrically neutral molecules, and they arise as a result of weak electrostatic attraction

between two atoms with permanent or induced dipole moments. Hydrogen bonds are also electrostatic interactions, and they occur between a weakly acidic donor group and an acceptor atom that bears a lone pair of electrons. Within a protein molecule both the donor and acceptor groups are usually the highly electronegative nitrogen and oxygen atoms, although sulphur atoms can also be involved in hydrogen bonding. In order for a hydrogen bond to form, the distance between donor and acceptor groups must be approximately 3Å. Hydrophobic interactions are the forces that hold non-polar molecules together. They play an important role in the stabilisation of a protein's folded conformation, as the interior of a protein is generally a densely packed core of hydrophobic amino acid side chains. It has been proposed that this hydrophobic effect is the major driving force behind protein folding (Dill, 1990).

These non-covalent interactions are all energetically weak in comparison to covalent bonds. The energy required to break a mole of covalent carbon-carbon bonds is about 350kJ. In comparison, approximately 20kJ/mol is required to disrupt a hydrogen bond, 40kJ/mol for an ionic bond, 4-8kJ/mol for a hydrophobic interaction and only 4kJ/mol to disrupt a van der Waals interaction. Whilst each of these interactions individually contribute only a small amount to a protein's overall stability, they predominate as the major stabilising forces because of their number. Generally speaking, the protein conformation with the lowest free energy, i.e. the most stable conformation, is the one with the maximum number of weak non-covalent interactions. Another reason why these weak interactions play an important role in protein stability is that they stabilise any polar and charged amino acid side chains within the core of the protein. For example, whilst one hydrogen bond makes only a small apparent contribution to the stability of a folded protein, the presence of a single hydrogen-bonding group without a partner within the hydrophobic core of the protein would be sufficiently destabilising so as to make the protein's conformation thermodynamically untenable.

Disulphide bonds are also known to contribute to protein stability, and these are examples of covalent interactions. These linkages occur via oxidation between the thiol groups of two cysteine residues. The cytoplasm of a cell is relatively reducing in

character, and this diminishes the stability of a disulphide bond, which is easily reduced. As such almost all proteins containing disulphide bonds are found in extracellular locations where the environment is more oxidising. Here the disulphide bonds confer additional stability to secreted proteins. As they are covalent linkages a much larger input of energy is required to disrupt them (approximately 210kJ/mol).

1.4.1 Factors contributing to thermal stability

There are many publications that review the studies performed to date that have attempted to answer the question of how enzymes from thermophilic organisms are able to maintain their stability at the elevated temperatures (for a recent example, see Vieille & Zeikus, 2001). The general opinion is that while certain features have been identified as contributing to stability at elevated temperatures in the numerous enzymes studied to date, these features are not universal ones that can be applied to any enzyme to guarantee an increase in its thermostability. Thermostability seems more to be a result of small structural modifications brought about by a few amino acid substitutions, and modulation of the forces and interactions discussed in the previous section that come together in a unique fashion for each individual enzyme. The fact that thermophilic and hyperthermophilic enzymes can be cloned and expressed in a mesophilic host, and that the recombinant enzymes usually display stability and activity equal to that of the native enzymes, highlight the point that these enzymes possess intrinsic factors which predispose them to stability and activity at higher temperatures. Studies into the basis of thermostability have been performed on families of enzymes containing both mesophilic and thermophilic members, and in some cases psychrophilic members also. They have concluded that there are common factors (single factors, or multiple factors in combination) within an enzyme family that do contribute to thermostability, but that these are often not general factors that apply across different families. An important point to consider here is that any differences identified between mesophilic and thermophilic proteins must be viewed in a structural context in order to fully appreciate their involvement in thermostability (Danson & Hough, 2002).

Common features that have been identified as contributors to thermal stability include an increased number of hydrogen bonds, improved electrostatic interaction through ionic bonds and networks, greater hydrophobicity, increased packing or core density through smaller cavities, shortening or deletion of loops, increased α -helical content, increased polar surface area, increased number of proline residues and decreased occurrence of thermolabile amino acid residues such as asparagine, glutamine, methionine and cysteine (Sternier & Liebl, 2001; Kumar *et al.*, 2000b). A number of these factors are thought to aid thermostability by reducing the flexibility of the protein. For example, loops are flexible regions within the secondary structure of a protein. As such it is thought that thermal denaturation may be initiated at these flexible sites. Shortening these loops, or making them less flexible by the introduction of stabilising amino acids (proline residues, for example), may protect the protein from denaturation at this point.

Interestingly, a recent statistical analysis of homologous mesophilic and thermophilic enzymes from 18 families (Kumar *et al.*, 2000b) concluded that the only factors responsible for increased thermostability across the whole selection of enzyme families were increased numbers of ionic bonds and hydrogen bonds between amino acid side chains. They concluded that the mesophilic and thermophilic proteins exhibit similar hydrophobicities, compactness, polar surface areas and main-chain and side-chain hydrogen bonding. They also did not see any obvious increase in the number of proline residues or in deletions that shorten loops. This study strengthens the opinion that thermostability cannot be defined in general terms for all thermophilic proteins, and demonstrates that while certain factors might contribute to thermostability in one protein they will not necessarily have the same effect in the next protein.

1.4.1.1 Examples of non-covalent interactions involved in thermostabilisation

In the studies performed to date that have attempted to address the question of how individual enzymes are stabilised at high temperatures, increased numbers of ionic bonds are frequently identified as important stabilising factors. Studies on glutamate dehydrogenase by Yip *et al.* (1995, 1998) have identified ion-pair networks as the major factor responsible for thermostability. Similarly, studies on the enzyme citrate synthase

have also shown the importance of ion-pair networks in maintaining thermostability. Russell *et al.* (1997) compared the crystal structures of three citrate synthases whose optimum growth temperatures span the biological temperature range (37, 55 and 100°C) and showed that the number of intersubunit ion-pairs increased with increasing temperature. Arnott *et al.* (2000) have further confirmed the involvement of these ion pairs in thermal stability by showing that disruption of the intersubunit ion-pair network in the citrate synthase whose optimum growth temperature is 100°C leads to a decrease in its thermostability.

Increased hydrophobic interactions are another example of non-covalent interactions that have been frequently cited as one of the mechanisms involved in stabilisation of proteins at high temperatures. As previously mentioned, hydrophobic interactions are generally accepted as being the major driving force behind protein folding (Dill, 1990). This fact is not due to any strong attraction between non-polar molecules, but rather results from a protein aiming to achieve the greatest thermodynamic stability possible by minimising the entropy decrease that would occur by ordering water molecules around non-polar, hydrophobic molecules. An example of where increased numbers of hydrophobic interactions have been cited as the responsible factor in increasing thermostability is the work of Haney *et al.* (1997). By comparing the three-dimensional structures of adenylate kinases from mesophilic, thermophilic and hyperthermophilic organisms they have identified an increase in the number of aliphatic amino acids, leading to a larger and more hydrophobic enzyme core, as the factor responsible for the increased thermostability seen in the thermophilic and hyperthermophilic enzymes.

1.4.1.2 Examples of covalent interactions involved in thermostabilisation

Disulphide bonds are the main covalent interactions that play a role in the stabilisation of proteins at high temperatures. As already discussed in section 1.4, disulphide bonds are known to give additional stability to the three-dimensional structure of active proteins, and in particular to those proteins that are secreted to the extracellular environment. Despite their stabilising nature they occur in unexpectedly low numbers in thermostable proteins. Cysteines are one of a number of thermolabile residues that are

found in decreased numbers in thermophilic proteins, and it may be the reduced presence of cysteine monomers that leads to the lower than expected frequency of disulphide bonds (Danson & Hough, 2002).

Considering the aims of this project, introducing a disulphide bond may be one way to increase the thermal stability of xylanase A from *N. patriciarum*. The idea of using non-native disulphide bonds to stabilise protein structure was first studied by Villifranca *et al.* (1983) with the enzyme dihydrofolate reductase, and since then has been applied in the quest to stabilise many other proteins. Xylanase A is a mesophilic enzyme that, in the animal feed industry, is expected to be active at mesophilic temperatures but to be stable at the high temperatures experienced during the feed pelleting process. The formation of an introduced disulphide bond should be possible as the enzyme will be synthesised in a mesophilic host, so the problems outlined above with the instability of cysteine residues should not pose a problem. On formation of a disulphide bond it would be hoped that the bond would help stabilise the enzyme during its incubation at elevated temperatures.

In support of this theory, one study has introduced a single disulphide bond, and a combination of two and three bonds, into a xylanase from *Bacillus circulans*, and has shown that the mutant enzymes are all more stable than the wild-type enzyme (Wakarchuk *et al.*, 1994). The mutants containing a single disulphide bond confer some additional thermostability to the xylanase, but the greatest improvement in stability was seen in the mutant with three internal disulphide bonds, where an increase in thermostability of 15°C was observed over the wild-type, as measured by residual activity.

1.5 ENGINEERING STABILITY

Protein engineering is a process whereby an enzyme's function or stability can be altered by modifying its amino acid sequence. The ability to alter the specific properties of an enzyme has attracted a great deal of interest from those industrial companies looking to use biological catalysts to improve their existing processes, or to carry out novel ones.

As already mentioned in section 1.1, there is increasing demand from industrial companies for enzymes possessing unusual properties that would enable improvements to be made in the efficiency of existing industrial processes. In addition to the properties found in enzymes from extremophilic organisms, such as activity at elevated temperature or extreme pH, the development of many non-natural properties would also be of benefit. Examples include alterations to substrate specificity and enantioselectivity, and stability and activity in artificial environments such as organic solvents. Xylanases are industrially relevant enzymes, and attempts have already been made to improve properties such as thermostability and activity at high pH so that the enzymes are more suited for use in the pulp and paper and animal feed industries.

The two key techniques commonly employed to engineer enzymic properties within the laboratory are rational design and random mutagenesis. Both methods have demonstrated varying degrees of success in their ability to alter the characteristics of industrially relevant enzymes. Random mutagenesis, also known as directed evolution, is becoming the increasingly popular option as it requires little prior knowledge of the enzyme under study. Rational design on the other hand requires detailed knowledge of the sequence and three-dimensional structure of a protein in order to accurately predict mutations that may result in the required improvement.

1.5.1 Rational design

Rational design, also known as site-directed mutagenesis, is the traditional method of protein engineering. It uses knowledge of the sequence and three-dimensional structure of a protein to design amino acid substitutions that are predicted to alter a characteristic of interest. Site-directed mutagenesis is also a useful tool for investigating the relationship between protein structure and function. It has been successfully used in the elucidation of enzyme catalytic and binding mechanisms, and has been applied in the quest to discover the structural basis behind characteristics such as thermostability and substrate specificity.

The chances of designing successful mutations by rational design are greatly increased by the availability of crystal structures of homologous enzymes possessing the desired trait. Consider thermostability, the characteristic of interest in this project. The chances of designing site-specific mutations that may lead to an increase in the thermostability of a mesophilic enzyme should be improved by structural knowledge of the naturally occurring thermostable homologues of the enzyme. However, as already discussed in section 1.4, thermostability is a difficult characteristic to predict accurately as no single factor is responsible for imparting stability at high temperatures. This makes the task of improving the thermal stability of a mesophilic enzyme by rational design significantly more challenging.

A successful example of the use of site-directed mutagenesis to increase the thermostability of an enzyme is the work carried out by Van den Berg *et al.* (1998). Based on comparisons with the more thermostable protein thermolysin, they have introduced 8 mutations into a thermolysin-like protease from *Bacillus stearothermophilus*, and have shown that the resulting mutant enzyme is 340 times more stable than the wild-type enzyme at 100°C. Rational design has also been used to successfully change the cofactor specificity of the enzyme isopropylmalate dehydrogenase from *Thermus thermophilus*. In this study, Chen *et al.* (1996) have used crystal structures and molecular modelling to make significant changes in the secondary structure of the enzyme in order to alter its cofactor specificity. The mutant enzyme, which is four times more active than the wild-type enzyme, contains four amino acid substitutions and an α -helix and loop in place of a β -turn. Its cofactor specificity has switched from a 100-fold preference for NAD to a 1000-fold preference for NADP.

Disadvantages of the rational design approach to protein engineering include that fact that crystal structures are not always known for a given enzyme. Even with structural information available the effects of multiple mutations are not easily predictable (Tobin *et al.*, 2000). An alternative approach if the crystal structure of an enzyme is not available is to produce a model based on the already determined crystal structures of other closely related proteins. This will provide a rough estimate of the three-

dimensional structure of a protein, although modelled structures are generally not as reliable as the true crystal structure as even small differences in amino acid sequence can have large effects on a protein's structure and the way in which it folds. Site-directed approaches to protein engineering based on a modelled structure can, therefore, be considerably less reliable than when the actual crystal structure is used as the basis for design.

Another disadvantage of site-directed mutagenesis is that often there is not a homologous enzyme displaying the desired characteristics available for comparison. Even if a homologue is known, it is not uncommon for two enzymes to strongly resemble each other in three-dimensional structure but have considerably different amino acid sequences (Arnold, 1998). These problems, coupled with the fact that the whole process of designing and introducing mutations and assessing the mutant enzyme's new characteristics is labour-intensive and time-consuming means that efforts have been made in recent years to develop an alternative method of engineering the properties of an enzyme.

1.5.2 Random mutagenesis

Random mutagenesis is emerging as a powerful tool with which to 'redesign' enzymes for use as biocatalysts in industrial applications. The main advantage of random mutagenesis over rational design is the fact that it requires no structural knowledge of the enzyme of interest in order to bring about improvements in a specific property. Previously, random mutations could be introduced into a gene using chemical mutagens such as formic acid, hydrazine or sodium nitrite (for example see Arase *et al.*, 1993). However, these methods are not ideal in exploring all potential mutations as they cannot generate all possible base substitutions (Fromant *et al.*, 1995). Over the last decade two alternative methods have been developed for the introduction of random mutations into gene sequences: directed evolution and DNA shuffling. These have replaced chemical mutagenesis to become the popular techniques with which to improve specific enzymic properties, and both involve stages of mutagenesis followed by screening to identify mutants displaying improvements in the desired function.

1.5.2.1 Directed evolution

The technique of random mutagenesis by directed evolution uses the theory of natural evolution to generate enzymes with improvements in specific properties. Natural evolution has shown that proteins are highly adaptable and are able to evolve in order to function in ever-changing environments. Generally, directed evolution involves the generation of a library of randomly mutated genes, followed by screening to identify those genes encoding enzymes displaying improvements in the desired property. The gene(s) encoding the improved enzymes are then subjected to further rounds of mutagenesis and screening in order to accumulate beneficial mutations (Kuchner & Arnold, 1997). Nature is able to evolve new proteins by randomly walking from a good starting point, and this system forms the basis for directed evolution experiments. By starting with an enzyme close, but not ideal, to what is required, it is possible to evolve it by accumulating small changes such that it retains its initial characteristics (for example, the ability to degrade xylan) but acquires new ones (such as increased stability at high temperature) (Arnold, 1996). Directed evolution uses the polymerase chain reaction to enzymatically introduce random mutations into a gene (Fromant *et al.*, 1995). This is achieved by using a polymerase lacking proofreading ability and by using unequal concentrations of the four deoxynucleoside triphosphates, and is also known as error-prone PCR. The screening process is the equivalent of natural selection, providing a selective pressure such that only mutants able to cope with this pressure are chosen for further rounds of mutation.

The main advantage of directed evolution over rational design is the lack of structural information required about the enzyme of interest. It is not necessary to know the crystal structure of the protein and how this relates to its function, nor is it necessary to have information about related enzymes from the same family in order to successfully improve a function of the enzyme. One limitation to the success of directed evolution experiments is the precision of the screening system. In order to identify a few improved mutant enzymes from the many thousands produced by error-prone PCR the screen must be sensitive to the properties of interest, reproducible with low inherent variability and efficient enough to screen many mutants quickly and effectively. Although the

mutational frequency can be controlled by the error-prone PCR conditions used, beneficial mutations are rare, with the majority being deleterious (Arnold *et al.*, 2001). This means that devising a screen capable of detecting the small functional changes expected from one or two amino acid substitutions can prove difficult. Despite the challenges of designing an accurate, reliable screen, directed evolution has proved successful in engineering numerous enzymic properties, including substrate specificity, enantioselectivity and thermostability (with and without an associated decrease in activity at lower temperatures) (See Table 1.1 for further examples). With the recent emergence of high-throughput screening processes, the application of directed evolution should soon be extended to many more industrial enzymes, and as such should increase the feasibility for creating new enzymic functions as well as improving existing ones (Georgiu & DeWitt, 1999).

There have been many attempts to use directed evolution to improve the thermostability of an enzyme. Successful examples include the work Gonzalez-Blasco *et al.* (2000). In this study they have used a single round of error-prone PCR and screening to isolate a mutant of β -glucosidase from *Paenibacillus polymyxa* that displays a half-life at 65°C of 12 minutes. This is in comparison to the wild-type enzyme, which displays no detectable activity at 55°C.

ALTERED PROPERTY	TARGET ENZYME
Increased thermostability	p-Nitrobenzyl esterase ¹
Increased activity in organic solvents	Subtilisin E ²
Altered substrate specificity	β -Galactosidase ³
Increased enantioselectivity	Lipases ⁴
Increased catalytic activity	Cytochrome P ₄₅₀ ⁵

Table 1.1 Examples of enzyme properties improved by directed evolution

Adapted from Affholter & Arnold, 1999. ¹Giver *et al.*, 1998; ²You & Arnold, 1996; ³Zhang *et al.*, 1997; ⁴Liebeton *et al.*, 2000; ⁵Joo *et al.*, 1999.

1.5.2.2 DNA shuffling

The technique of DNA shuffling was first introduced by Stemmer in 1994 (Stemmer, 1994a). Rather than a method of introducing random point mutations into a gene, it is a method for homologous recombination of genes by random fragmentation and PCR-mediated reassembly. Like random mutagenesis by error-prone PCR, DNA shuffling is based on the evolutionary principle of mutation and natural selection (screening being the laboratory equivalent of natural selection). DNA shuffling requires homologous sequences that are separated by regions of variability. By shuffling together closely related genes it should be possible to combine the phenotypes of the similar enzymes in order to produce mutants displaying properties from all 'parent' sequences. An advantage of the DNA shuffling approach is that by backcrossing mutants with excess wild-type DNA it is possible to remove neutral mutations that do not cause functional changes (Stemmer, 1994b).

In recent years DNA shuffling has been used in conjunction with directed evolution by error-prone PCR in order to increase its power as a protein engineering tool. It is, however, a useful technique in its own right and there are examples where it has been successfully used to alter or improve enzyme function. One such example is the work of Zhang *et al.* (1997), where *E. coli* β -galactosidase has been evolved into an efficient β -fucosidase through seven rounds of shuffling and screening. The final mutant demonstrated 1000-fold increase in specificity for *o*-nitrophenyl fucopyranoside over its previously preferred substrate *o*-nitrophenyl galactopyranoside.

When coupling the two directed evolution techniques together, DNA shuffling is typically used after error-prone PCR and screening in order to recombine improved mutants identified from the random mutagenesis stage. By combining the adaptive mutations introduced by random mutagenesis, the DNA shuffling step allows additional enhancements to be made to the property of interest, and provides a more improved mutant with which to begin the whole process of directed evolution and screening again.

An example of the power of combining both error-prone PCR and recombination is the work of Zhao and Arnold (1999). They have used directed evolution to effectively convert subtilisin E from *Bacillus subtilis* into its thermophilic homologue thermitase, from *Thermoactinomyces vulgaris*. The mutant enzyme was over 200 times more stable at 65°C than the wild-type enzyme, and it displayed an increase of 17°C in its temperature optimum. While subtilisin E and thermitase differ at 157 amino acid positions (subtilisin E is 381 amino acids and thermitase is 279 amino acids), it only took eight amino acid substitutions introduced by directed evolution and recombination to turn one enzyme into a functional equivalent of the other. Of the eight substitutions, which are all situated on the surface of the enzyme, only two are found in thermitase. The remaining substitutions include some known stabilising mutations in addition to mutations not previously reported as being thermostabilising. Most of the substitutions are located in loops connecting regions of secondary structure and are thought to increase thermostability by reducing the entropy of these flexible loops. One substitution is thought to increase thermostability by the improvement of a hydrogen bond. The mechanisms of thermostabilisation of four of the eight mutations are still under investigation.

Giver *et al.* (1998) have also successfully used a combination of error-prone PCR and recombination by DNA shuffling to improve the thermostability of *p*-nitrobenzyl esterase from *Bacillus subtilis*. Over six generations of random mutagenesis, recombination and screening they have increased the melting temperature of the esterase by more than 14°C to 66.5°C. Of importance in this example is the fact that the thermostability of the enzyme has been improved without compromising its catalytic activity at lower temperatures. It has often been thought that thermostability comes at a cost of decreased activity at lower temperatures (Shoichet *et al.*, 1995). This study by Giver *et al.* (1998) has shown that by designing the screen to select for both properties it is possible to improve thermal stability whilst retaining low temperature activity. These results are encouraging when the aims of this project are considered.

1.5.3 Successful examples of protein engineering in xylanases

Considering that the aims of this project are to increase the thermostability of xylanase A from *Neocallimastix patriciarum*, it is encouraging to find examples in the literature where various protein engineering techniques have been successfully applied to improve characteristics of other xylanases.

Attempts to engineer xylanases by rational design have succeeded in increasing both catalytic activity and thermostability. By targeting conserved residues within the enzyme Moreau *et al.* (1994) increased both the catalytic activity and thermostability of xylanase A from *Streptomyces lividans*. Georis *et al.* (2000) have modelled the structures of the thermostable xylanase A from *Thermomonospora fusca* and the mesophilic xylanase 1 from *Streptomyces* sp. S38, and then introduced some of the features identified as contributing to the higher thermostability of xylanase A into xylanase 1. They have shown that the introduction of an additional aromatic interaction can increase both the thermostability and thermophilicity of xylanase 1 (i.e. they have increased both the enzyme's stability and activity at higher temperatures). Another successful site-directed mutagenesis study has stabilised a xylanase from *Bacillus circulans* by the introduction of both intra- and inter-molecular disulphide bonds (Wakarchuk *et al.*, 1994).

There are also successful examples of the use of random mutagenesis to improve thermal stability, catalytic activity and alkalophilicity of xylanases. Arase *et al.* (1993) used chemically induced random mutagenesis to improve the thermostability of xylanase A from *Bacillus pumilus*. DNA shuffling was used by Shibuya *et al.* (2000) to improve both the thermostability and hydrolytic activity of xylanase B from *Streptomyces lividans*. Here the stability of xylanase B has been improved by shuffling together its gene with the gene encoding xylanase A from *Thermomonospora fusca*, a naturally thermostable enzyme with a temperature optimum of 75°C. The best mutant produced in this study demonstrated a temperature optimum the same as *T. fusca* xylanase A, and additionally produced 40% more reducing sugar at this temperature than xylanase A. A recent study by Chen *et al.* (2001) has used directed evolution by error-prone PCR to improve the activity of a catalytic domain from a *Neocallimastix patriciarum* xylanase

in alkaline conditions. They identified eight amino acid substitutions in six mutants that lead to an increased activity at pH 8.5 (where the wild-type enzyme does not demonstrate any activity), and introduced seven of these mutations into the enzyme by site-directed mutagenesis. The resulting enzyme was more thermostable at 60°C and more alkaline tolerant at pH 10 than the wild-type xylanase.

1.5.4 Alternatives to protein engineering

An alternative approach to protein engineering in order to obtain industrially relevant enzymes is to look to nature and screen for the required catalytic activity. It is estimated that less than 1% of microorganisms from extremophilic environments can be cultured at present (Hugenholtz & Pace, 1996). The remaining 99% represents a largely unexploited resource, and efforts to selectively culture these currently ‘unculturable’ organisms based on required catalytic activity will surely lead to the discovery of many more industrially useful catalysts (Danson & Hough, 1998). Ito *et al.* (1998) have adopted this approach to isolate enzymes for use in laundry and dishwasher detergents. Detergent enzymes need to function under alkaline conditions, and Iko *et al.* have isolated a number of alkaliphilic *Bacillus* strains that secrete useful detergent enzymes such as cellulases, proteases and α -amylases.

1.6 OBJECTIVES

The objectives of this project are essentially two-fold. The first is to increase the thermal stability of the second catalytic domain of xylanase A (xylA.cd2) from *Neocallimastix patriciarum*; the second is to retain its high levels of activity at lower temperatures. Two individual methods will be utilised in attempts to fulfil these objectives. The first method will be to design and introduce site-specific mutations that are predicted to increase the thermal stability of xylA.cd2. This will be achieved by comparing a structural model of the protein to the published crystal structures of thermostable family 11 xylanases. The second method will be to apply directed evolution techniques to the xylanase A second catalytic domain, in order to produce a library of random xylA.cd2 mutants. Using a suitable screening system the library will be screened in order to identify those mutants

that retain activity at lower temperatures but also demonstrate an increased stability at elevated temperatures.

Chapter 2

MATERIALS AND METHODS

2.1 MOLECULAR BIOLOGY MATERIALS AND METHODS

2.1.1 Materials

SeaKem® LE agarose was purchased from FMC Bioproducts, Rockland, ME, USA and 1kb DNA molecular weight marker was purchased from GibcoBRL Life Technologies, Paisley, UK. *E. coli* JM109 competent cells were obtained from Promega, Madison, WI, USA. IPTG and X-Gal were purchased from Calbiochem-Novabiochem Corporation, La Jolla, CA, USA. PCR Primers were synthesised by MWG-Biotech GmbH, Ebersberg, Germany. pUC18 plasmid vector, BamHI digested pUC18, M13 sequencing and reverse primers and deoxynucleoside triphosphates (dNTP's) were all purchased from Amersham Pharmacia Biotech, Uppsala, Sweden. QIAprep Spin Miniprep Kit, QIAquick PCR Purification Kit and QIAEX II Gel Extraction KIT were all obtained from Qiagen Ltd, Hilden, Germany. Rapid DNA ligation kit was purchased from Boehringer-Mannheim, Mannheim, Germany. Vent DNA polymerase, restriction endonucleases and reaction buffers were supplied by New England Biolabs, Hitchin, Hertfordshire, UK. All other reagents used in the molecular biology methods were supplied by Sigma, Poole, Dorset, UK.

2.1.2 Agarose gel electrophoresis

DNA was analysed by agarose gel electrophoresis. 1% (w/v) agarose gels (agarose dissolved in TAE buffer (40mM Tris-acetate, 1mM EDTA, pH 8.3) by heating) containing 0.5µg/ml ethidium bromide were placed in an electrophoresis tank and covered with TAE buffer. DNA samples were loaded with the appropriate volume of 6x loading buffer (40% (w/v) sucrose, 0.25% (w/v) bromophenol blue, 0.25% (w/v) xylene cyanol) and electrophoresed at a constant voltage of 80 V until the xylene cyanol dye front was 1cm from the end of the gel. DNA, visible by the presence of ethidium bromide, was visualised under UV transillumination and estimation of the size of DNA

fragments was by comparison to the 1kb DNA molecular weight marker run simultaneously on the gel.

2.1.3 Polymerase chain reaction

Amplification of the xylanase A second catalytic domain from the full-length gene was carried out by PCR using primers designed to the flanking region of the catalytic domain. Full details of all primers can be found in the Appendix. For expression of xylA.cd2 from the plasmid vector pUC18 both forward and reverse primers were designed with a BamH1 restriction site to aid cloning of the PCR product into pUC18 commercially digested with BamH1. The reverse primer was also required to incorporate a stop codon. A total of 20pmol of each primer was used in a reaction. Vent DNA polymerase was used in a total reaction volume of 100µl. Final concentrations in the reaction mixture were as follows: 0.2mM of each deoxynucleoside triphosphate (dATP, dCTP, dGTP, dTTP), 2mM MgCl₂ and 1U Vent DNA polymerase. Approximately 1µg of template DNA was added and the reaction was incubated in buffer supplied by the manufacturer. The final reaction mixture was overlaid with 20µl mineral oil to prevent evaporation. A 'hot-start' PCR technique was used, where the reaction mixture is heated to 96°C for 5 minutes prior to the addition of the polymerase. The following conditions were then repeated for 30 cycles before a final 10 minutes extension at 72°C:

96°C denaturation step	1 min 15 s
55°C annealing step	1 min 30 s
72°C extension step	2 min

A Cetus DNA thermal cycler (Perkin-Elmer, Norwalk, CT, USA) was used to perform the reactions. 10µl of each PCR reaction was run on a 1% agarose gel, as previously described in section 2.1.2, to visualise the product. Products were purified as described in section 2.1.4.2.

2.1.4 Purification of PCR products

2.1.4.1 Gel purification

PCR products were purified by running on an agarose gel and using the QIAEX II Gel Extraction Kit according to the manufacturer's instructions. Products were resuspended in a final volume of 30µl distilled water.

2.1.4.2 Column purification

PCR products were purified using the QIAquick PCR Purification Kit according to the manufacturer's instructions and were resuspended in a final volume of 50µl elution buffer (10mM Tris-Cl, pH8.5, supplied with kit).

2.1.5 Restriction digestion of DNA

Plasmid DNA and PCR products were digested by restriction endonucleases in a reaction volume of 20µl. Commonly approximately 2µg of plasmid DNA, prepared as described in section 2.1.8, or 100ng of PCR product were incubated with 10 or 20 units of enzyme (according to the manufacturer's instructions) in the buffer supplied. The reaction was allowed to proceed for 3 hours at 37°C. BSA (100µg/ml) was included in some reactions according to the manufacturer's instructions. Where the products of a digestion were to be used for cloning, the reaction was further incubated at 65°C for 20 minutes to inactivate the remaining enzyme.

2.1.6 Ligation

PCR products were ligated into the appropriately digested plasmid vector using the Rapid DNA Ligation kit in a total volume of 20µl. An insert to vector ratio of 3 to 1 was commonly used. Reactions were carried out according to the manufacturer's instructions.

2.1.7 Transformation of DNA into *E. coli* - heat shock method

Ligated DNA was transformed into *E. coli* strain JM109 as follows: 3µl of ligation reaction was added to 40µl of competent *E. coli* cells on ice and the mixture was mixed

gently before incubating on ice for 20 minutes. The cells were then heat shocked at 42°C for 1 minute before being returned to ice for a further 2 minutes. 1ml of LB broth (10g/L bacto-tryptone, 10g/L sodium chloride, 5g/L yeast extract) was added to the cells and this mixture was incubated at 37°C for 1 hour with shaking. Cells were then spread onto LB agar plates (LB broth with 15g/L agar) supplemented with 100µg/ml ampicillin, to select for cells that have been transformed with the ligated plasmid DNA, and incubated overnight at 37°C.

2.1.8 Preparation of plasmid DNA

E. coli strain JM109 transformed with the plasmid of interest was cultured overnight at 37°C in 5ml of LB broth supplemented with 100µg/ml ampicillin. Plasmid DNA was prepared using the QIAprep Spin Miniprep Kit according to the manufacturer's instructions and eluted in 50µl elution buffer (10mM Tris-Cl, pH8.5, supplied with kit).

2.1.9 DNA sequencing

DNA sequencing was performed on an ABI Prism™ 377 automated sequencer (PE Applied Biosystems, Fostercity, CA, USA) using the Big Dye™ Terminator Cycle Sequencing Ready Reaction Kit (PE Applied Biosystems). Sequences were analysed using the Wisconsin Package, version 8.0 (Genetics Computer Group, Madison, WI, USA).

2.2 PROTEIN MATERIALS AND METHODS

2.2.1 Materials

Acrylamide/bis-acrylamide mixture (Ultrapur protogel™) was purchased from National Diagnostics, Atlanta, GA, USA. APS, SDS broad range markers and Bio-Rad Protein Assay reagent were obtained from Bio-Rad, Hercules, CA, USA. Bovine serum albumin standard (2mg/ml) was supplied by Pierce, Rockford, IL, USA. HiTrapQ High Performance 5ml anion exchange columns were supplied by Amersham Pharmacia Biotech, Uppsala, Sweden. TEMED (N, N, N', N'-tetramethylethylenediamine) and RBB-xylan (4-O-methyl-D-glucurono-D-xylan-remazol brilliant blue R) were purchased from Sigma, St. Louis, MO, USA. Amicon YM-30 Centriplus® centrifugal filter devices

and 0.22 μ m syringe driven filter units were purchased from Millipore, Bedford, MA, USA. All other chemicals and reagents were supplied by either Fisons, Loughborough, Leicestershire, UK or Sigma, Poole, Dorset, UK.

2.2.2 Bradford protein estimation assay

Protein concentration was determined using the Bio-Rad Protein Assay, which is essentially as described by Bradford (1974). In brief, samples of unknown protein concentration were diluted accordingly in 0.9% NaCl solution and incubated with 900 μ l Bio-Rad Protein Assay reagent for 15 minutes at room temperature. The absorbance of the samples was measured at 595nm and protein concentration was determined by comparison to a standard curve generated using samples containing known concentrations of bovine serum albumin.

2.2.3 Sodium dodecyl sulphate-polyacrylamide gel electrophoresis (SDS-PAGE)

SDS-PAGE was performed according to the method of Laemmli (1970) using an Atto Corporation Mini-Atto System. A 12.5% running gel solution (5ml Ultrapure protogel™ (30% (v/v) acrylamide/0.8 % (v/v) bis-acrylamide), 3ml running gel buffer (1.5M Tris, 0.4% (w/v) SDS, pH 8.9), 4ml dH₂O) was polymerised by the addition of 50 μ l of 10 % APS and 12.5 μ l TEMED. A stacking gel (0.9ml Ultrapure protogel™, 2.4ml stacking gel buffer (0.48M Tris, 0.4% (w/v) SDS, pH 6.8), 3.6ml dH₂O, 50 μ l 10% (w/v) APS, 10 μ l TEMED) was poured on top of the polymerised running gel, and wells were formed for loading the samples. The gel was placed in an electrophoresis tank and submerged in tank buffer (0.052M Tris, 0.1% (w/v) SDS, 0.4% (w/v) glycine). Protein samples were loaded on to the gel in an equal volume of 2x loading buffer (0.125M Tris, 4% (w/v) SDS, 20% (w/v) sucrose, 0.08% (w/v) bromophenol blue, 10 (v/v) β -mercaptoethanol) and were electrophoresed at 10mA through the stacking gel and 20mA through the running gel. After electrophoresis the gel was stained for 20 minutes with Coomassie staining solution (0.25% (w/v) Coomassie blue R, 45.4% (v/v) methanol, 9.2% (v/v) acetic acid) and destained overnight with destain solution (5% (v/v) methanol, 7.5% (v/v) acetic acid). The molecular weight of proteins visible as bands after the gel had been stained was determined by comparison to standards of known

molecular weight that were run simultaneously on the gel. (broad range markers were commonly used: rabbit muscle myosin (200kDa), *E. coli* β -galactosidase (116.25kDa), rabbit muscle phosphorylase B (97.4kDa), bovine serum albumin (66.2 kDa), hen egg white ovalbumin (45kDa), bovine carbonic anhydrase (31kDa), soybean trypsin inhibitor (21.5kDa), hen egg white lysozyme (14.4kDa), bovine pancreas aprotinin (6.5kDa)).

2.2.4 Zymogram analysis

Xylanase-active protein bands were identified using a novel Zymogram technique. The method is essentially as described for performing SDS-PAGE, with the inclusion of RBB-xylan in the running gel. RBB-Xylan was dissolved in the water component of the running gel at 0.1%, and the gel was then prepared as described in section 2.2.3. 4 μ g of purified protein, or 10 μ g of cell extract proteins, were loaded onto the gel and run as previously described. After electrophoresis the gel was incubated overnight in 25% (v/v) isopropanol with gentle shaking to renature the proteins. The gel was then washed four times for 30 minutes at 4°C with 0.1M sodium acetate buffer (pH 5.5). It was then incubated at 37°C in pre-warmed PC buffer (phosphate-citrate buffer, pH 6.5) with 100 μ g/ μ l BSA until clearing zones became visible. The proteins were then stained with Coomassie staining solution and destained as described above.

2.2.5 Purification of XylA.cd2

XylA.cd2 was purified from *E. coli* JM109 harbouring the pUC18.cd2 plasmid vector. JM109 cells were grown in 5ml LB broth supplemented with 100 μ g/ml ampicillin overnight at 37°C. This culture was then used to inoculate 250ml LB-ampicillin broth (2.5ml of overnight culture into 250ml LB-ampicillin broth), which was incubated at 37°C for 16 hours. The cell extract was then prepared as outlined below.

2.2.5.1 Preparation of cell extract

Cell extract was prepared by harvesting the cells by centrifugation at 1250g for 10 minutes at 4°C, and resuspending the cell pellet in 1/25 of the original culture volume of 20mM Tris-HCl, pH 8.0. Cells were disrupted by sonication with 4 x 30 second bursts,

at 8-10 microns, peak to peak (3mm probe, 150 watt Ultrasonic Disintegrator, MSE Scientific Instruments, Crawley, Sussex, UK) with cooling on ice between ultrasonic bursts. Disrupted cells were centrifuged for 20 minutes at 8000g at 4°C to give the supernatant as the cell extract and the pellet as the cell debris. The debris was resuspended in 1/50 the original culture volume of 20mM Tris-HCl, pH 8.0. Both cell extract and debris were stored at 4°C until further use.

2.2.5.2 Anion exchange chromatography

Separation of XylA.cd2 from the cell extract proteins was achieved using reverse anion exchange chromatography. A HiTrap Q High Performance 5ml anion exchange column was equilibrated with 20mM Tris-HCl, pH 8.0, and cell extract was applied to the column using an FPLC System (Amersham Pharmacia Biotech, Uppsala, Sweden). XylA.cd2 protein was washed through the column with equilibration buffer and collected in the unbound fraction. The bound protein was collected by washing the column with elution buffer (equilibration buffer containing 1M NaCl).

2.2.5.3 Concentration of purified protein

Purified protein was concentrated in an Amicon YM30 Centriplus® centrifugal filter device, (molecular weight cut-off 30kDa) by centrifuging at 3000g in a swing-out bucket rotor at 4°C until reduced to a suitable volume.

2.3 ASSAY MATERIALS AND METHODS

2.3.1 Materials

Tris was supplied by BDH, Poole, Dorset, UK. Oat spelt xylan was purchased from Fluka Chemie AG, Buchs, Switzerland. Congo Red, 3,5-dinitrosalicylic acid, phenol and D(+)xylose, were purchased from Sigma, Poole, Dorset, UK. All other chemicals and reagents were supplied by either Fisons, Loughborough, Leicestershire, UK or Sigma, Poole, Dorset, UK.

2.3.2 Dinitrosalicylic acid (DNS) assay

Xylanase activity was determined using a modification of the DNS assay, originally described by Miller (1959). 100µl of enzyme sample (diluted if necessary in PC buffer with 1mg/ml BSA) was incubated with 400µl of 0.2% soluble xylan (in 50mM Tris, pH8.0) (see section 2.3.2.1 for production of soluble xylan) at 37°C for 15 minutes. The reaction was terminated by the addition of 500µl DNS reagent (1% (w/v) DNS, 0.2% phenol (v/v), 1% (w/v) sodium hydroxide, 0.002% (w/v) glucose and 0.05% (w/v) sodium sulphite). The samples were heated to 100°C for 20 minutes before being placed on ice for 10 minutes and centrifuged at 12,000g for 5 minutes. The absorbance of the samples was measured at 575nm against a blank sample (100µl of PC buffer used in place of the 100µl sample). The amount of xylanase activity in the samples was determined by comparison to a standard curve, generated using standard solutions of D(+)xylose in PC buffer with 1mg/ml BSA. The standard xylose solutions were in a total volume of 500µl, and after addition of 500µl of DNS reagent were treated as described above. The calculated amount of xylanase activity was expressed as µmoles of xylose equivalents produced per minute per mg enzyme.

2.3.2.1 Preparation of soluble xylan

Soluble xylan used in the DNS assay was prepared as follows: 20g of oat spelt xylan were resuspended in 200ml distilled water and the pH was adjusted with 1M NaOH to pH 10.0. After stirring at room temperature for 1 hour the pH was adjusted with 1M acetic acid to pH 7.0. After centrifugation at 20,000g for 10 minutes the supernatant was removed and freeze-dried until no liquid remained. The dried soluble xylan fraction was resuspended as a 0.2% solution in 50mM Tris, pH 8.0 when required for the xylanase assay.

2.3.3 Congo Red overlay assay

Xylanase activity was determined for the XylA.cd2 in *E. coli* JM109 by the Congo Red overlay assay, essentially as described by Teather & Wood (1982): JM109 cells harbouring the pUC18.cd2 plasmid vector were grown overnight on LB-ampicillin agar

plates then overlayed with 7ml xylan agar (0.25% (w/v) oat spelt xylan, 1.5% (w/v) agar in PC buffer, pH6.5). After incubation for 2 hours at 37°C the top agar was stained with 1% Congo Red solution for 10 minutes, then destained by washing three times with 10ml 1M NaCl, each wash being for 15 minutes. Cells that were xylanase active had a visible clearing zone, or orange 'halo', around them.

Chapter 3

CLONING, EXPRESSION, PURIFICATION AND CHARACTERISATION OF RECOMBINANT *N. PATRICIARUM* XYLANASE A SECOND CATALYTIC DOMAIN

3.1 INTRODUCTION

It is known from previous studies (Gilbert *et al.*, 1992) that *E. coli* harbouring a clone coding for only the second xylanase A catalytic domain from *N. patriciarum* expresses 15 times more protein than *E. coli* expressing the full-length enzyme. These previous studies are the basis for the initial aims of this project, which are to clone, express, purify and characterise the isolated second catalytic domain from xylanase A.

This chapter will describe the cloning of the second catalytic domain of *Neocallimastix patriciarum* xylanase A from the full-length gene into the plasmid vector pUC18, the expression of this xylA.cd2 clone in *E. coli* strain JM109 and the purification to near homogeneity of the recombinant protein by anion exchange chromatography. It will then go on to describe characterisation of the recombinant xylA.cd2 with respect to its specific activity, temperature optimum for enzymic activity and thermal stability.

3.2 MATERIALS AND METHODS

All methods used in this chapter not outlined below can be found in chapter 2.

3.2.1 Materials

Neocallimastix patriciarum xylanase A full-length gene was kindly supplied as a pBluescript clone by Dr Geoff Hazlewood. All other materials used in this section are as outlined in chapter 2, sections 2.1.1, 2.2.1 and 2.3.1.

3.2.2 PCR amplification of the xylA.cd2 fragment and ligation into pUC18

As described in section 2.1.3, the second catalytic domain was amplified from the full-length gene by PCR using primers 1 and 2, designed to the flanking regions either side of the catalytic domain. Full details of all primers can be found in the Appendix. Both forward and reverse primers contained a BamHI restriction site, and the purified PCR product was digested with BamHI, as described in section 2.1.5, before being ligated into BamHI commercially digested pUC18 plasmid vector using the Rapid DNA Ligation Kit (section 2.1.6). This construct is known as pUC18.cd2.

3.2.3 Expression of recombinant xylA.cd2 in *E. coli*

pUC18.cd2 was transformed into *E. coli* strain JM109 using the heat shock method (section 2.1.7). The Congo Red overlay assay was employed to identify which clones had the xylA.cd2 insert ligated in the correct orientation in the pUC18 plasmid. Once this was determined, and the xylA.cd2 insert had been sequenced to ensure that no errors had been introduced during the PCR reaction, the xylA.cd2 protein was expressed from a 250ml culture of LB supplemented with 100µg/ml ampicillin as described in section 2.2.5.

3.2.4 Purification of recombinant xylA.cd2 from *E. coli*

E. coli cells harbouring the pUC18.cd2 plasmid were harvested after approximately 16 hours of growth. The cells were disrupted by sonication and a cell extract was prepared as described in section 2.2.5.1. The cell extract was applied to a HiTrap Q High

Performance 5ml anion exchange column equilibrated with 20mM Tris-HCl, pH8.0, and the xylA.cd2 protein was collected in the unbound fraction.

3.2.5 Determination of specific activity

The DNS assay was performed as outlined in section 2.3.2 to determine the specific activity of the purified xylA.cd2 protein. In order to determine a suitable dilution of the enzyme to ensure that the initial rate of reaction was being measured, standard assays were performed using varying dilutions of xylA.cd2 from 1/250 to 1/10,000. Protein concentration was determined as described in section 2.2.2.

3.2.6 Determination of temperature optimum for activity

The temperature optimum for activity of the purified xylA.cd2 protein was determined using the DNS assay essentially as described in section 2.3.2, the only difference in method being that the enzyme sample and substrate were incubated together for 15 minutes at various temperatures, rather than just at 37°C. A 1/5000 dilution of the enzyme was used in these reactions, and the temperatures studied were 18, 30, 40, 45, 50, 55, 58, 60, 62, 65, 70 and 80°C.

3.2.7 Thermal inactivation of xylA.cd2

The stability of purified xylA.cd2 protein at elevated temperatures was determined by thermal inactivation studies. The appropriate amount of PC buffer with 1mg/ml BSA was pre-heated to 58, 60, 62 or 64°C and using an initial 1/50 dilution of xylA.cd2, which was stored on ice, an appropriate volume was added to the heated buffer to give a final dilution of 1/5000. At various times 100µl aliquots were taken out of the heated enzyme solution and quickly placed into a pre-chilled tube in an ice/water bath. To determine the activity of the enzyme prior to heating, a separate 1/5000 dilution was made using the initial 1/50 dilution, and this was stored on ice until all the other samples had been collected. Xylanase activity was then determined in all the samples using the DNS assay, as described in section 2.3.2.

3.3 RESULTS

3.3.1 Construction of the pUC18.cd2 clone

Primers were designed to the flanking regions of the second catalytic domain, both of which contained the necessary coding sequence to ensure the introduction of a BamHI restriction site. In addition the reverse primer was also designed to incorporate a stop codon. The sequence of primers 1 and 2 can be found in the Appendix. Figure 3.1 shows the full xylanase A gene sequence.

```

1  TTTTATTATA TCAATCTCTA ATTTATTTTT TTAGGAAAAA AATAAAAAAA
51  TAAATATAAT AAATATTAGA GAGTAATATT TAAAAACAAA GAAATTTAAA
101 AACGTTTATT TAGTTATTTT TTTTACTGGT TAAAAAAAAA ATAAAAAACA
151 AAATTAATAA AGATATTTTT GAAAAATATT GAATTAGAAA AAAAAATGAGA
201 ACTATTAAAT TCTTTTTCGC AGTAGCTATT GCAACTGTTG CTAAGGCCCA
251 ATGGGGTGGA GGTGGTGCCT CTGCTGGTCA AAGATTAACC GTCGGTAATG
301 GTCAAACCCA ACATAAGGGT GTAGCTGATG GTTACAGTTA TGAAATCTGG
351 TTAGATAACA CCGGTGGTAG TGGTTCTATG ACTCTCGGTA GTGGTGCAAC
401 CTTCAAGGCT GAATGGAATG CATCTGTAA CCGTGGTAAC TTCCTTGCCC
451 GTCGTGGTCT TGACTTCGGT TCTCAAAAGA AGGCAACCGA TTACAGCTAC
501 ATTGGATTGG ATTATACTGC AACTTACAGA CAAACTGGTA GCGCAAGTGG
551 TAACTCCCGT CTCTGTGTAT ACGGTTGGTT CCAAACCGT GGAGTTCAAG
601 GTGTTCCATT GGTAGAATAC TACATCATTG AAGATTGGGT TGACTGGGTC
651 TCAGATGCAC AAGGTAGAAT GGTAACCATT GATGGAGCTC AATATAAGAT
701 TTTCCAAATG GATCACACTG GTCCAACAT CAATGGTGGT AGTGAAACCT
751 TTAAGCAATA CTTCAGTGTC CGTCAACAAA AGAGAACTTC TGGTCATATT
801 ACTGTCTCAG ATCACTTTAA GGAATGGGCC AAACAAGGTT GGGGTATTGG
851 TAACCTTTAT GAAGTTGCTT TGAACGCCGA AGGTTGGCAA AGTAGTGGTA
901 TAGCTGATGT CACCAAGTTA GATGTTTACA CAACCCAAAA AGGTTCTAAT
951 CCTGCCCCTA CCTCCACTGG TACTGTTCCA AGCAGTTCTG CTGGTGGAAG
1001 TACTGCCAAT GGTAAAAAGT TTACTGTCGG TAATGGACAA AACCAACATA

```

The diagram shows the full xylanase A gene sequence. A BamHI restriction site (GAATTC) is indicated by a bracket above the sequence at position 151. A stop codon (TGA) is indicated by a bracket above the sequence at position 1001.

```

1051  AGGGTGTCAA CGATGGTTTC AGTTATGAAA TCTGGTTAGA TAACACTGGT
1101  GGTAACGGTT CTATGACTCT CGGTAGTGGT GCAACTTTCA AGGCTGAATG
1151  GAATGCAGCT GTTAACCGTG GTAACCTCCT TGCCCGTCGT GGTCTTGACT
1201  TCGGTTCTCA AAAGAAGGCA ACCGATTACG ACTACATTGG ATTAGATTAT
1251  GCTGCTACTT ACAAACAAAC TGCCAGTGCA AGTGGTAACT CCCGTCTCTG
1301  TGTATACGGA TGGTTCCAAA ACCGTGGACT TAATGGCGTT CCTTTAGTAG
1351  AATACTACAT CATTGAAGAT TGGGTTGACT GGGTTCCAGA TGCACAAGGA
1401  AAAATGGTAA CCATTGATGG AGCTCAATAT AAGATTTTCC AAATGGATCA
1451  CACTGGTCCA ACTATCAATG GTGGTAGTGA AACCTTTAAG CAATACTTCA
1501  GTGTCCGTCA ACAAAGAGA ACTTCTGGTC ATATTACTGT CTCAGATCAC
1551  TTTAAGGAAT GGGCCAAACA AGGTTGGGGT ATTGGTAACC TTTATGAAGT
1601  GGCTTTGAAC GCCGAAGGTT GGCAAAGTAG TGGTGTGCT GATGTCACCT
1651  TATTAGATGT TTACACAAC CCAAAGGGT CTAGTCCAGC CACCTCTGCC
1701  GCTCCTCGTA CTACTACCCG TACTACTACT CGTACCAAGT CTCTTCCAAC
1751  CAATTACAAT AAGTGTTCTG CTAGAATTAC TGCTCAAGGT TACAAGTGTT
1801  GTAGCGATCC AAATTGTGTT GTTTACTACA CTGATGAGGA TGGTACCTGG
1851  GGTGTTGAAA ACAACGACTG GTGTGGTTGT GGTGTTGAAC AATGTTCTTC
1901  CAAGATCACT TCTCAAGGTT ACAAGTGTTG TAGCGATCCA AATTGCGTTG
1951  TTTTCTACAC TGATGACGAT GGTAAATGGG GTGTTGAAAA CAACGACTGG
2001  TGTGGTTGTG GTTTCTAAGC AGTAAAATAC TAATTAATAA AAAATTAAAG
2051  AATTATGAAA AATTTAAATT TAAAAATTTA AAAGAATTAT GAAAAATTTA
2101  AATTTAAAAA TTTAAAAAAA ACTAATTTAG TAAAAAATTA AAGAATTATT
2151  GAAAATTTTA AATGTAAAAA TTTAAAAAAT ACAAATTTGT AAAAAAAAT
2201  GAAAGAATTA TGAAAAATTA AAATGTAAAA GTTTAAAAAA TACAAATTTG
2251  TAAGAAAAAT AAAGAATTAT AAAAAAATA AAGAATTATG AAAAACCCTAA
2301  ATGTAAAGAA AAAAAAATAA AAAAAAATAA AAAAAAATAA

```

Figure 3.1 *N. patriciarum* xylanase A gene sequence

└─► Indicates start of xylanase A coding region. * over bold text indicates stop codon. Second catalytic domain coding region is highlighted in bold text. Large arrows indicate position of primers used to amplify second catalytic domain.

3.3.1.1 PCR amplification of xylanase A second catalytic domain

A PCR fragment of the expected size, 703bp, was produced (Figure 3.2) (675bp xylA.cd2 coding region, plus primer extensions of 10bp (5') and 18bp (3')). After digestion with BamHI, the PCR fragment was ligated into pre-digested pUC18 plasmid vector and the resulting clones were transformed into *E. coli* strain JM109 cells. Successful transformants were selected for by growth on LB-agar plates containing 100µg/ml ampicillin, and successful ligation of the xylA.cd2 insert into each plasmid was confirmed by restriction digest of plasmid prepared from single colonies. Digestion with BamHI gives two bands when run on an agarose gel: one corresponding to the insert and the other corresponding to the plasmid (Figure 3.3)

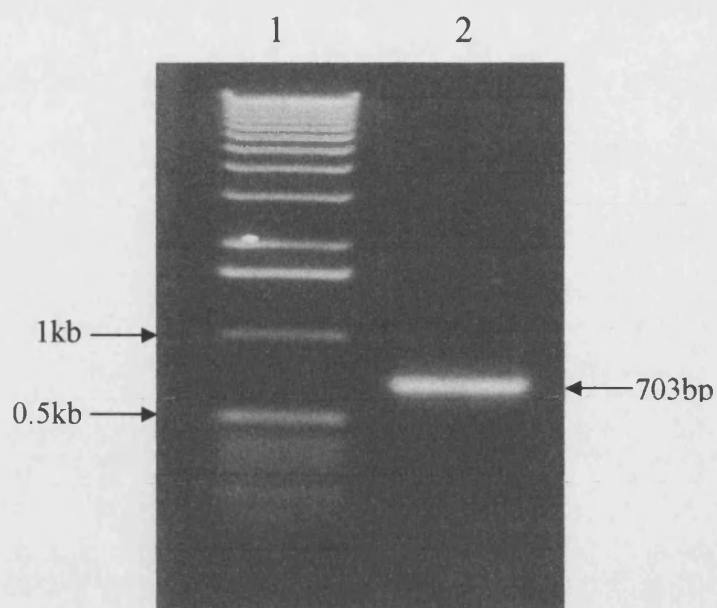


Figure 3.2 Identification of xylA.cd2 PCR product by agarose gel electrophoresis

Lane 1, 1kb DNA molecular weight markers; lane 2, 703bp PCR product.

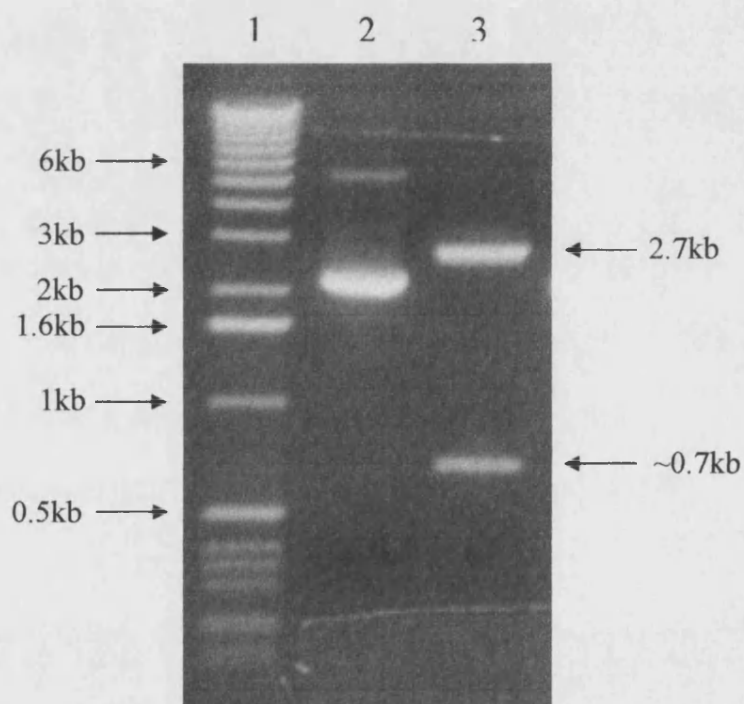


Figure 3.3 BamHI digested pUC18.cd2, to confirm the cloning of xylA.cd2 insert into pUC18 plasmid

Lane 1, 1kb DNA molecular weight markers; lane 2, undigested pUC18.cd2 (supercoiled & relaxed circle); lane 3, BamHI digested pUC18.cd2 (~700bp insert band & 2.7kb plasmid band).

3.3.1.2 Identification of clones with correctly oriented *xylA.cd2* insert

To determine that the PCR fragment had ligated into the pUC18 vector in the correct orientation, *E. coli* cells containing the plasmid clones were subjected to the Congo Red overlay assay. Those cells that contained the plasmid with insert ligated in the correct orientation showed a clearing zone around them, while the ones containing the plasmid with insert ligated in the reverse orientation showed no visible clearing zones, indicating no xylanase activity (Figure 3.4).



Figure 3.4 Congo Red assay confirming xylanase activity of pUC18.cd2 clones

These clones are all displaying xylanase activity (note the yellow halos around the individual streaks).

3.3.1.3 Sequencing of the PCR insert

Sequencing of the PCR insert was performed using the M13 universal sequencing and reverse primers. One sequencing reaction from each direction allowed the full insert sequence to be obtained. Comparison of this sequence to the published full-length gene sequence confirmed that no errors had been introduced during the PCR reaction. The xylA.cd2 sequence can be seen in Figure 3.5. As the xylA.cd2 insert is cloned into pUC18 in frame with the lacZ promoter there are a few upstream amino acid residues preceding the sequence shown in Figure 3.5. These are M I T N S S S V P G D P.

3.3.2 XylA.cd2 purification

Recombinant xylA.cd2 was expressed in *E. coli* strain JM109 cells from a pUC18.cd2 clone. A summary of the purification results can be seen in Table 3.1.

Approximately 2.3g (wet weight) of cells were harvested from a 250ml culture of JM109 cells harbouring the pUC18.cd2 plasmid after 16 hours of growth. After resuspension and lysis by sonication the cell extract contained approximately 35.4mg of protein, and demonstrated a specific xylanase activity of 2010U/mg.

The cell extract was applied to a HiTrap Q High Performance 5ml anion exchange column and the xylA.cd2 protein was washed through in the unbound fraction. Although quite dilute - the unbound fraction was eluted in approximately 18ml as compared to the 3ml of cell extract applied to the column – the unbound fraction showed very high xylanase activity. The total amount of protein in the fraction was approximately 5.7mg, and the xylanase specific activity was calculated as 10,400U/mg.

SDS-PAGE analysis (Figure 3.6) showed the xylA.cd2 within the unbound fraction to be over 90% pure (estimated visually). Zymogram analysis of the various purification stages showed a clearing zone around a band at approximately 27kDa, indicating that this is the molecular weight of the recombinant xylA.cd2 protein (Figure 3.7).

```

AAGTTTACTGTCGGTAATGGACAAAACCAACATAAGGGTGTCAACGATGGTTTCAGTTAT
1  -----+-----+-----+-----+-----+-----+ 60
TTCAAATGACAGCCATTACCTGTTTTGGTTGTATTCCCACAGTTGCTACCAAAGTCAATA

K F T V G N G Q N Q H K G V N D G F S Y

GAAATCTGGTTAGATAAACTGGTGGTAACGGTTCTATGACTCTCGGTAGTGGTGCAACT
61  -----+-----+-----+-----+-----+-----+ 120
CTTTAGACCAATCTATTGTGACCACCATTGCCAAGATACTGAGAGCCATCACCACGTTGA

E I W L D N T G G N G S M T L G S G A T

TTCAAGGCTGAATGGAATGCAGCTGTTAACCGTGGTAACTTCCTTGCCCGTCGTGGTCTT
121 -----+-----+-----+-----+-----+-----+ 180
AAGTTCCGACTTACCTTACGTCGACAATTGGCACCATTGAAGGAACGGGCAGCACCAGAA

F K A E W N A A V N R G N F L A R R G L

GACTTCGGTTCTCAAAAGAAGGCAACCGATTACGACTACATTGGATTAGATTATGCTGCT
181 -----+-----+-----+-----+-----+-----+ 240
CTGAAGCCAAGAGTTTTCTTCCGTTGGCTAATGCTGATGTAACCTAATCTAATACGACGA

D F G S Q K K A T D Y D Y I G L D Y A A

ACTTACAAACAACTGCCAGTGCAAGTGGTAACTCCCGTCTCTGTGTATACGGATGGTTC
241 -----+-----+-----+-----+-----+-----+ 300
TGAATGTTTGTGTTGACGGTCACGTTACCATTTAGGGCAGAGACACATATGCCTACCAAG

T Y K Q T A S A S G N S R L C V Y G W F

CAAAACCGTGGACTTAATGGCGTTCCTTTAGTAGAATACTACATCATTGAAGATTGGGTT
301 -----+-----+-----+-----+-----+-----+ 360
GTTTTGGCACCTGAATTACCGCAAGGAAATCATCTTATGATGTAGTAACCTCTAACCCAA

Q N R G L N G V P L V E Y Y I I E D W V

GACTGGGTTCCAGATGCACAAGGAAAAATGGTAACCATTGATGGAGCTCAATATAAGATT
361 -----+-----+-----+-----+-----+-----+ 420
CTGACCCAAGGTCTACGTGTTCTTTTTACCATTGGTAACTACCTCGAGTTATATTCTAA

D W V P D A Q G K M V T I D G A Q Y K I

TTCCAAATGGATCACACTGGTCCAACTATCAATGGTGGTAGTGAAACCTTTAAGCAATAC
421 -----+-----+-----+-----+-----+-----+ 480
AAGGTTTACCTAGTGTGACCAGGTTGATAGTTACCACCATCACTTTGGAAATTCGTTATG

F Q M D H T G P T I N G G S E T F K Q Y

TTCAGTGTCCGTCAACAAAAGAGAACTTCTGGTCATATTACTGTCTCAGATCACTTTAAG
481 -----+-----+-----+-----+-----+-----+ 540
AAGTCACAGGCAGTTGTTTTCTCTTGAAGACCAGTATAATGACAGAGTCTAGTGAAATTC

F S V R Q Q K R T S G H I T V S D H F K

```

```

GAATGGGCCAAACAAGGTTGGGGTATTGGTAACCTTTATGAAGTTGCTTTGAACGCCGAA
541 -----+-----+-----+-----+-----+-----+ 600
CTTACCCGGTTTGTTCCAACCCATAACCATTGGAAATACTTCAACGAAACTTGCGGCTT

E W A K Q G W G I G N L Y E V A L N A E

GGTTGGCAAAGTAGTGGTGGTGGCTGATGTCACCTTATTAGATGTTTACACAACCTCCAAAG
601 -----+-----+-----+-----+-----+-----+ 660
CCAACCGTTTTCATCACCACAACGACTACAGTGGAATAATCTACAAATGTGTTGAGGTTTC

G W Q S S G V A D V T L L D V Y T T P K

GGTTCTAGTCCAGCCTAG
661 -----+----- 678
CCAAGATCAGGTCGGATC

G S S P A *

```

Figure 3.5 **Sequence of xylA.cd2**

The translated amino acid sequence is shown below the gene sequence using the single letter amino acid codes.

Purification step	Total protein (mg)	Total activity (units*)	Specific activity (units*/mg)	Yield (%)	Purification factor (x fold)
Cell extract	35.4	71,000	2010	100	1
HiTrap Q anion exchange unbound fraction	5.7	59,700	10,400	84	5.17

Table 3.1 Summary of purification of xylA.cd2 from *E. coli* strain JM109

Samples after each step were analysed for xylanase activity using the DNS assay and for protein concentration using the Bio-Rad protein estimation assay. Yield is expressed relative to the total amount of enzyme activity present in the cell extract. Purification factor is expressed relative to the specific activity of the enzyme in the cell extract. *One unit of enzyme activity is defined as that which releases 1 μ mol product (expressed as xylose equivalents) per minute.

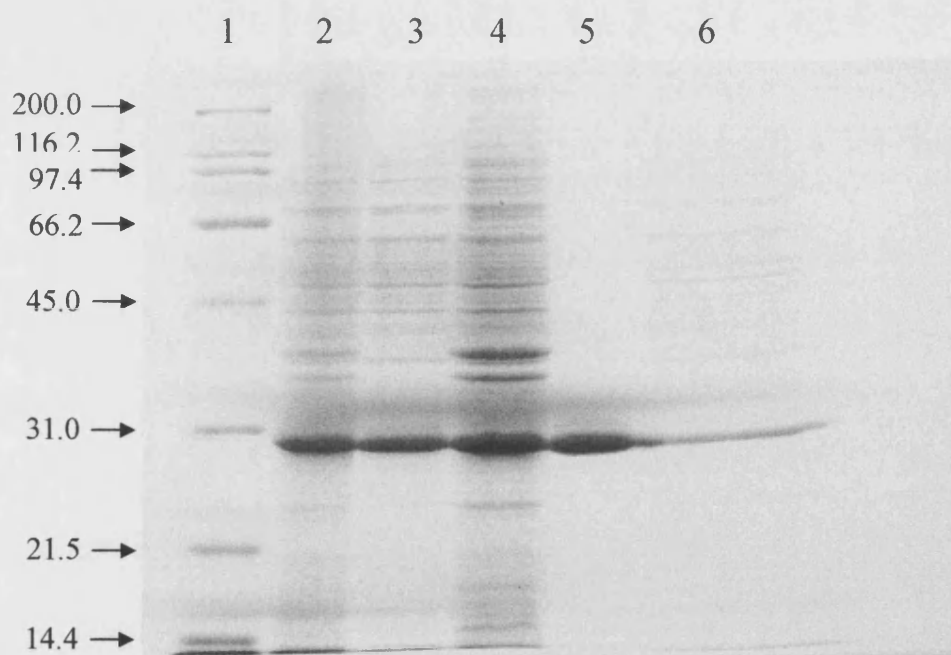


Figure 3.6 SDS-PAGE analysis of the purification stages of xylA.cd2

Lane 1, SDS-PAGE Broad range markers; lane 2, Total cells; lane 3, Cell extract; lane 4, Cell debris; lane 5, HiTrap Q anion exchange unbound fraction; lane 6, HiTrap Q anion exchange total bound protein.

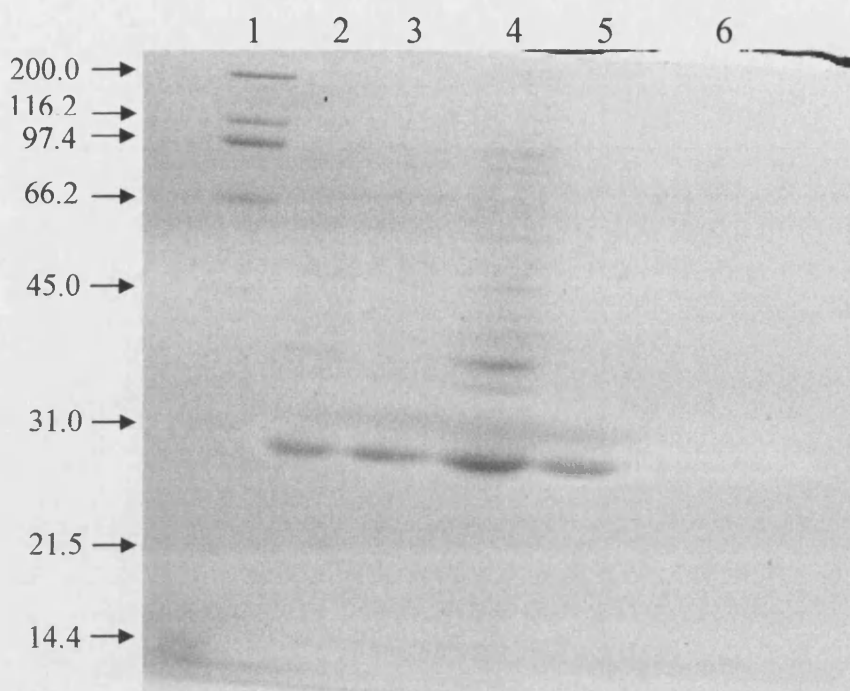


Figure 3.7 Zymogram of purification stages of xylA.cd2

Clearing zones indicate areas of xylanase activity. Lane 1, SDS-PAGE Broad range markers; lane 2, Total cells; lane 3, Cell extract; lane 4, Cell debris; lane 5, HiTrap Q anion exchange unbound fraction; lane 6, HiTrap Q anion exchange total bound protein.

3.3.3 XylA.cd2 characterisation

3.3.3.1 Determination of appropriate enzyme dilution and specific activity

When performing characterisation studies on an enzyme it is important to ensure that the initial rate of reaction is being measured. If over the time course of an assay the reaction reaches near-completion then a false representation of the enzymes characteristics will be obtained. In order to determine the correct dilution of xylA.cd2 to use in the studies of its activity with temperature and thermal stability, and also to determine its specific activity, a series of standard assays were carried out using varying volumes of a 1/250 dilution of xylA.cd2. It was determined that a 1/5000 dilution of the purified xylA.cd2 would be an appropriate dilution to use in order to ensure initial rates were being measured. Figure 3.8 graphically represents these results. The purified xylA.cd2 enzyme demonstrated a specific activity of 10,400 units per mg of protein.

3.3.3.2 Temperature optimum for activity

XylA.cd2 was assayed at various temperatures from 18°C to 80°C, and these results are shown in Figure 3.9. Blank reactions (with 100µl PC buffer in place of the 100µl enzyme dilution) were carried out at each temperature to account for any degradation of the soluble xylan substrate at the higher temperatures, although no significant increase in absorbance of the blank samples was observed. The maximum activity of the purified xylA.cd2 was observed at 55°C.

3.3.3.3 Thermal Inactivation

Temperatures just above the observed optimum were chosen to study the thermal stability of purified xylA.cd2. These results are represented graphically in Figure 3.10 and show that purified xylA.cd2 has a half-life of approximately 15 minutes at 58°C, reducing to a half-life of less than 1 minute at 64°C. An Arrhenius plot can be constructed, according to the Arrhenius equation (Equation 3.1), by plotting $\ln(k)$ against $1/T$ for each temperature studied. The slope of this straight-line plot gives $-E_a/R$, which can be used to determine the activation energy for the inactivation process of purified xylA.cd2 (Figure 3.11).

$$k = Ae^{-E_a/RT} \quad \text{Equation 3.1}$$

Where

- A is the pre-exponential factor
- R is the universal gas constant ($8.314 \text{ J} \cdot \text{K}^{-1} \text{ mol}^{-1}$)
- T is the absolute temperature (K)
- E_a is the activation energy for the reaction (kJ/mol)

From the Arrhenius plot E_a is calculated as 478kJ/mol.

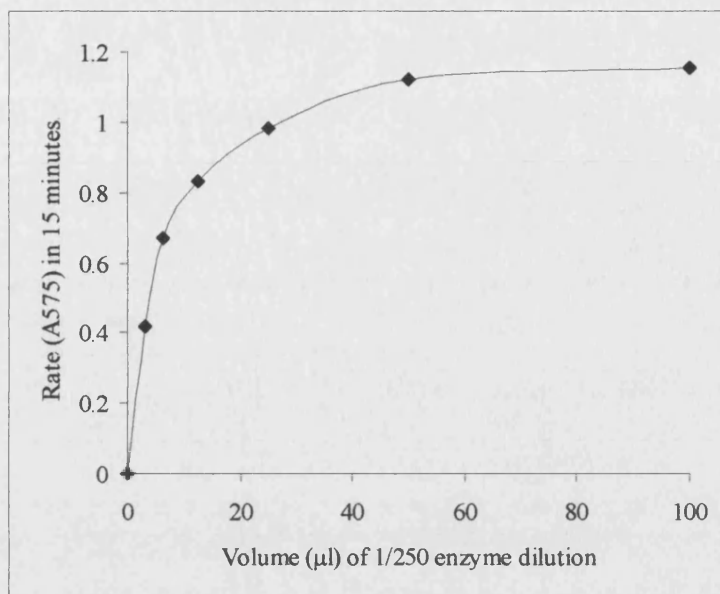


Figure 3.8 XylA.cd2 activity against volume of a 1/250 enzyme dilution

Each point represents the mean of duplicate assays

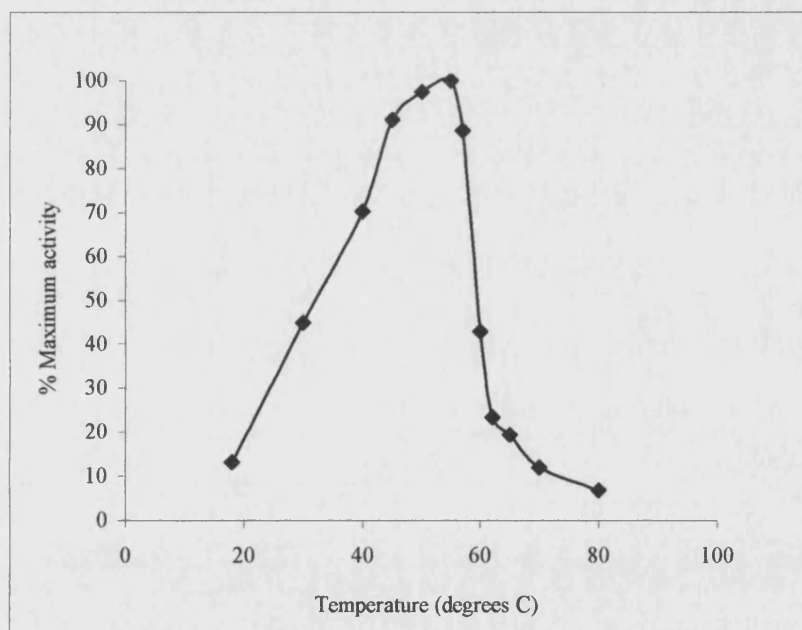


Figure 3.9 Temperature activity curve for xylA.cd2

Activities are expressed as a percentage of activity at 55°C, as this was the temperature at which the maximum activity was observed. Each point represents the mean of 4 assays.

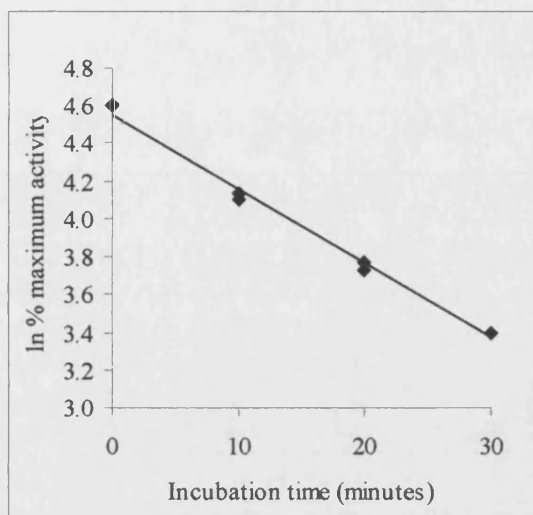


Figure 3.10a

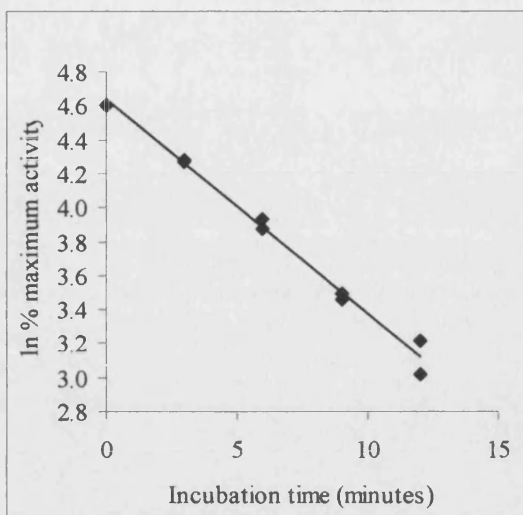


Figure 3.10b

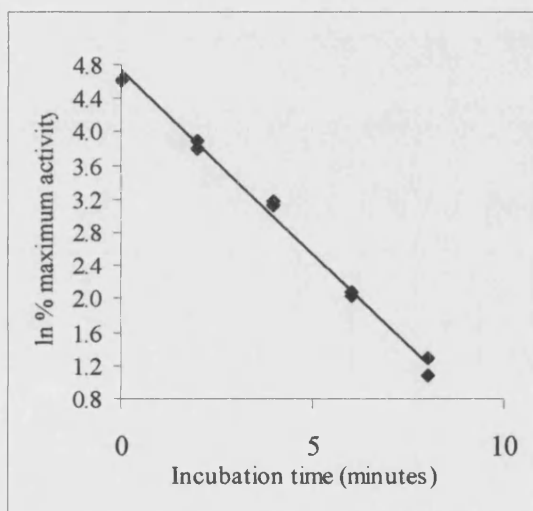


Figure 3.10c

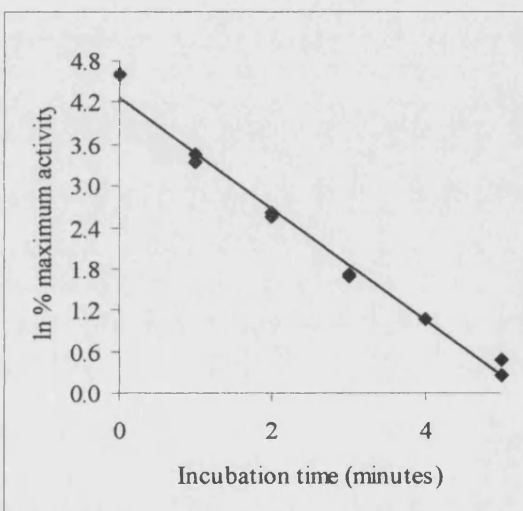


Figure 3.10d

Figure 3.10 Thermal inactivation of xylA.cd2

Data are shown as ln (% activity) against incubation time (% activity being calculated as a percent of maximum activity, seen at time 0). Lines of best fit, calculated by linear regression, are shown.

Figure 3.10a Thermal inactivation of xylA.cd2 at 58°C

Figure 3.10b Thermal inactivation of xylA.cd2 at 60°C

Figure 3.10c Thermal inactivation of xylA.cd2 at 62°C

Figure 3.10d Thermal inactivation of xylA.cd2 at 64°C

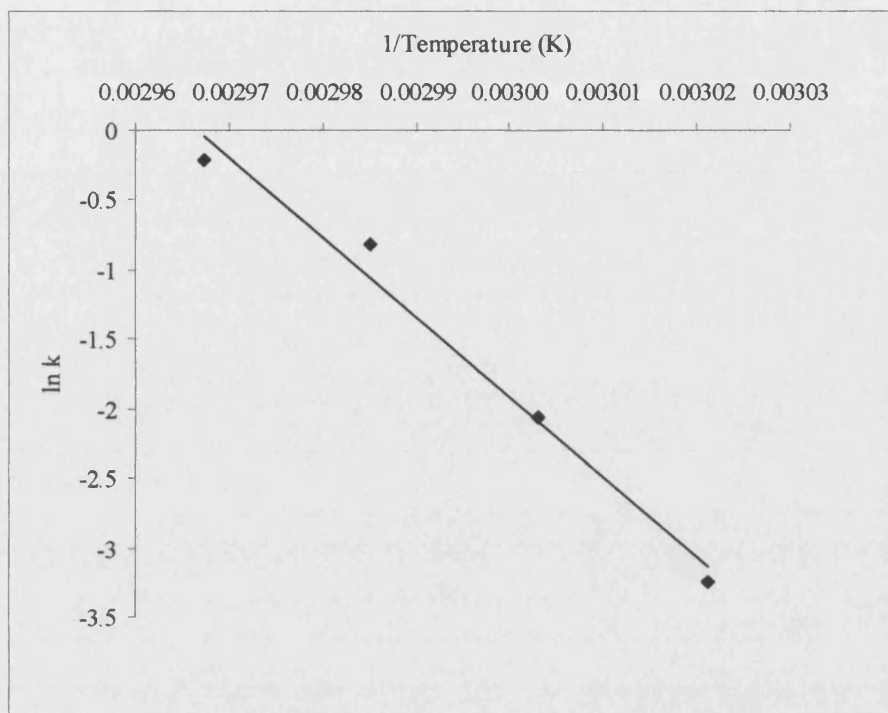


Figure 3.11 Arrhenius plot for xylA.cd2 thermal inactivation data

Data from Figure 3.10 are represented as an Arrhenius plot, according to the Arrhenius equation (Equation 3.1). Linear regression has been used to calculate a line of best fit through the data.

3.4 DISCUSSION

3.4.1 Cloning and expression

The second catalytic domain of *Neocallimastix patriciarum* xylanase A has been cloned into the plasmid vector pUC18 and expressed in *E. coli* strain JM109. pUC18 is a high copy number plasmid that is recommended for use in error-prone PCR experiments (described in Chapter 6). As the xylA.cd2 does not have its own translation initiation sequence it has been cloned in frame with the lacZ promoter of pUC18 to enable translation to occur via this promoter and start codon. As a result the expressed xylA.cd2 will have 12 additional residues, coded for by the first few bases of the lacZ gene, at its N-terminus. These preceding amino acids could influence both the activity and stability properties of the xylA.cd2 enzyme, although definite conclusions about their precise effects cannot be drawn without a comparison to an expressed xylA.cd2 lacking these additional residues.

3.4.2 Recombinant xylA.cd2 purification

The purification of recombinant xylA.cd2 from cell extract was achieved in a one step procedure by anion exchange chromatography. An 84% yield, constituting 19% of the total protein, was obtained. The expressed protein was estimated by SDS-PAGE analysis to be over 90% pure. This level of purity is more than sufficient for the characterisation studies carried out.

Interestingly, the anion exchange chromatography worked as a ‘negative’ purification step; that is, it enabled purification of xylA.cd2 from the remaining cell extract proteins by eliminating it from the column unbound, while the majority of the remaining proteins stayed bound to the anion exchange matrix. This would suggest that xylA.cd2 should actually bind to a cation exchange matrix, with the remaining proteins eluting unbound. If this were the case then it may serve to increase the purity of the protein by switching to a cation exchanger, as controlling the elution of xylA.cd2 from the matrix may also lead to further separation from the few contaminating proteins, and as such increase its purity.

The specific activity of purified recombinant xylA.cd2 is almost twice that of purified full-length xylanase A (10,400U/mg compared with 5980U/mg (Gilbert *et al.*, 1992)). This factor is of obvious advantage when the industrial application of xylA.cd2 is considered. An enzyme having twice the specific activity of another would convert its substrate to product at twice the rate. Alternatively, only half the amount of xylA.cd2 would be necessary to complete the equivalent conversion of substrate to product. Either of these points could be considered economically advantageous.

3.4.3 Temperature activity and thermal stability

Performing DNS assays on purified xylA.cd2 over a range of temperatures has shown that the optimum temperature for activity, i.e. the temperature at which maximum activity is seen, is 55°C. Beyond this temperature inactivation is rapid, with over 50% of activity lost with an increase of just 5°C over the 15 minute time-course of the assay. Assaying xylA.cd2 for activity at varying temperatures measures both reversible and irreversible denaturation, and this rapid loss of activity may be due to a combination of both these effects.

The thermal inactivation studies measure the effects of irreversible denaturation only, and they confirm the observation from the temperature activity profile that rapid inactivation is seen above the temperature optimum. At 58°C the half-life of xylA.cd2 is approximately 15 minutes, but this reduces rapidly with only relatively small increases in temperature. At 60°C the half-life is reduced by over half to 6 minutes, and by 62°C it is reduced again by over half to approximately 2 minutes. At 64°C the inactivation is so rapid that it becomes difficult to measure accurately using this method of study, but it can be estimated as less than one minute. XylA.cd2 is not expected to display any exceptional thermostability, as its biological source is a mesophilic organism. The aim of this project is to increase the thermostability of xylA.cd2 whilst retaining its activity at lower temperatures. Successful attempts to increase the thermostability of proteins have often achieved an increase in stability at the cost of a decrease in activity at lower temperatures, i.e. the temperature activity profile of the protein has been shifted to the right. In order to fulfil the aims of this project it will be necessary to broaden the peak of the temperature activity profile (or even increase the peak to higher temperatures) and

increase the half-life of xylA.cd2 at higher temperatures, but retain the activity at sub-optimal temperatures.

Chapter 4

STRUCTURAL STUDIES OF *NEOCALLIMASTIX PATRICIARUM* XYLANASE A SECOND CATALYTIC DOMAIN

4.1 INTRODUCTION

Site-directed mutagenesis is a powerful tool for exploring the role of specific amino acid residues, or the interaction of multiple residues, within a protein. Three-dimensional crystal structures greatly enhance the chances of accurately predicting the effect a change in residue would have on the overall protein structure, and as such are important tools in the design of site-directed mutagenesis experiments. In cases where the crystal structure of a protein is not available it is possible to design a model of the protein of interest using known structures of homologous proteins. This model can then be used in the same way to design site-specific mutations.

The crystal structure of *Neocallimastix patriciarum* xylanase A is not known. For the purpose of this project a model had been designed using the crystal structures of closely homologous family 11 xylanases present in the Protein Data Bank. Sequence alignment of xylanases similar to the second catalytic domain of *N. patriciarum* xylanase A shows that xylanase II (PDB code 1ENX) from *Trichoderma reesei* is most closely matched, and this was used as the primary template for constructing the model. Some additions and deletions of residues in *N. patriciarum* xylA.cd2 were found to correspond more closely to xylanase 1 (PDB code 1UKR) from *Aspergillus niger*, so this was used as a secondary template.

4.2 METHODS

4.2.1 Sequence manipulation

Manipulation of related xylanase sequences in order to produce an alignment and consensus sequence was performed using the Wisconsin Package, version 8.0 (Genetics Computer Group, Madison WI, USA). The *N. patriciarum* xylA.cd2 sequence was manually manipulated to ensure that conserved residues (e.g. catalytic residues, large aromatic residues) aligned with those present in the other sequences. Care was also taken to ensure that the location of any conserved residues in the thermostable xylanases used in the alignment, for which an involvement in maintaining the stability of the enzyme has been suggested, were mapped onto the xylA.cd2 sequence.

4.2.2 Molecular modelling

The three-dimensional structure of the template was visualized using the *O* graphics program. Beginning at the N-terminus of the template each amino acid residue was mutated, replacing the template residue with that of the *N. patriciarum* sequence. Residues present in the template but absent from xylA.cd2 were deleted, and residues present in xylA.cd2 but absent from the template were added and their structures modelled using the *O* program database: *O* has a database of well-refined structures and this can be searched to find the 20 loops that best fit the conformation of the inserted stretch of residues. Each conformation is given a value reflecting its likelihood, and the final choice of conformation is left to the user.

4.2.3 Preliminary analysis of side-chain positions

As the *O* graphics program does not account for the various possible amino acid side-chain conformations when the initial mutations from template to model are made, it is necessary to examine the model and alter any unfavourable side-chain conformations. This was done manually using *O*'s database of commonly found conformations for each amino acid side-chain.

4.2.4 Detailed analysis of the structural model

The *PROCHECK* program suite (Laskowski *et al.*, 1993) was used to obtain a more detailed analysis of the structural model. The conformation of the main chain atoms of a protein is determined by the ϕ (phi) and ψ (psi) angles of each amino acid. Rotation around the C_{α} -N bond and C_{α} -C bond gives the ϕ and ψ angles of rotation, respectively. *PROCHECK* compares the model to well-refined structures of a similar resolution and checks for 'unusual' backbone atom conformations. In order to ensure that unusual conformations are in fact unusual, and not a characteristic of the protein, the template structure is also submitted as a check. *PROCHECK* displays the pairs of ϕ and ψ angles for each amino acid in a Ramachandran plot, making unfavourable main chain conformations easy to identify.

The model was also submitted to the *Verify 3D* website (Luthy *et al.*, 1992). This program analyses individual residues, giving each one a score based on a comparison of its actual environment as opposed to its ideal environment. For example, a hydrophobic residue on the external surface of the protein would rate a very low score. Very low or negative scores generally indicate serious errors in the structural model

4.3 RESULTS

4.3.1 Sequence homology

The sequence data and crystal structure coordinates of template candidates were obtained from the Protein Data Base. Eight homologues of the *N. patriciarum* xylA.cd2 were aligned manually alongside the xylA.cd2 sequence and the most similar sequence was found to be that of xylanase II from *Trichoderma reesei* (Figure 4.1 shows alignment of *N. patriciarum* xylA.cd2 sequence with template sequences and thermostable sequences only). *N. patriciarum* xylA.cd2 was found to have two large insertions not found in any of the other eight xylanases (residues 89-95 and 130-135 as numbered in Figure 4.1). These insertions corresponded to loop regions in the template structure and were modelled as extensions of these existing loops, as large insertions positioned in a secondary structural element are predicted to severely disrupt the function of the enzyme. The shape and orientation of the inserted loops were predicted from conformations suggested by the *O* graphics program. Care was taken to ensure that the loops did not clash with any pre-existing structure.

4.3.2 Model analysis

The first Ramachandran plot produced (not shown) showed 80.7% of residues in most favoured regions, and a further 14.2% in allowed regions. This left seven residues in generously allowed regions and two in disallowed regions. These latter two regions are unsatisfactory and as such the ϕ and ψ bond angles of these residues were progressively altered until the residues moved into acceptable regions of the plot. Figure 4.2 shows the final Ramachandran plot with all residues in acceptable regions, 82.9% of which are in the most favoured region. Figure 4.3 shows the final model of *N. patriciarum* xylA.cd2.

	1				50
xylAKFT	VGNGQNQHKG	VNDGFSYEI
lukrMKVTAA	FAGLLVTAF	APVPEPVLVS	RSAGINYVQN
lenx	MVSFTSLIAA	SPPSRASCRP	AAEVESVAVE	KRQTIQPGTG	YNNGYFYSYW
lpvxGTTPNSEG	WHDGYYYSWW
lyna	.MVGFTPVAL	AALAATGALA	FPAGNATELE	KRQTTPNSEG	WHDGYYYSWW
	51				100
xylA	LDNTGGNGSM	TLGSGATFKA	EWNAAVNRGN	FLARRGLDFG	SQKKATDYDY
lukr	YN.GNLGDF	YDESAGTFSM	YWEDGVS.SD	FVVGLGW...TTGSS
lenx	ND.GHGGVTY	TNGPGGQFSV	NWSNS...GN	FVGGKGWQ..PGTKN
lpvx	SD.GGGDSTY	TNNSGGTYEI	TWNG...GN	LVGGKGWN..PGLNA
lyna	SD.GGAQATY	TNLEGGTYEI	SWG DG...GN	LVGGKGWN..PGLNA
	101				150
xylA	IGLDYAATK	QTASASGNSR	LCVYGWFQNR	GLNGVPLVEY	YIIEDWVDWV
lukr	KAITYSAEYS	A...SGSSSY	LAVYGWVNY.PQAEY	YIVEDYGDYN
lenx	KVINP.SGSY	N...PNGNSY	LSVYGWSRN.PLIEY	YIVENFGTYN
lpvx	RAIHF.TGVY	Q...PNGTSY	LSVYGWTRN.PLVEY	YIVENFGSSN
lyna	RAIHF.EGVY	Q...PNGNSY	LAVYGWTRN.PLVEY	YIVENFGTYD
	151				200
xylA	PDAQGKM...	VTIDGAQYKI	FQMDHT.GT	INGGSETFKQ	YFSVRQQKRT
lukr	PCSSATSLGT	VYSDGSTYQV	CTDTRTNEPS	ITGTS.TFTQ	YFSVRESTR
lenx	PSTGATKLGE	VTSDGSVYDI	YRTQRVNQPS	IIGTA.TFYQ	YWSVRRNHRS
lpvx	PSSGSTDLGT	VSDGSTYTTL	GQSTRYNAPS	IDGTQ.TFNQ	YWSVRQDKRS
lyna	PSSGATDLGT	VEDGSIYRL	GKTTRVNAPS	IDGTQ.TFDQ	YWSVRQDKRT
	201				250
xylA	SGH...ITVS	DHFKEWAKQG	WGIGNLYE.V	ALNAEGWQSS	GVADVTLILDV
lukr	SG...TVTVA	NHFNFWAQHG	FGN.SDFNYQ	MAVEAWSGA	GSASVITSS.
lenx	SG...SVNTA	NHFNFAWQOG	LTL.GTMDYQ	IVAVEGYFSS	GSASITVS..
lpvx	SG...TVQTG	CHFDAWASAG	LNVTGDHYYQ	IVATEGYFSS	GYARITVADV
lyna	SG...TVQTG	CHFDAWARAG	LNVNGDHYYQ	IVATEGYFSS	GYARITVADV
	251				300
xylA	YTTPKGSSPA
lukr
lenx
lpvx	G.....
lyna	G.....

Figure 4.1 Sequence alignment of *N. patriciarum* xylA.cd2 with template and thermostable xylanases only

xylA, xylanase A from *Neocallimastix patriciarum*; lukr, xylanase 1 from *Aspergillus niger*; lenx, xylanase II from *Trichoderma reesei*; lpvx, xylanase from *Paecilomyces varioti* Banier; lyna, xylanase from *Thermomyces lanuginosus*. Residues in yellow represent the catalytic residues; red represents the cysteines involved in disulphide bond formation in the two thermostable enzymes (with the corresponding xylA.cd2 residues highlighted also); green represents the aromatic residue (possible target for increasing thermostability); blue represents the two residues involved in defining the active site cleft entrance size (possible targets for increasing substrate specificity).

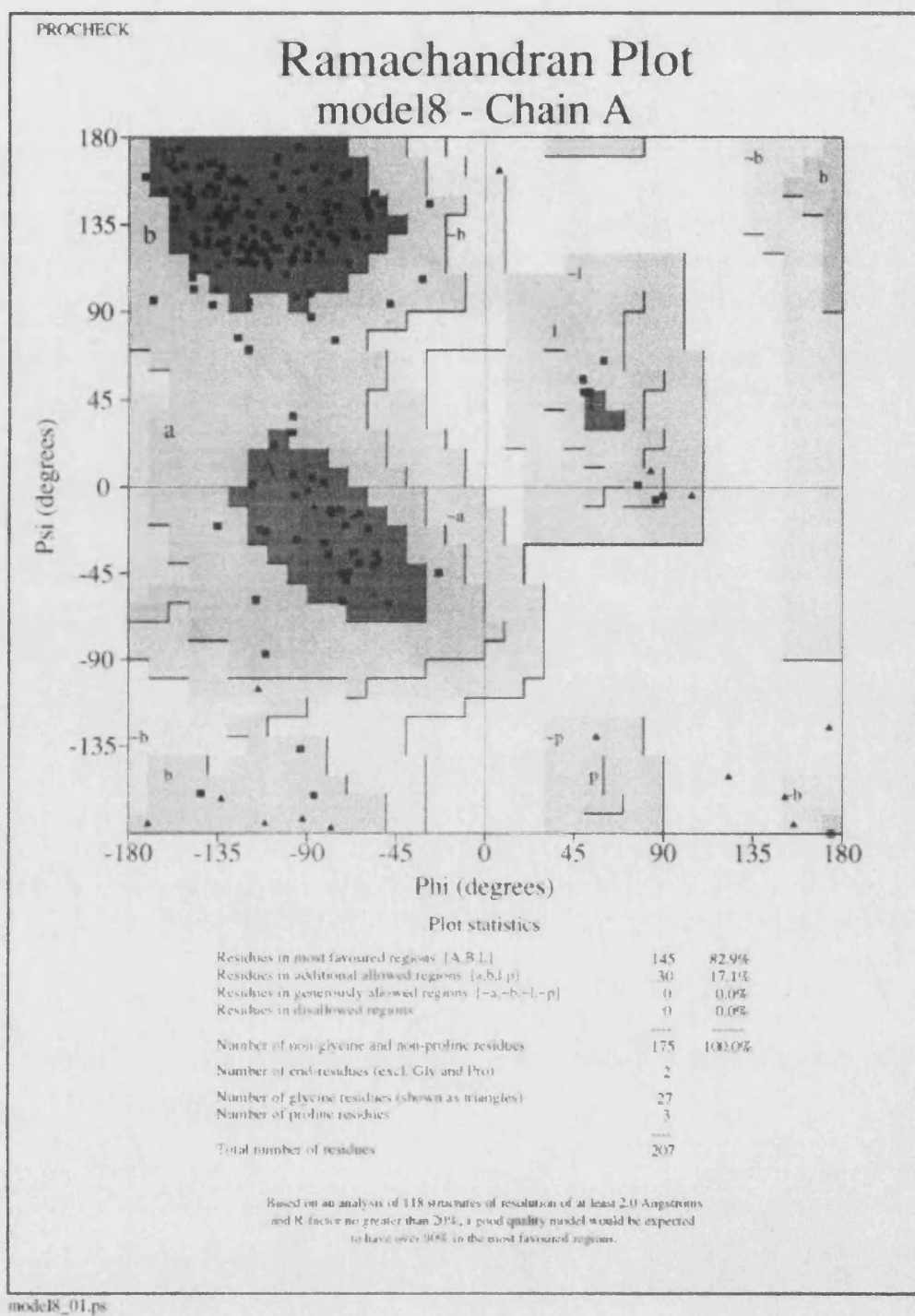


Figure 4.2 Final Ramachandran plot for xylA.cd2 model

Plot created using the PROCHECK program. All residues are positioned in allowed regions of the plot.

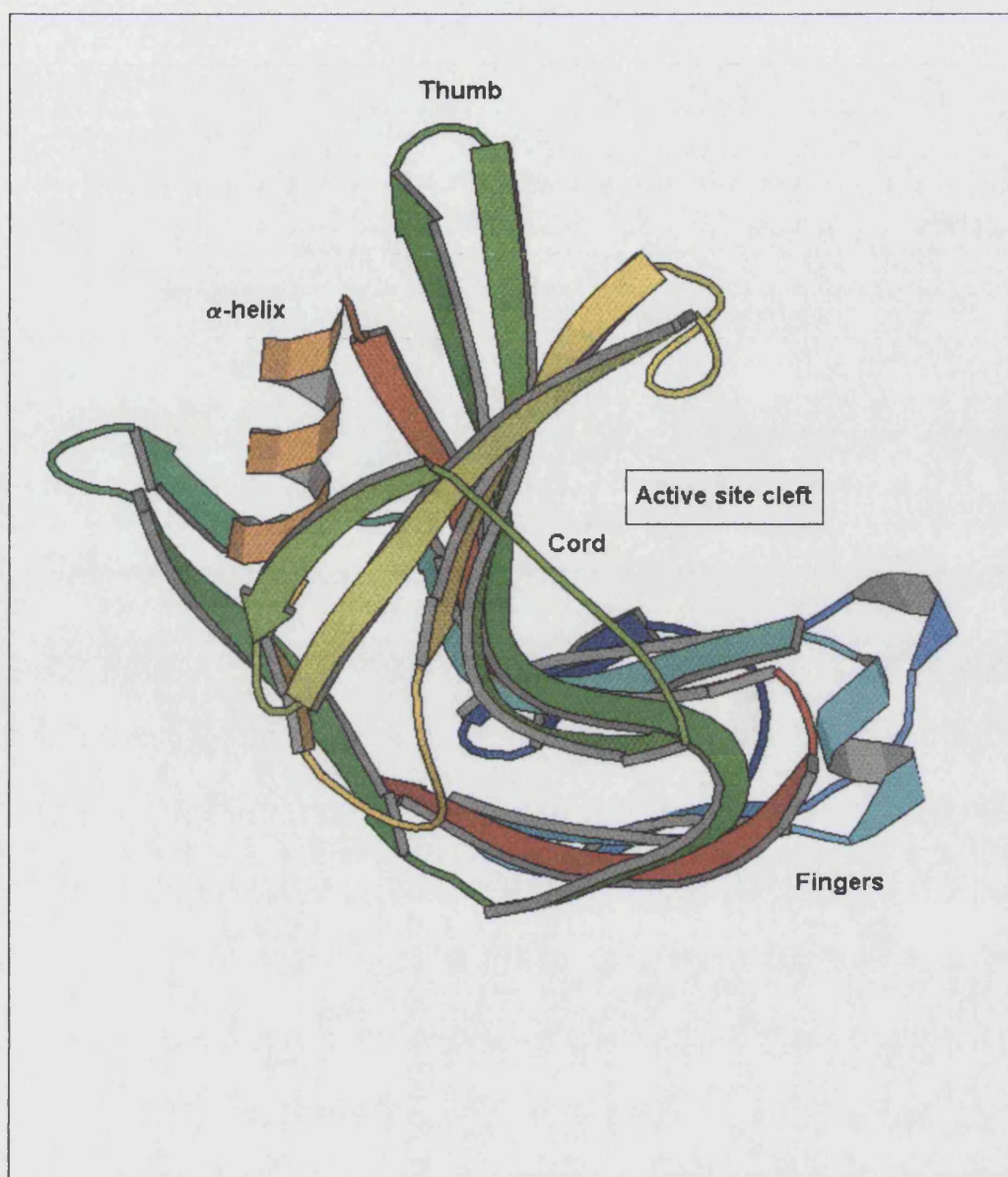


Figure 4.3 Final model of *Neocallimastix patriciarum* xylanase A second catalytic domain

Blue highlights the N-terminus, red highlights the C-terminus.

4.4 FEATURES OF MODEL

Producing models of a protein structure allows visualisation of what the protein may look like. It cannot, however, be expected to produce an exact image of the actual protein. Although the actual crystal structure of another homologous enzyme is used as a template, it can only be used as a guide to suggest what structure the unknown protein may adopt. Sequence variations between the two proteins, including insertions and deletions, will obviously affect the way in which the modelled protein will fold. By using the crystal structure of an enzyme as homologous as possible as a template, the chances of predicting a reasonably accurate model are increased.

4.4.1 Conserved sequences and their functional properties

4.4.1.1 *Structural features*

The three-dimensional structure of family 11 xylanase catalytic domains is unique to family 11 xylanases, with family 10 xylanases showing a completely different fold in their structure. The family 11 catalytic domain is a single domain composed mainly of two curved β -sheets. Its appearance has been likened to a right hand, with four 'fingers' and an opposing 'thumb' held in a grasping position around a cylindrical active site cleft. A long cord joins the thumb to one of the fingers. The structure of a protein is determined by its amino acid residues, and the interaction of these residues with each other. Proline and glycine residues are particularly important in determining the general structure of a protein as these can allow the amino acid chain to 'bend' into otherwise difficult conformations according to their own conformation. Glycines at positions 59, 135 and 206, along with Pro 148, have all been identified as important residues for allowing the backbone chain to twist and form hairpin bends in other xylanase structures, and these are conserved in this model.

4.4.1.2 *Binding activity*

During catalysis the xylanase holds the polysaccharide xylan chain in position in the active site cleft, similar to a hand grasping a bar or rope. Through sequence homology with the template enzyme and other family 11 xylanases it can be proposed that the

model residues Trp 24, Tyr 97, Tyr 114, His 145 and Trp 202 all interact with the xylan substrate by either forming hydrogen bonds or by packing against the sugar rings of the substrate. The hydrogen bonding causes conformational changes within the protein structure, for example Pro 114 converts from *cis* to *trans*, which enables the ‘fingers’ of the enzyme to curl around the polysaccharide chain.

4.4.1.3 Catalytic activity

Family 11 xylanases have two conserved catalytic residues, both of which are glutamic acids. They are situated on opposite sides of the active site cleft and are involved in a catalytic mechanism thought to be similar to that of lysozyme. One glutamate acts as an acid/base catalyst while the other acts as a nucleophile to stabilise the reaction intermediate. The sequence alignment has shown that these two glutamic acids are located at positions 112 and 200 in the *N. patriciarum* xylA.cd2 (highlighted in yellow in Figure 4.1). Glu 200 is the acid/base catalyst, and conformation of it and its environment is thought to be determined by Asn 53, Leu 55 and Tyr 97. Glu 112 is the nucleophile, and its surrounding residues (Tyr 114, Glu 159 and Tyr 193) are thought to form a hydrogen bond network that is capable of fine-tuning the properties of this residue.

4.4.2 Non-conserved sequences

The major difference between *N. patriciarum* xylA.cd2 and other family 11 xylanases of similar sequence (and presumably structure) is the insertion of four sections of amino acid residues. The major insertions were modelled into the structure as loops, as insertion into a β -sheet or α -helix was predicted to cause major disruptions within the structure and as a result would be likely to disrupt the activity of the enzyme. Their positions and conformations are however an estimation, and can only be accurately determined by actual structure determination. It could be predicted that these residues may in some way interact with the first catalytic domain of the *N. patriciarum* xylanase A, and are missing from other family 11 xylanases as these are single catalytic domain enzymes. Again this can only be verified by obtaining the actual crystal structure of the full-length xylanase A protein.

4.5 IMPROVEMENT OF THERMOSTABILITY

To date there are crystal structures available for four family 11 xylanases isolated from thermophilic organisms: one from *Paecilomyces varioti* Bainier (Kumar *et al.*, 2000a), and one from *Thermomyces lanuginosus* (formerly *Hemicola lanuginosa*) (Gruber *et al.*, 1998), both of which are from thermophilic fungi, one from *Dictyoglomus thermophilum*, which is a thermophilic bacterium (McCarthy *et al.*, 2000), and one from *Bacillus* strain D3 (Harris *et al.*, 1997). All these enzymes have structural variations that are not seen in the structures of mesophilic family 11 xylanases, and which are therefore thought to confer thermostability. A comparison of the *N. patriciarum* xylA.cd2 sequence data and the structural data from these thermophilic enzymes has allowed suggestions to be made for improvements to the enzyme that may lead to an increase in its thermostability.

4.5.1 Disulphide bonds

Both the *P. varioti* (PDB code 1PVX) and *T. lanuginosus* (PDB code 1YNA) xylanases have a disulphide bond between residues Cys 110 and Cys 154 that connects the C-terminus of a β -strand (B9) with the N-terminus of an α -helix (residues highlighted in red in Figure 4.1). This bond is situated in the 'hinge' region of the enzyme, i.e. the point at which a conformational change occurs on binding of the polysaccharide substrate into the active site cleft. It is thought that the presence of a disulphide bond makes this hinge region more compact and thus more stable in the thermophilic enzymes.

Attempts have already been made to enhance the thermostability of a mesophilic xylanase by the introduction of a disulphide bond equivalent to the one seen in the thermostable enzymes. Wakarchuk *et al.* (1994) have introduced a disulphide bond into a *Bacillus circulans* xylanase and have shown that on its own it does confer an increase in stability. This suggests that a similar increase in stability may be achieved by introducing the equivalent disulphide bond into *N. patriciarum* xylA.cd2. Sequence alignment shows that the residues equivalent to Cys 110 and Cys 154 in xylA.cd2 are Ile 133 and Asp 177. Mutation of these residues by site-directed mutagenesis should result

in the introduction of a disulphide bond on expression of the protein, which would hopefully lead to an increase in its thermostability. Figure 4.4 shows the xylA.cd2 model structure, and indicates the location of the residues that could be mutated to introduce a disulphide bond.

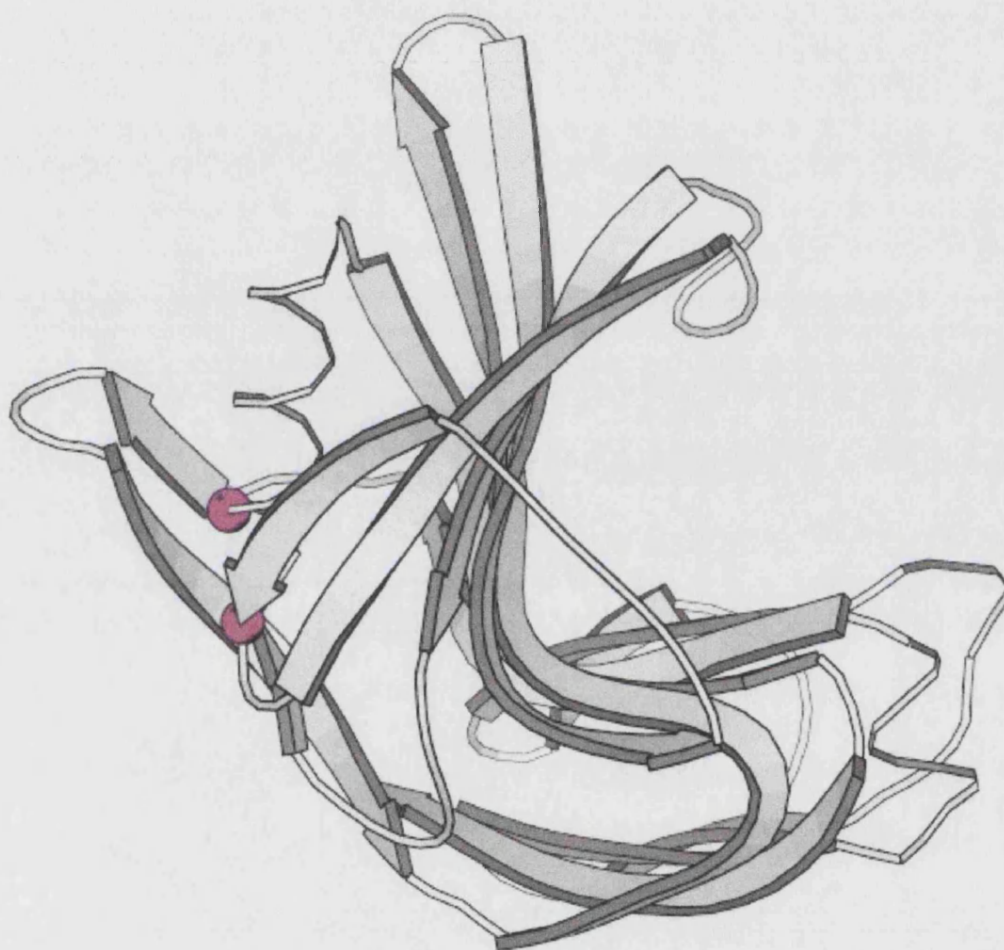


Figure 4.4 Model structure of *N. patriciarum* xylA.cd2

Pink spheres indicate location of 2 residues that could be mutated to cysteine residues in attempts to introduce a disulphide bond.

4.5.2 Ionic interactions

Ionic interactions can occur between oppositely charged pairs of residues, and are frequently cited as having positive effects on protein stability at elevated temperatures (Yip *et al.*, 1995; Russell *et al.*, 1997; Vetriani *et al.*, 1998). This is confirmed in the case of 1PVX and 1YNA, the two thermostable xylanases discussed above. Both studies on these enzymes have calculated the number of ionic interactions between charged residues in the xylanase, and have compared them to the number of ionic interactions seen in similar family 11 xylanases from mesophilic organisms. 1YNA from *T. lanuginosus*, which is optimally active at 70°C, has 25 ion pairs and 1PVX from *P. varioti*, which is optimally active around 60°C, has 17 ion pairs (an ion pair was proposed where the distance between two oppositely charged residues was below 8Å). These values can be put into context when compared with a mesophilic xylanase, for example xylanase I from *Trichoderma reesei*, which has 13 ion pairs. From the modelled structure of *N. patriciarum* xylA.cd2 it can be predicted that it also has 13 ion pairs. The studies on 1YNA and 1PVX showed that both the enzymes had an increase in the number of ionic interactions around the disulphide bond/hinge region when compared to mesophilic family 11 xylanases. It was suggested that these interactions, along with the presence of the disulphide bond, were responsible for stabilising the structure at this point and as a result stabilising the enzyme as a whole. Although the studies of 1YNA and 1PVX could not conclusively determine whether any of the other additional ion pair interactions were having a direct effect on thermostability, it was proposed that the general stabilisation of the enzymes as a whole through increased numbers of ion pairs went some way to explain the enhanced stability seen. Another possible way to increase the stability of xylA.cd2 would be to incorporate more ionic interactions, in particular around the introduced disulphide bond, through the introduction of charged residues in positions equivalent to those in the two thermostable xylanases.

4.5.3 Aromatic residues

The study of the *Bacillus* strain D3 family 11 xylanase proposed that a major factor in the enhanced stability seen over its mesophilic counterpart was the presence of surface aromatic residues. The equivalent mesophilic xylanase (from *Bacillus circulans*) only

has three of its 29 aromatic amino acids on the surface, where the thermostable D3 xylanase has eight additional aromatic residues and they are all situated on the surface of the protein. The study proposes that these additional surface aromatic amino acids are positioned in clusters and form 'sticky patches' on the surface of the protein. These are thought to facilitate aggregation of protein molecules when the aromatic clusters from neighbouring proteins 'stick' together, and this aggregation is proposed to confer extra stability on the enzyme molecules at elevated temperatures.

The *N. patriciarum* xylA.cd2 model indicates that it has three aromatic residues that may be possible candidates for the formation of a surface aromatic cluster. Two of these however are situated on an extended loop and so their conformations are not as reliable. The third, Tyr 82, is located on the surface of the protein away from the active site cleft on the 'wrist' of the structure (residue highlighted in green in Figure 4.1). Site-directed mutagenesis could again be employed to substitute neighbouring residues for aromatic ones in an attempt to increase the thermostability of the molecule by improving its protein-protein aggregation.

4.5.4 Other engineering possibilities

Xylan is a very diverse polysaccharide that can have numerous side-chain substituents bound to its xylose backbone, and its constitution depends on its biological source. One of the reasons why only particular types of xylan are permitted into the active site cleft of particular xylanases must be the volume of the cleft, and the size of the entrance to it. A great deal of industrial interest would be attracted if a xylanase could be engineered to have broad range specificity. This may be possible by altering the residues that limit the size of the substrate. In 1PVX from *P. varioti* the closest residues along the active site cleft are Pro 126, which is situated at the tip of the 'thumb', and Trp 18, which is situated at the end of β -strand 2 (highlighted in blue in Figure 4.1). These two residues are 6Å apart. The sequence alignment shows that the equivalent residues in xylA.cd2 are Pro 148 and Trp 24, and these are the closest residues along the active site cleft. If mutations could be made that would increase the gap between these two residues then

the specificity of xylA.cd2 may be altered and this in turn may lead to the production of a xylanase with wider ranging specificity.

4.6 CONCLUSIONS

The aim of this section of work was to design a model of the *N. patriciarum* xylA.cd2, and to use this model to suggest site-specific mutations that may lead to an increase in the thermostability of the enzyme. Comparison of the sequence data and modelled structure of xylA.cd2 to the known crystal structures of other family 11 xylanases has allowed three main suggestions to be made about possible targets for increasing thermostability: introducing a disulphide bond, increasing the number of ion pair interactions, and formation of a surface aromatic cluster. Of these three suggestions the most straightforward to introduce by site-directed mutagenesis is a disulphide bond, as this requires only the mutation of two residues. In addition, the disulphide bond is a feature visible in the thermostable enzymes and is already proven to increase thermostability. Ionic interactions would be more difficult to introduce accurately, as although a trend of increasing numbers of ion pairs is seen when mesophilic and thermophilic enzymes are compared, the actual location of ion pairs is difficult to predict (it is thought that increased numbers of ion pairs generally lead to overall stabilisation of the enzyme, rather than specific interactions in a particular location). Introduction of a surface aromatic cluster would involve the introduction of a number of aromatic residues to interact with the existing Tyr 82. Aromatic residues have large, bulky side-chains and their introduction may cause disruption to the core structure of the enzyme, leading to a loss of activity.

The final decision was to introduce a sulphide bond into *N. patriciarum* xylA.cd2, and this work is described in detail in chapter 5.

Chapter 5

CONSTRUCTION AND CHARACTERISATION OF A SITE-DIRECTED MUTANT OF THE SECOND CATALYTIC DOMAIN OF *N. PATRICIARUM* XYLANASE A

5.1 INTRODUCTION

Using structural information obtained from a model of *N. patriciarum* xylA.cd2, and by making comparisons of this model to known structures of thermostable xylanases, it has been proposed that the introduction of a disulphide bond may lead to an increase in the thermostability of the xylA.cd2 enzyme (Chapter 4). The aim of this section of work is to introduce into xylA.cd2 an equivalent disulphide bond to that found in thermostable xylanases. This will be achieved using site-directed mutagenesis to mutate residues 133 and 177 of the xylA.cd2 enzyme into cysteine residues (positions equivalent to those in the thermostable enzymes).

This chapter will describe the construction of this disulphide bond mutant by site-directed mutagenesis using the megaprimer PCR technique, the cloning of this mutant enzyme into the plasmid vector pUC18 and its expression and purification from *E. coli* strain JM109. It will then go on to describe the characterisation of the xylA.cd2 mutant enzyme with respect to its specific activity, temperature optimum for enzymic activity and thermal stability. Conclusions shall be drawn on the success of introducing a disulphide bond as a means of increasing thermostability by comparing the characteristics of this xylA.cd2 mutant enzyme with those of the recombinant xylA.cd2 (described in Chapter 3).

5.2 MATERIALS AND METHODS

All methods used in this chapter not outlined below can be found in chapter 2.

5.2.1 Materials

DTNB was purchased from Sigma, Poole, Dorset, UK. All other materials used in this section are as outlined in chapter 2, sections 2.1.1, 2.2.1 and 2.3.1.

5.2.2 Construction of disulphide bond mutant xylA.cd2

A three-step PCR process using mutagenic primers was used to construct the xylA.cd2 site-directed mutant. The technique, also referred to as Mega-primer PCR, uses the product from the first round of PCR as a primer in the second round, and then the product from the second round of PCR as a primer in the final round (Figure 5.1). Full details of all primers can be found in the Appendix. The site-directed mutagenesis involved the introduction of two separate mutations within the xylA.cd2 coding sequence, to convert two existing codons into cysteine codons. The first reaction (Figure 5.1a) used the full-length xylanase A gene as a template, with primer 2 and a mutagenic forward primer (primer 3, see Figure 5.1) containing the first of the base mutations to be introduced. This reaction gave a product of 179bp, which was run on a 2.0% agarose gel and purified as described in section 2.1.4.1. This purified product, named megaprimer 1, was then used as the reverse primer in the second round reaction (Figure 5.1b), along with the same full-length xylanase A gene template and a second mutagenic forward primer (primer 4, see Figure 5.1), containing the second of the two base mutations to be introduced. This second reaction gave a product of 310bp, which contained both of the introduced base changes. It was purified again as described in section 2.1.4.1 by running on a 1.8% agarose gel, and used in the final reaction (Figure 5.1c) as the reverse primer (megaprimer 2) along with primer 1 and the full-length xylanase A template. The product of this reaction gave the full coding sequence for xylA.cd2 containing both the introduced mutations.

The reactions were carried out essentially as described in section 2.1.3. The only variation was that for the second round reaction the annealing time was extended to 2

minutes, and for the third round reaction the annealing time was extended again to 4 minutes.

Cloning of this PCR fragment containing the two mutations into pUC18 was as described for xylA.cd2 in section 3.2.2. The product was digested with BamHI (section 2.1.6) and ligated into BamHI-digested pUC18 plasmid vector using the Rapid DNA Ligation Kit (section 2.1.7). This construct is known as pUC18.mutant.cd2.

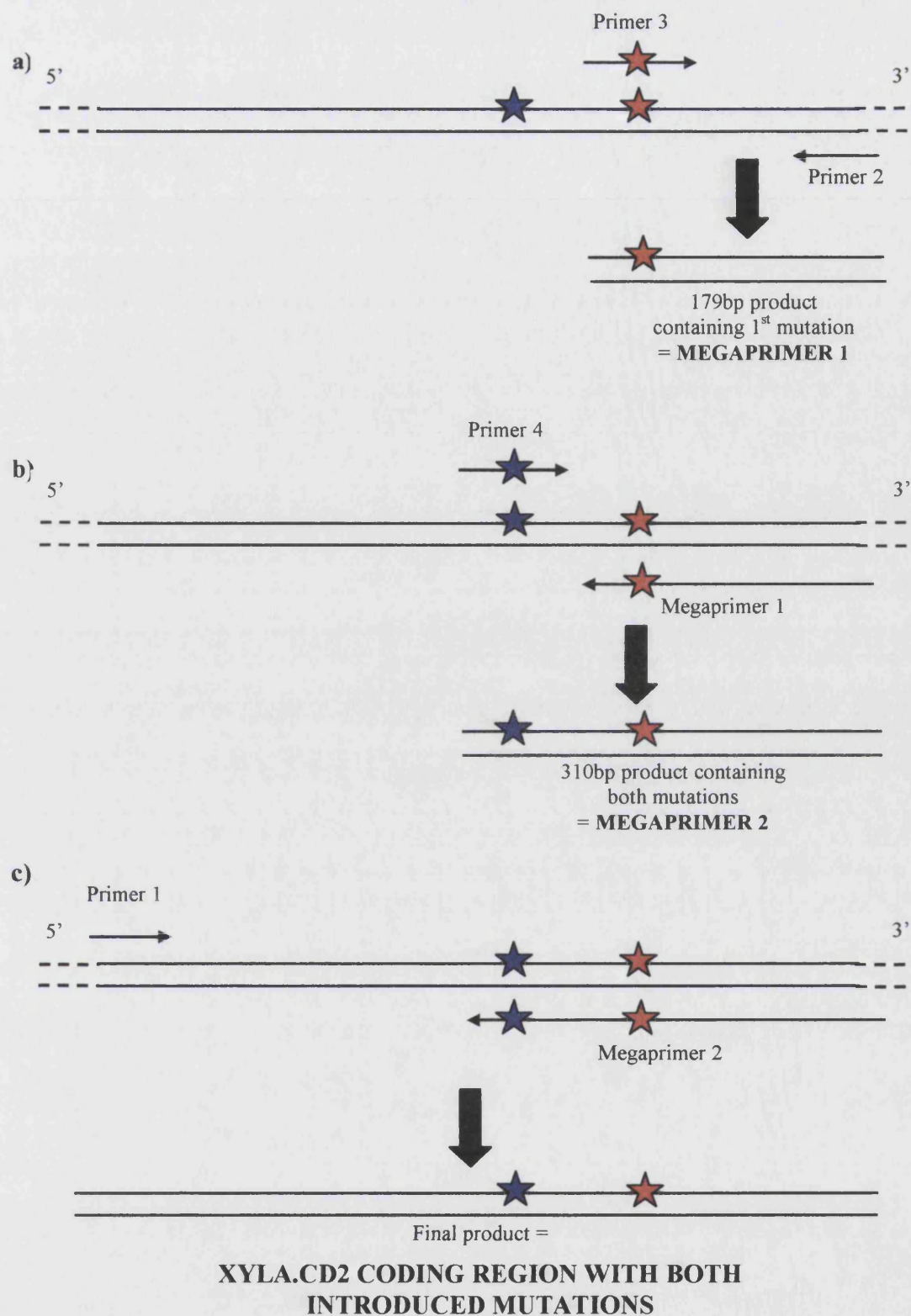


Figure 5.1 Schematic diagram representing the PCR strategy for construction of the site-directed xylA.cd2 mutant

Blue and red stars indicate location of the mutations.

5.2.3 Expression of recombinant mutant xylA.cd2 in *E. coli*

pUC18.mutant.cd2 was transformed into *E. coli* strain JM109 using the heat shock method (section 2.1.7). As for xylA.cd2 (section 3.2.3), the Congo Red overlay assay was employed to identify which clones had the mutant xylA.cd2 insert ligated in the correct orientation in the pUC18 plasmid. Once this was determined, the mutant xylA.cd2 insert was sequenced to ensure that the mutations had been successfully introduced into the coding sequence, and that no other errors had been introduced during the PCR reactions.

The mutant xylA.cd2 protein was expressed from a 250ml culture of LB supplemented with 100µg/ml ampicillin as described in section 2.2.5.

5.2.4 Purification of mutant xylA.cd2 from *E. coli*

The mutant xylA.cd2 protein was purified in the same way as the original xylA.cd2. *E. coli* cells harbouring the pUC18.mutant.cd2 plasmid were harvested after approximately 16 hours of growth. The cells were disrupted by sonication and a cell extract was prepared as described in section 2.2.5.1. The cell extract was applied to a HiTrap Q High Performance 5ml anion exchange column equilibrated with 20mM Tris-HCl, pH8.0, and the mutant xylA.cd2 protein was collected in the unbound fraction.

5.2.5 Identification of disulphide bond

In order to confirm that a disulphide bond has actually formed between the introduced cysteine residues 5, 5'-dithiobis-(2-nitrobenzoic acid) (DTNB) can be used as a reagent to react with free thiol groups. DTNB will react with exposed thiol groups within a protein to form a mixed disulphide and 5-thio-2-nitrobenzoate (TNB), a coloured product that can be detected by measuring the absorbance of a reaction mixture at 412nm (Figure 5.2). In order to detect all cysteine residues within the xylA.cd2 protein, the DTNB assay must be performed in the presence of 6M guanidine to ensure complete unfolding of the protein.

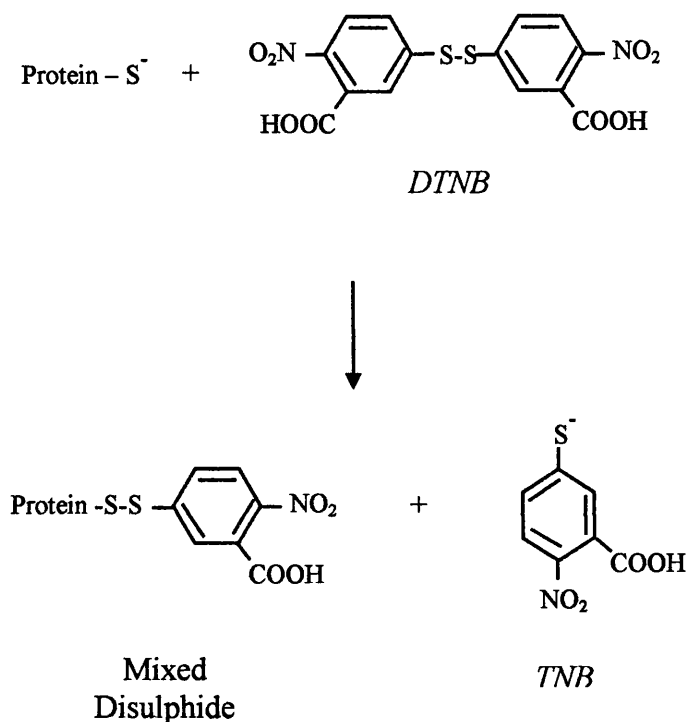


Figure 5.2 Schematic diagram demonstrating the reaction of DTNB with a protein thiol group

The DTNB assay was performed to infer the presence of a disulphide bond within the mutant xylA.cd2 protein. The assay was performed on both the original and mutant xylA.cd2 proteins, in order for a comparison to be made between the two. Both purified proteins were firstly concentrated approximately 25 fold, then the appropriate amount of each was added to a 1ml cuvette along with the other reagents to give a final protein concentration of 0.25mg/ml (which equates to a 0.01mM solution). The total reaction was performed in a final volume of 1ml. Table 5.1 shows the reagents used and their amounts.

REAGENTS USED	MUTANT XYLA.CD2 REACTION	ORIGINAL XYLA.CD2 REACTION
Purified protein	~250µg (27µl of 9.12mg/ml stock)	~250ug (38µl of 6.6mg/ml stock)
6M Guanidine	750µl	750µl
10mM DTNB	10µl	10µl
20mM Tris-HCL, pH8.0	213µl	202µl

Table 5.1 Reagents and amounts used in DTNB assay

Assays were performed in a 1ml plastic cuvette.

After thorough mixing and incubation at room temperature for 5 minutes the absorbance of both samples was read at 412nm.

5.2.6 Characterisation of mutant xylA.cd2

The mutant xylA.cd2 protein was characterised in the same way as the original xylA.cd2 protein. Its specific activity was determined as outlined in section 3.2.5, with DNS assays being performed using varying dilutions of the mutant xylA.cd2 to determine a suitable dilution of the enzyme to ensure that the initial rate of reaction was being measured. Its temperature optimum for activity was determined as described in section 3.2.6, and its thermal stability was determined by thermal inactivation studies as described in section 3.2.7.

5.3 RESULTS

5.3.1 Construction of mutant xylA.cd2 clone

The xylA.cd2 coding sequence was altered by site-directed mutagenesis, using mutagenic primers to introduce base changes into the sequence that will cause amino-acid changes in the expressed protein. The first set of mutations was required at bases 1413 and 1414 (numbering corresponds to base positions in the full-length xylanase A gene). These are the first two bases of the triplet ATT, coding for amino acid residue Ile 133. These two bases were mutated to give a triplet code in the mutant coding sequence of TGT, which codes for cysteine. The second set of mutations was required at bases 1545 and 1546. These are the first two bases of the triplet GAT, coding for amino acid residue Asp 177. Again, these two bases were mutated to give TGT, which is the triplet code for cysteine. The sequence of the mutagenic primers 3 and 4 can be found in the Appendix.

5.3.1.1 PCR amplification and introduction of site-directed mutations

The mutant xylA.cd2 coding sequence was created in a three-step PCR procedure. All reactions used the full-length xylanase A gene as a template, the only variable aspect being the combination of primers used. The first PCR reaction introduced the first set of mutations, and its 179bp product (Figure 5.3) was purified and used as a primer (megaprimer 1) in the second reaction. The second PCR reaction introduced the second of the two sets of mutations, and created a product of 310bp (Figure 5.4), which was purified and used as a primer (megaprimer 2) in the third reaction. The third PCR reaction amplified the full coding sequence for the second catalytic domain, and using megaprimer 2 as the reverse primer ensured that both sets of mutations were included in the final product. As for the amplification of the original xylA.cd2 (section 3.3.1.1) the final product (Figure 5.5) was 703bp.

The PCR fragment was digested with BamHI and ligated into pre-digested pUC18 plasmid vector. The resulting clones were transformed into *E. coli* strain JM109 cells, and successful transformants were selected for by growth on LB-agar plates containing 100µg/ml ampicillin. As with the original xylA.cd2 clone, successful ligation of the

mutant xylA.cd2 insert into each plasmid was confirmed by restriction digest of plasmid prepared from single colonies. Digestion with BamHI gives two bands of the expected sizes when run on an agarose gel (Figure 5.6).

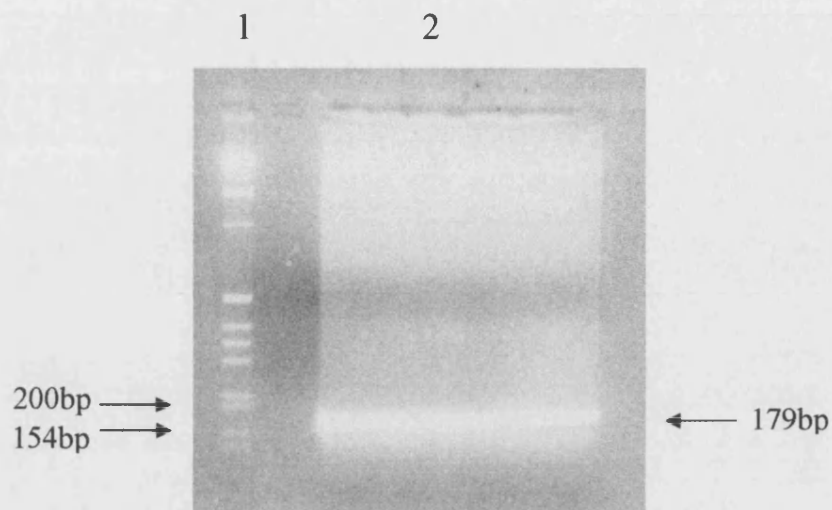


Figure 5.3 Identification of PCR reaction 1 product (megaprimer 1) by agarose gel electrophoresis

Lane 1, 1kb DNA molecular weight markers; lane 2, 179bp PCR product.

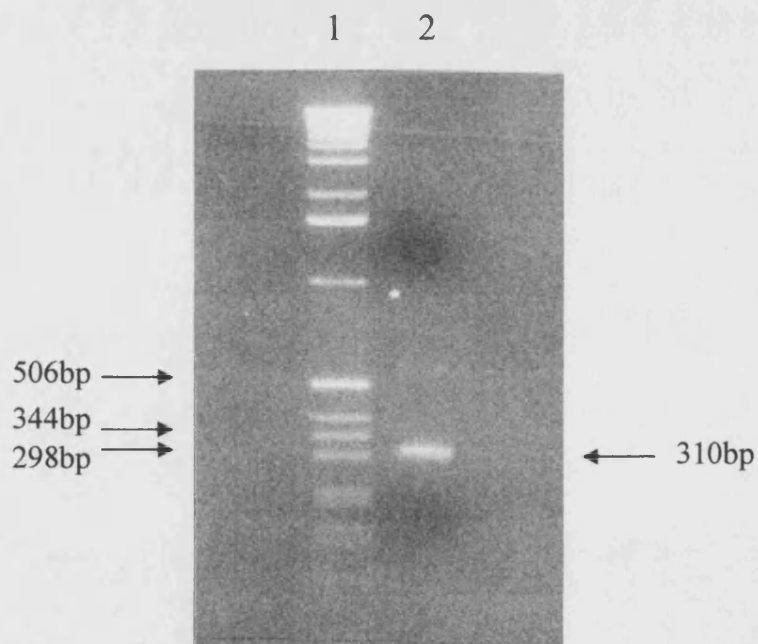


Figure 5.4 Identification of PCR reaction 2 product (megaprimer 2) by agarose gel electrophoresis

Lane 1, 1kb DNA molecular weight markers; lane 2, 310bp PCR product.

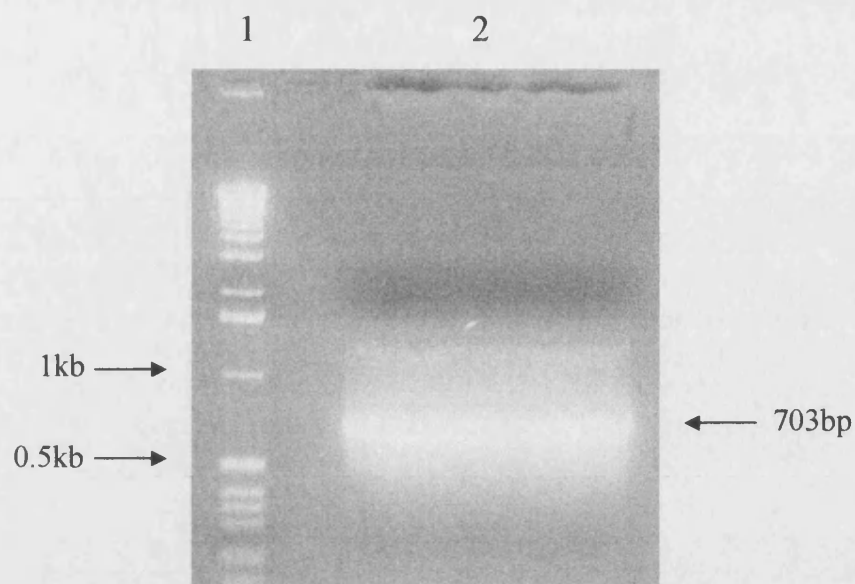


Figure 5.5 Identification of final mutant xylA.cd2 PCR product by agarose gel electrophoresis

Lane 1, 1kb DNA molecular weight markers; lane 2, 703bp PCR product.

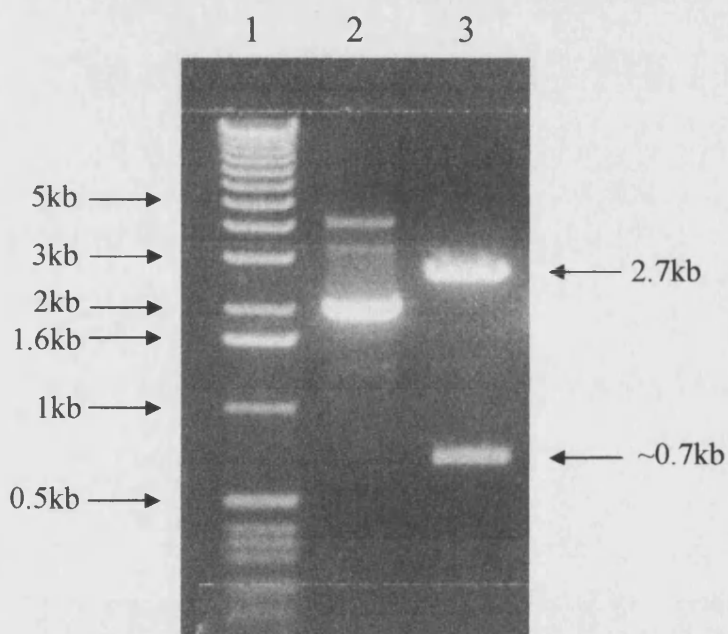


Figure 5.6 BamHI digested pUC18.mutant.cd2, to confirm the cloning of mutant xylA.cd2 insert into pUC18 plasmid

Lane 1, 1kb DNA molecular weight markers; lane 2, undigested pUC18.mutant.cd2 (supercoiled & relaxed circle); lane 3, BamHI digested mutant pUC18.cd2 (~700bp insert band & 2.7kb plasmid band).

5.3.1.2 Identification of clones with correctly oriented mutant insert

The Congo Red overlay assay was used to determine whether *E. coli* cells were harbouring pUC18 plasmid clones with the mutant xylA.cd2 PCR insert ligated in the correct orientation. Those cells that contained the plasmid with insert ligated in the correct orientation showed a clearing zone around them, while the ones containing the plasmid with insert ligated in the reverse orientation showed no visible clearing zones, indicating no xylanase activity (Figure 5.7).

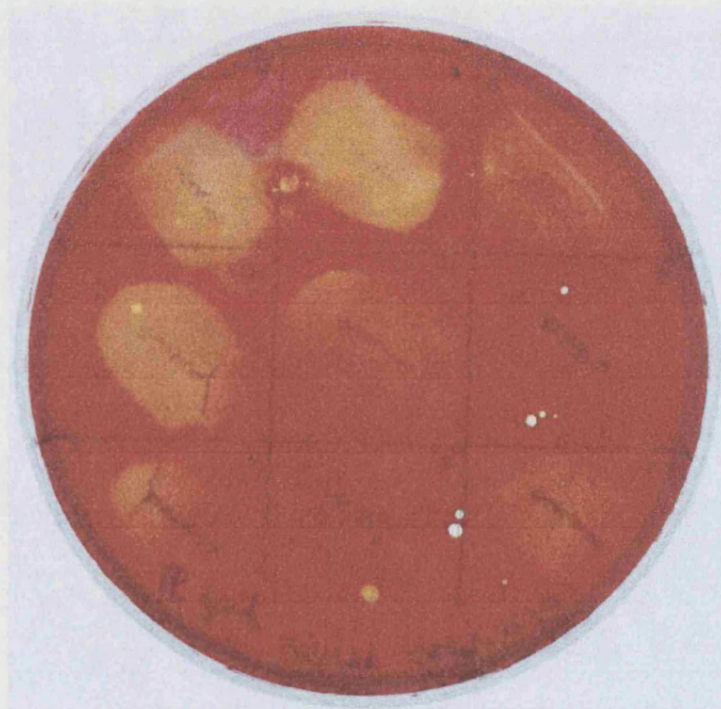


Figure 5.7 Congo Red assay confirming xylanase activity of pUC18.mutant.cd2 clones

Not all clones are displaying xylanase activity (note the yellow halos around individual streaks that are xylanase active).

5.3.1.3 Sequencing of the mutant xylA.cd2 PCR insert

Sequencing of the mutant xyl.cd2 PCR insert was performed using the M13 universal sequencing and reverse primers. The sequence obtained showed that the specific mutations had been introduced into the coding sequence, and that no other sequence errors had been introduced during the PCR amplification. Figure 5.8 shows the mutant xylA.cd2 sequence.

5.3.2 Mutant xylA.cd2 purification

Mutant xylA.cd2 protein was expressed in *E. coli* strain JM109 cells from a pUC18.mutant.cd2 clone, and purified in the same way as the original xylA.cd2 protein. Table 5.2 summarises the purification results.

Approximately 2.2g (wet weight) were harvested from a 250ml culture of JM109 cells harbouring the pUC18.mutant.cd2 plasmid after 16 hours of growth. After resuspension and lysis by sonication the cell extract contained approximately 37mg of protein, and demonstrated a specific xylanase activity of 1970U/mg.

The cell extract was applied to a HiTrap Q High Performance 5ml anion exchange column and the mutant xylA.cd2 protein was washed through in the unbound fraction. The unbound fraction was eluted in approximately 19ml and again, as with the original xylA.cd2, it showed very high xylanase activity despite being quite dilute (the amount of cell extract applied to the column was approximately 3ml). The total amount of protein in the fraction was approximately 5.1mg, and the xylanase specific activity was calculated as 10,600U/mg.

SDS-PAGE analysis (Figure 5.9) showed the mutant xylA.cd2 within the unbound fraction to be over 90% pure (estimated visually). Zymogram analysis of the various purification stages showed a clearing zone around a band at approximately 27kDa, indicating that this is the molecular weight of the recombinant xylA.cd2 protein (Figure 5.10).


```

AAGTTTACTGTCGGTAATGGACAAAACCAACATAAGGGTGTCAACGATGGTTTCAGTTAT
1  -----+-----+-----+-----+-----+-----+ 60
TTCAAATGACAGCCATTACCTGTTTTGGTTGTATTCCCACAGTTGCTACCAAAGTCAATA

K F T V G N G Q N Q H K G V N D G F S Y

GAAATCTGGTTAGATAACACTGGTGGTAACGGTCTATGACTCTCGGTAGTGGTGCAACT
61 -----+-----+-----+-----+-----+ 120
CTTTAGACCAATCTATTGTGACCACCATTGCCAAGATACTGAGAGCCATCACCACGTTGA

E I W L D N T G G N G S M T L G S G A T

TTCAAGGCTGAATGGAATGCAGCTGTTAACCGTGGTAACCTTCCTTGCCCGTCGTGGTCTT
121 -----+-----+-----+-----+-----+ 180
AAGTTCCGACTTACCTTACGTCGACAATTGGCACCATTGAAGGAACGGGCAGCACCAGAA

F K A E W N A A V N R G N F L A R R G L

GACTTCGGTTCTCAAAAGAAGGCAACCGATTACGACTACATTGGATTAGATTATGCTGCT
181 -----+-----+-----+-----+-----+ 240
CTGAAGCCAAGAGTTTTCTTCCGTTGGCTAATGCTGATGTAACCTAATCTAATACGACGA

D F G S Q K K A T D Y D Y I G L D Y A A

ACTTACAAACAACTGCCAGTGCAAGTGGTAACCTCCCGTCTCTGTGTATACGGATGGTTC
241 -----+-----+-----+-----+-----+ 300
TGAATGTTTGTGTTGACGGTCACGTTACCATTTGAGGGCAGAGACACATATGCCTACCAAG

T Y K Q T A S A S G N S R L C V Y G W F

CAAAACCGTGGACTTAATGGCGTTCCTTTAGTAGAATACTACATCATTGAAGATTGGGTT
301 -----+-----+-----+-----+-----+ 360
GTTTTGGCACCTGAATTACCGCAAGGAAATCATCTTATGATGTAGTAACCTCTAACCCAA

Q N R G L N G V P L V E Y Y I I E D W V

GACTGGGTTCCAGATGCACAAGGAAAAATGGTAACCTTGTGATGGAGCTCAATATAAGATT
361 -----+-----+-----+-----+-----+ 420
CTGACCCAAGGTCTACGTGTTCCCTTTTTACCATTGGTAACCTACCTCGAGTTATATTCTAA

D W V P D A Q G K M V T ■ D G A Q Y K I

TTCAAATGGATCACACTGGTCCAACATCAATGGTGGTAGTGAAACCTTTAAGCAATAC
421 -----+-----+-----+-----+-----+ 480
AAGGTTTACCTAGTGTGACCAGGTTGATAGTTACCACCATCACTTTGGAAATTCGTTATG

F Q M D H T G P T I N G G S E T F K Q Y

TTCAGTGTCCGTCAACAAAAGAGAACTTCTGGTCATATTACTGTCTCATTGCTCACTTTAAG
481 -----+-----+-----+-----+-----+ 540
AAGTCACAGGCAGTTGTTTTCTCTTGAAGACCAGTATAATGACAGAGTCTAGTGAAATTC

F S V R Q Q K R T S G H I T V S ■ H F K

```

```

GAATGGGCCAAACAAGGTTGGGGTATTGGTAACCTTTATGAAGTTGCTTTGAACGCCGAA
541 -----+-----+-----+-----+-----+-----+ 600
CTTACCCGGTTTGTTCCAACCCATAACCATTTGGAAATACTTCAACGAAACTTGCGGCTT

E W A K Q G W G I G N L Y E V A L N A E

GGTTGGCAAAGTAGTGGTGTGCTGATGTCACCTTATTAGATGTTTACACAACTCCAAAG
601 -----+-----+-----+-----+-----+-----+ 660
CCAACCGTTTCATCACCACAACGACTACAGTGAATAATCTACAAATGTGTTGAGGTTTC

G W Q S S G V A D V T L L D V Y T T P K

GGTTCTAGTCCAGCCTAG
661 -----+----- 678
CCAAGATCAGGTCGGATC

G S S P A *

```

Figure 5.8 **Sequence of mutant xylA.cd2**

The translated amino acid sequence is shown below the gene sequence using the single letter amino acid codes. The base changes introduced by PCR are highlighted in bold text, and the introduced cysteine residues are highlighted in red.

Purification step	Total protein (mg)	Total activity (units*)	Specific activity (units*/mg)	Yield (%)	Purification factor (x fold)
Cell extract	36.9	72,800	1970	100	1
HiTrap Q anion exchange unbound fraction	5.1	54,300	10,600	75	5.38

Table 5.2 Summary of purification of mutant xylA.cd2 from *E. coli* strain JM109

Samples after each step were analysed for xylanase activity using the DNS assay and for protein concentration using the Bio-Rad protein estimation assay. Yield is expressed relative to the total amount of enzyme activity present in the cell extract. Purification factor is expressed relative to the specific activity of the enzyme in the cell extract. *One unit of enzyme activity is defined as that which releases 1 μ mol product (expressed as xylose equivalents) per minute.

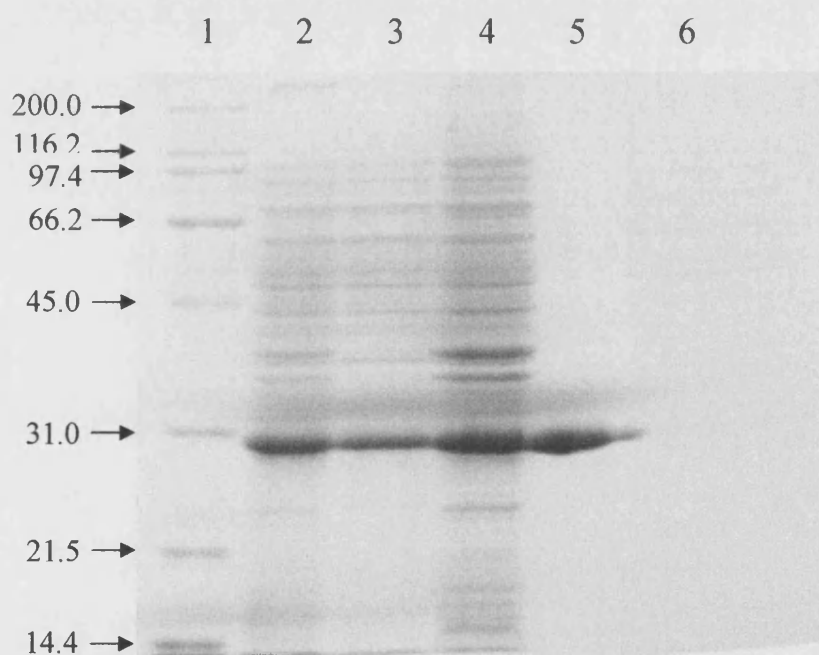


Figure 5.9 SDS-PAGE analysis of the purification stages of mutant xylA.cd2

Lane 1, SDS-PAGE Broad range markers; lane 2, Total cells; lane 3, Cell extract; lane 4, Cell debris; lane 5, HiTrap Q anion exchange unbound fraction; lane 6, HiTrap Q anion exchange total bound protein.

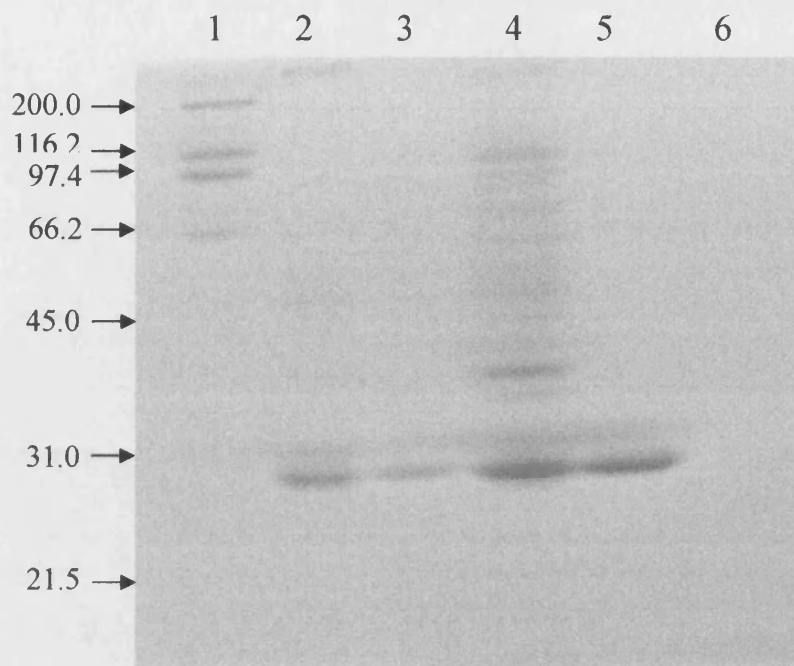


Figure 5.10 Zymogram of purification stages of mutant xylA.cd2

Clearing zones indicate areas of xylanase activity. Lane 1, SDS-PAGE Broad range markers; lane 2, Total cells; lane 3, Cell extract; lane 4, Cell debris; lane 5, HiTrap Q anion exchange unbound fraction; lane 6, HiTrap Q anion exchange total bound protein.

5.3.3 Mutant xylA.cd2 characterisation

5.3.3.1 Identification of disulphide bond

The DTNB assay was used to determine the number of free thiol groups in both the original and mutant xylA.cd2 proteins, as a means of deducing whether the two introduced cysteine residues have actually formed a disulphide bond. The absorbance values gained from the reactions with both original and mutant proteins were almost equal, and using the reasoning set out below this result suggests that both proteins contain an equal number of free thiol groups:

- $A = \epsilon cl$, (where A = absorbance, ϵ = molar absorption coefficient, c = concentration of protein and l = pathlength), therefore concentration = $A/\epsilon l$
- For original xylA.cd2, 0.01mM protein + excess DTNB $\rightarrow \Delta A_{412} = 0.155$
- So, concentration of SH groups = $0.155/13,600 \times 1 \text{ M}$
= 0.0114mM SH groups
- Therefore number of SH groups per xylA.cd2 molecule = $0.0114/0.01$
= **1.14**
- For mutant xylA.cd2, 0.01mM protein + excess DTNB $\rightarrow \Delta A_{412} = 0.162$
- So, concentration of SH groups = $0.162/13,600 \times 1 \text{ M}$
= 0.0119mM SH groups
- Therefore number of SH groups per mutant xylA.cd2 molecule = $0.0119/0.01$
= **1.19**

These calculations suggest that both original and mutant xyl.cd2 proteins contain the same number of free thiol groups.

5.3.3.2 Determination of appropriate enzyme dilution and specific activity

Standard DNS assays were performed on the purified mutant xylA.cd2 enzyme to determine an appropriate dilution to use in the studies of its activity with temperature and thermal stability, and also to determine its specific activity. A series of assays were carried out using varying volumes of a 1/250 dilution of the mutant xylA.cd2, and it was determined that a 1/5000 dilution would be an appropriate dilution to use to ensure that initial rates were being measured. Figure 5.11 graphically represents these results. The purified mutant xylA.cd2 enzyme demonstrated a specific activity of 10,600 units per mg of protein.

5.3.3.3 Temperature optimum for activity

As for the original xylA.cd2 enzyme, the mutant xylA.cd2 was assayed at various temperatures from 18°C to 80°C, and these results are shown in Figure 5.12. Blank

reactions (with 100 μ l PC buffer in place of the 100 μ l enzyme dilution) were carried out at each temperature to account for any degradation of the soluble xylan substrate at the higher temperatures, although no significant increase in absorbance of the blank samples was observed. The maximum activity of the purified xylA.cd2 was observed at 55°C.

5.3.3.4 Thermal inactivation

The same temperatures as used to study the original xylA.cd2 enzyme were used to study the thermal stability of the mutant enzyme, so that a direct comparison between the two could be made. These results are represented graphically in Figure 5.13 and show that the purified mutant enzyme has a half-life of just less than one hour at 58°C, which reduces to 1.2 minutes at 64°C. Figure 5.14 shows the Arrhenius plot of these data (plotted according to equation 3.1), and allows the activation energy for the inactivation process (E_a) of the mutant xylA.cd2 to be calculated as 624kJ/mol.

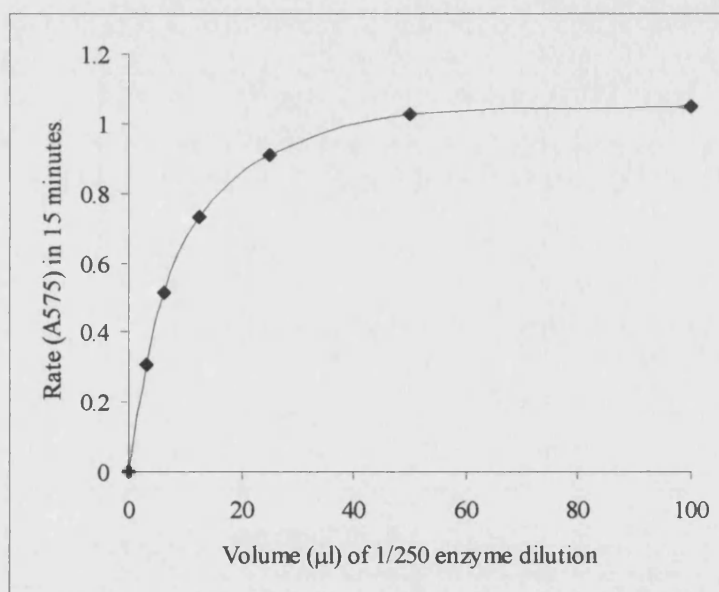


Figure 5.11 Mutant xylA.cd2 activity against volume of a 1/250 enzyme dilution

Each point represents the mean of duplicate assays.

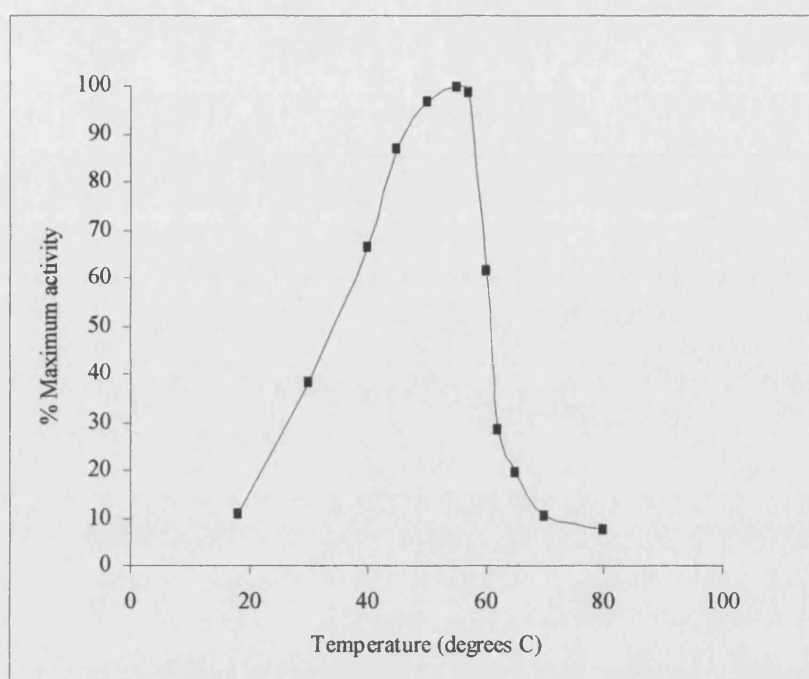
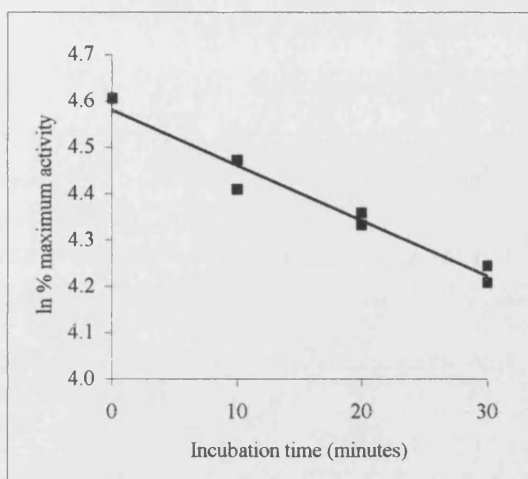
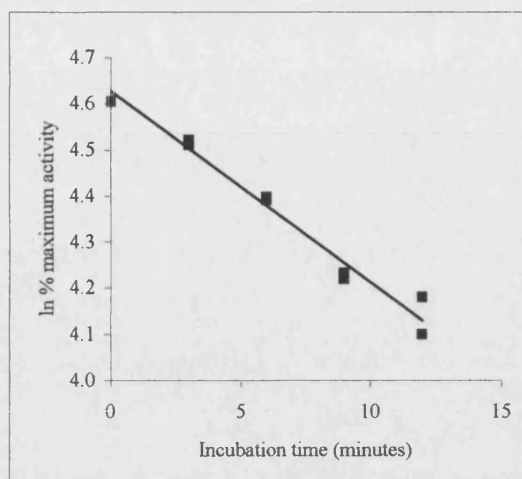
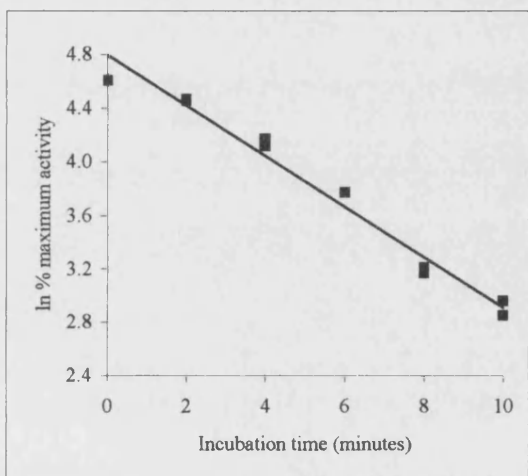
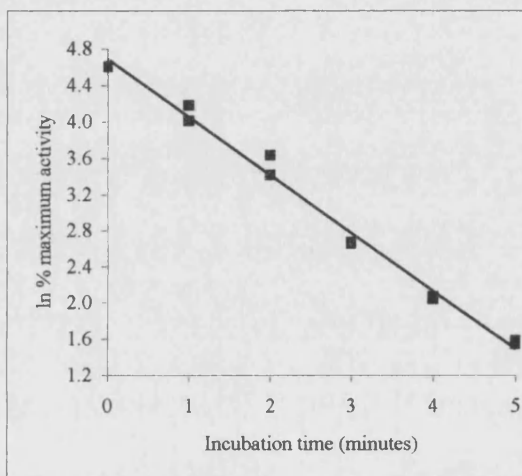


Figure 5.12 Temperature activity curve for xylA.cd2

Activities are expressed as a percentage of activity at 55°C, as this was the temperature at which maximum activity was observed. Each point represents the mean of 4 assays.

**Figure 5.13a****Figure 5.13b****Figure 5.13c****Figure 5.13d****Figure 5.13 Thermal inactivation of mutant xylA.cd2**

Data are shown as ln (% activity) against incubation time (% activity being calculated as a percent of maximum activity, seen at time 0). Lines of best fit, calculated by linear regression, are shown.

Figure 5.13a Thermal inactivation of mutant xylA.cd2 at 58°C

Figure 5.13b Thermal inactivation of mutant xylA.cd2 at 60°C

Figure 5.13c Thermal inactivation of mutant xylA.cd2 at 62°C

Figure 5.13d Thermal inactivation of mutant xylA.cd2 at 64°C

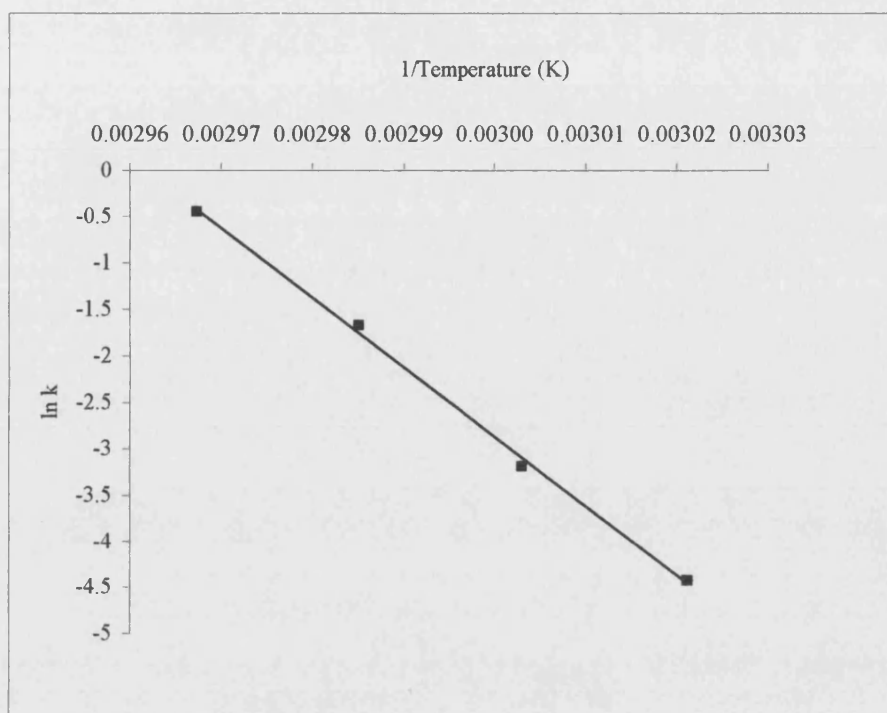


Figure 5.14 Arrhenius plot for mutant xylA.cd2 thermal inactivation data

Data from Figure 5.13 are represented as an Arrhenius plot, according to the Arrhenius equation (Equation 3.1). Linear regression has been used to calculate a line of best fit through the data.

5.3 DISCUSSION

5.3.1 Construction of a site-directed mutant xylA.cd2 enzyme and confirmation of the introduction of a disulphide bond

This chapter has described the construction of a disulphide bond mutant of *N. patriciarum* xylA.cd2. Site-directed mutagenesis has been used to introduce the necessary base changes into the xylA.cd2 coding sequence by PCR such that in the translated protein amino acid residues 133 and 177 have been mutated from an isoleucine and an aspartic acid to cysteine residues.

The DTNB assay has been used as a means to 'deduce' that a disulphide bond has indeed been formed in the mutant protein between the two introduced cys residues. DTNB can be used to quantitatively determine the number of free thiol groups in a protein. The original xylA.cd2 protein has only one cys residue, whereas the mutant xylA.cd2 has three. Of these three it was hoped that two would have formed a disulphide bond, thus leaving only one free thiol group in the mutant protein. Unfolding both the original and mutant xylA.cd2 proteins with 6M guanidine and incubating them in excess 10mM DTNB gave almost the same absorbance reading when measured at 412nm. As both proteins were present in the reaction mixture in equal molar amounts, this suggests that they both have the same number of free thiol groups in them, and as such it could be predicted from these data that the two cysteine residues introduced into the mutant have formed a disulphide bond.

Mutant xylA.cd2 was expressed and purified in the same way as the original xylA.cd2. A slightly lower yield of 75% was obtained for the mutant protein, which constituted 18% of the total protein. SDS-PAGE analysis showed the purified mutant xylA.cd2 to be over 90% pure. Its specific activity, measured to be 10,600U/mg, is almost identical to that of the original xylA.cd2 (10,400U/mg). This indicates that the introduction of a disulphide bond has not altered the three-dimensional structure of the mutant enzyme in a way that may have caused a conformational change in or near the active site. This can be proposed as any change in the enzymes structure that affects its active site would be

reflected in its catalytic efficiency, and as a result a decrease in specific activity would be expected.

5.3.2 Comparison of mutant to original xylA.cd2 enzyme

Assaying the mutant xylA.cd2 over a range of temperatures had shown that its optimum temperature for activity is 55°C. When these data are compared with that of the original xylA.cd2 it can be seen that both enzymes have a very similar temperature activity profile. Figure 5.15 shows both profiles on the same axes, and it can clearly be seen that both profiles share the same optimum temperature. Closer inspection shows that the mutant enzyme has a greater percentage maximum activity when assayed at 58°C, in comparison to the original enzyme over the same incubation time. This trend is also visible at 60°C, but beyond this point both profiles follow the same path, with percent maximum activity values being almost identical. The overall aims of the project are to increase the stability of xylA.cd2 without affecting its activity at lower temperatures. This comparison of temperature activity between the mutant and wild-type enzymes suggests that the introduction of a disulphide bond has had no real effect on the overall activity of xylA.cd2 at any temperature. However, this does not indicate that the stability of the enzyme at elevated temperatures remains unaffected.

Comparison of the thermal inactivation rates for the two enzymes reveals that there is a notable difference between them. At all temperatures studied the mutant is more than twice as stable as the original enzyme. At 58°C, which is only 3 degrees above the optimum temperature for activity, the mutant has a half-life 3.5 fold higher than the original xylA.cd2. This increase in half-life remains at least 2.5 fold higher for all the other temperatures studied. Figure 5.16 shows a graphical comparison of the thermal inactivation data for both original and mutant xylA.cd2, and Figure 5.17 shows a comparison of the thermal inactivation data represented as an Arrhenius plot. The activation energy (E_a) for the inactivation process for the mutant enzyme has been calculated as 624kJ/mol. This is larger than the E_a for the original xylA.cd2 (which is calculated as 478kJ/mol) and supports the observation that the mutant enzyme is more

stable than the original. Table 5.3 summarises the comparison of data obtained for the original and mutant xylA.cd2 enzymes.

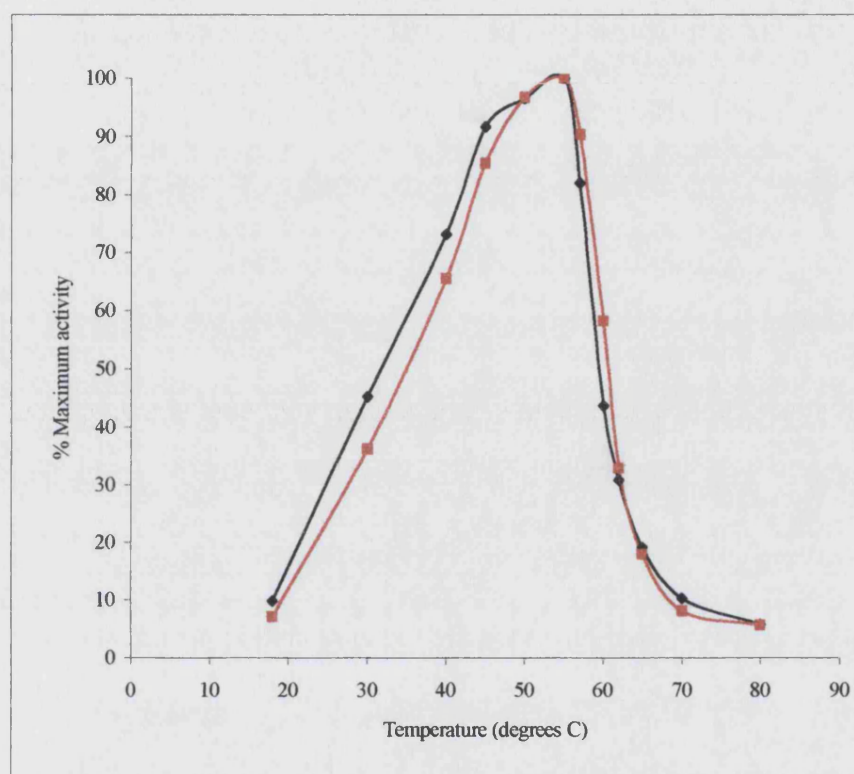
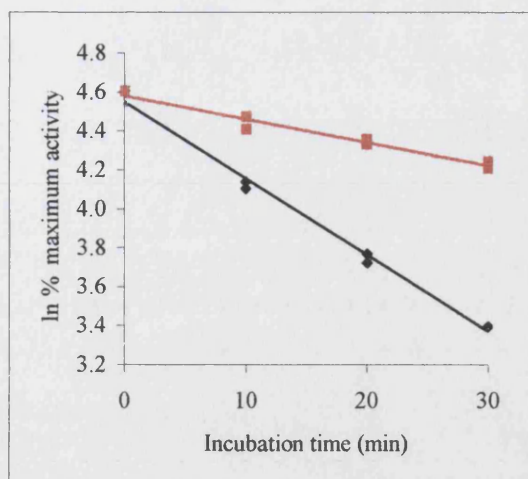
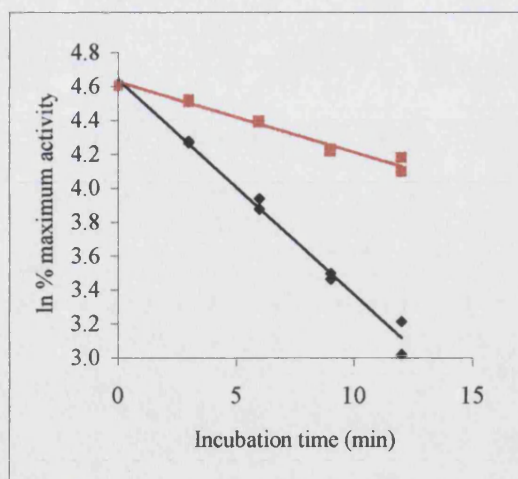
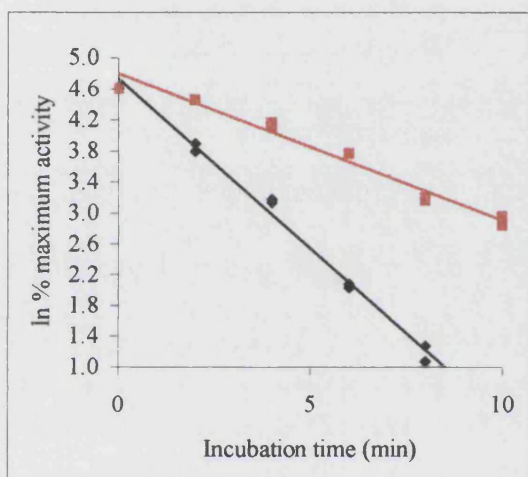
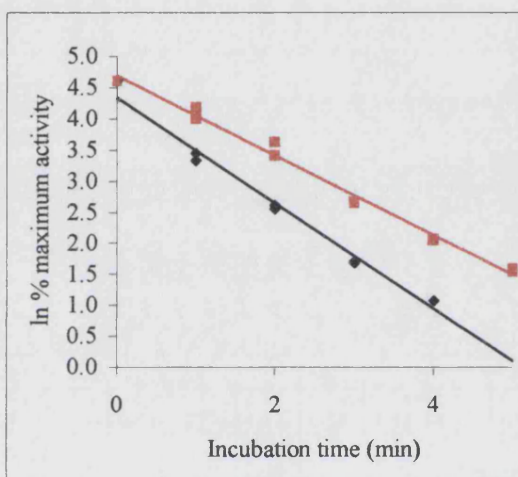


Figure 5.15 Comparison of temperature activity profiles for original and mutant xylA.cd2

Activities are expressed as a percentage of activity at 55°C, as this demonstrated to be the temperature at which the maximum activity was observed. Black line represents original xylA.cd2; red line represents mutant xylA.cd2. Each point represents the mean of 4 assays.

**Figure 5.16a****Figure 5.16b****Figure 5.16c****Figure 5.16d****Figure 5.16 Comparison of thermal inactivation data from original & mutant xylA.cd2**

Data are shown as \ln (% activity) against incubation time (% activity being calculated as a percent of maximum activity, seen at time 0). Black line represents original xylA.cd2; red line represents mutant xylA.cd2. Lines of best fit, calculated by linear regression, are shown.

Figure 5.16a Thermal inactivation at 58°C

Figure 5.16b Thermal inactivation at 60°C

Figure 5.16c Thermal inactivation at 62°C

Figure 5.16d Thermal inactivation at 64°C

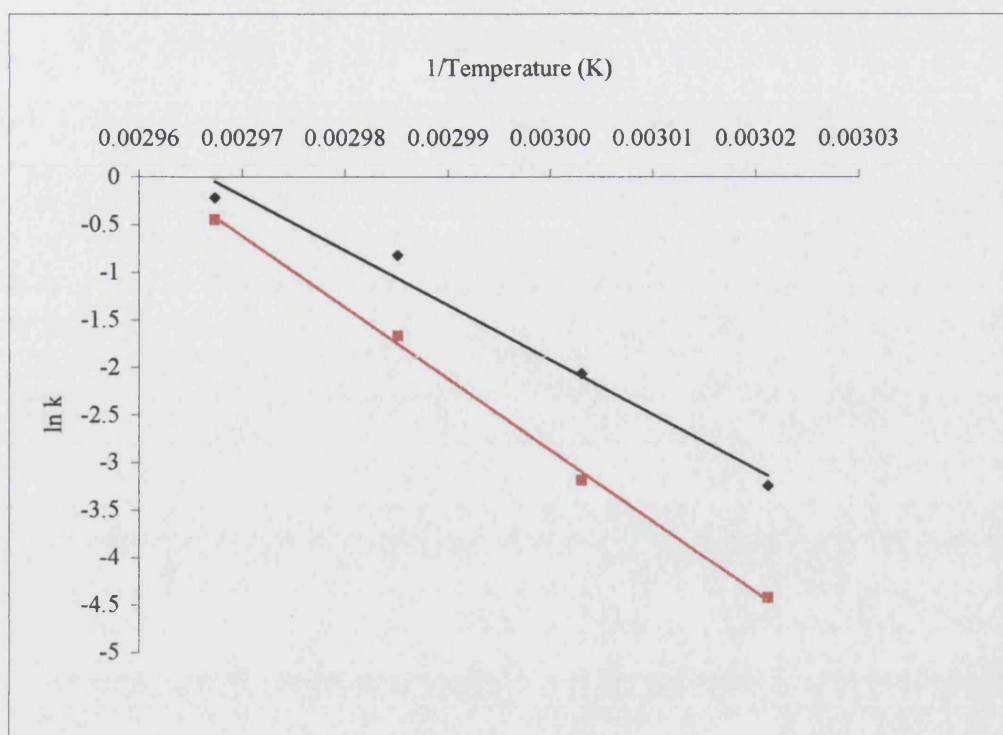


Figure 5.17 Comparison of Arrhenius plots for original and mutant xylA.cd2 thermal inactivation data

Data from Figure 5.16 are represented as an Arrhenius plot, according to the Arrhenius equation (Equation 3.1). Black line represents original xylA.cd2; red line represents mutant xylA.cd2. Linear regression has been used to calculate a line of best fit through the data.

	ORIGINAL XYLA.CD2	MUTANT XYLA.CD2
Temperature Optimum	55°C	55°C
$T_{1/2}$ at 58°C	16 min	56 min
$T_{1/2}$ at 60°C	5.75 min	17 min
$T_{1/2}$ at 62°C	1.9 min	4.7 min
$T_{1/2}$ at 64°C	0.5 min	1.2 min
E_a for inactivation	478 kJ/mol	624 kJ/mol

Table 5.3 Comparison of temperature optimum and thermal stability data for original and mutant xylA.cd2 enzymes

$T_{1/2}$ represents half-life; E_a represents activation energy for the inactivation process.

5.4 CONCLUSIONS

This chapter has described attempts to increase the thermal stability of *N. patriciarum* xylA.cd2 by constructing a site-directed mutant enzyme with an equivalent disulphide bond to that found in thermostable xylanases. Characterisation of the mutant enzyme and comparison to data obtained from the original xylA.cd2 enzyme show that while the mutant does not demonstrate a detectable increase in its temperature optimum for activity, it is notably more stable than the original enzyme at temperatures above 55°C. A DTNB assay has been used to deduce that the two introduced cysteine residues have actually formed a disulphide bond, and the fact that the mutant enzyme has an almost identical specific activity to the original xylA.cd2 suggests that the substitution of residues and introduction of a disulphide bond have not compromised the structure of the enzyme in a way that leads to a decrease in activity.

These results support the idea that thermal stability is not caused simply by a single change within the structure of a protein. It is often suggested that thermophilic enzymes demonstrate an increased stability over their mesophilic counterparts by a combination of effects, for example increased numbers of ion pairs and hydrogen bonds, decreased flexibility, increased compactness, and this seems to be the case here. While the introduction of a disulphide bond does appear to have contributed to an increase in stability of the xylA.cd2 enzyme, it has not 'transformed' the enzyme from mesophilic to thermophilic. It is, however, a good basis for improvement, and in conjunction with other thermostabilising features may facilitate a greater stability in the xylA.cd2 enzyme.

Chapter 6

CONSTRUCTION OF A RANDOM MUTANT LIBRARY AND INITIAL SCREENING

6.1 INTRODUCTION

Directed evolution is a powerful tool that is being increasingly employed over rational design approaches to generate enzymes demonstrating new or improved properties. Evolution in a laboratory situation can be used to explore non-natural enzymic functions in addition to improving existing properties. From an industrial point of view directed evolution presents the opportunity to modify and improve important biocatalysts, and this is the basis behind this section of work.

As previously described, the industrial application of the second catalytic domain of *N. patriciarum* xylanase A is as an animal feed additive. In keeping with the aims of this project, which are to improve the thermal stability of xylA.cd2 whilst retaining its activity at lower temperatures, directed evolution has been utilised in attempts to generate mutant forms of the enzyme that display increased thermostability. Successful improvements of any property using directed evolution are usually achieved by a process of mutation and screening that is repeated several times. Screening for the desired property in a library of random mutants is, therefore, of considerable importance as it may be required to identify only small improvements at each individual stage. The screen described in this chapter studies the thermal stability of the mutant xylA.cd2 enzymes *in situ*, within the *E. coli* cells transformed with the random mutant library.

The basis of directed evolution is to introduce random errors into the coding sequence of the enzyme of interest using an error-prone PCR technique. Error-prone PCR is similar to standard PCR (as described in section 2.1.3), the main difference being the concentration of MgCl₂ and deoxynucleoside triphosphates used in the reaction. By varying these concentrations the DNA polymerase is forced into making errors by misincorporating bases when copying the DNA template. *Taq* DNA polymerase is used

in place of the usual Vent polymerase as the former has a reduced proof-reading ability, and as such will be more prone to making errors when copying the template.

This chapter will describe the generation of a random mutant library of xylA.cd2 clones, and the initial agar plate-based screening method employed to identify positive mutants. It will also describe the characterisation of four mutants identified from the screen that demonstrate potential improvements in stability. Conclusions about the success of the random mutagenesis method and screening process are drawn by comparing the characteristics of the four mutant enzymes to those of the original xylA.cd2 enzyme.

6.2 MATERIALS AND METHODS

All methods used in this chapter not outlined below can be found in Chapter 2.

6.2.1 Materials

Taq DNA polymerase and 5-bromo-4-chloro-3-indoyl- β -D-galactopyranoside (X-gal) were purchased from Sigma, Poole, Dorset, UK. Electroporation competent Epicurian Coli® cells were purchased from Stratagene, La Jolla CA, USA (Genotype: *el4- (McrA) Δ (mcrCB-hsd SMR-mrr)171 end1 supE44 thi-1 gyrA96 relA1 lac recB recJ sbcC umuC::Tn5 (kanr) uvr C [F'proAB lacIqZA (M15 Tn10 (Tetr))]*). All other materials used in this section are as outlined in Chapter 2, sections 2.1.1, 2.2.1 and 2.3.1.

6.2.2 Random mutagenesis technique: Error-prone PCR

Random mutations were introduced into the *xylA.cd2* coding sequence by error-prone PCR (EP-PCR). Reactions were carried out using pUC18.cd2 as the template DNA. The *cd2* insert was amplified by *Taq* DNA polymerase using primers 5 and 6, designed to a region of the pUC18 vector flanking the poly-cloning site. Full details of all primers can be found in the Appendix. A total of 45pmol of each primer was used in all reactions. Three separate rounds of EP-PCR were performed. In each round 4 separate reactions were carried out: one control reaction (using non-error inducing conditions) and 3 reactions using a 1/1000, 1/10,000 and 1/100,000 dilution of the template DNA respectively. Each reaction used 5 μ l of the diluted template DNA. In the first round the template DNA was pUC18.cd2. In the subsequent rounds the product from the previous round that used the most dilute template to achieve a product was used as the template. Table 6.1 summarises the concentrations of deoxynucleoside triphosphates and MgCl₂ used in the control and error-prone reactions.

	CONTROL REACTION	ERROR-PRONE REACTION
MgCl ₂	2.0mM	3.85mM
dATP	0.2mM	0.22mM
dCTP	0.2mM	0.20mM
dGTP	0.2mM	0.34mM
dTTP	0.2mM	2.40mM

Table 6.1 Summary of concentrations of deoxynucleoside triphosphates and MgCl₂ used in EP-PCR reactions

5U *Taq* DNA polymerase were used in each reaction, which was incubated in buffer supplied by the manufacturer. The final reaction mixture was overlaid with 20µl mineral oil to prevent evaporation. A 'hot-start' PCR technique was used, where the reaction mixture is heated to 96°C for 5 minutes prior to the addition of the polymerase. The following conditions were then repeated for 30 cycles before a final 10 minutes extension at 72°C:

94°C denaturation step	1 min
55°C annealing step	1 min
72°C extension step	2 min 30 s

10µl of each reaction was run on a 1% agarose gel, as described in section 2.1.2, to check the products and choose the most appropriate one to use as the template in the next round of EP-PCR. The third round products were purified by phenol/chloroform extraction as follows: 100µl of a 1:1 phenol:chloroform solution was added to the PCR reaction and vortexed vigorously before centrifugation at 12,000g for 1 min. The DNA in the top layer was precipitated by the addition of 10µl of 3M ammonium sulphate solution. 100µl of isopropanol was then added and the solution incubated at -20°C for 30

minutes before centrifugation again at 12,000g for 15 minutes. The supernatant was removed and the pellet resuspended in 20µl distilled water.

6.2.3 Construction of the random mutant library and transformation into *E. coli*

The purified products of the EP-PCR reactions were digested with both HindIII and EcoRI, as described in section 2.1.5, before being ligated into HindIII and EcoRI digested pUC18 plasmid vector using the Rapid DNA Ligation Kit (section 2.1.6). The product of this ligation reaction is a random mutant library of xylA.cd2 in pUC18. The random mutant library was transformed into Epicurian Coli® electroporation competent cells by electroporation, as follows: 3µl of DNA from the random mutant library was added to 30µl of electroporation competent Epicurian Coli® in a pre-chilled 0.2mm electroporation cell on ice. The cells were electroporated using a Biorad Gene Pulser™ at 1.7kV with a 1ms pulse, immediately after which 1ml of LB broth, pre-incubated to 37°C, was added to the cells. After incubation at 37°C for 1 hour the cells were spread onto LB-agar plates supplemented with 100µg/ml ampicillin and 40µg/ml X-gal and incubated overnight at 37°C. For analysis of library size and estimation of the number of xylanase active clones, varying volumes of the transformed cells were spread onto LB-agar plates supplemented with 100µg/ml ampicillin, 40µg/ml X-gal and 500µg/ml RBB-xylan.

6.2.4 Agar plate screen: Heat inactivation and RBB-xylan overlay assay

Thermal stability of the randomly mutated enzymes was assessed by performing a heat inactivation step on the *E. coli* cells transformed with the random mutant library. The transformants were grown overnight at 37°C on LB-agar plates supplemented with 100µg/ml ampicillin. The resulting colonies were incubated for 30 minutes at 85°C before being immediately transferred to -20°C for 10 minutes. Once cooled down the plates were overlaid with 7ml xylan blue agar (500µg/ml xylan blue, 2% (w/v) agar in 20mM tris-HCl, pH 7.5) and incubated at 37°C until clearing zones became visible in the xylan-blue agar around the colonies (approximately 2 hours). Plasmid was prepared from colonies retaining xylanase activity after this heat inactivation step, and was

retransformed into Epicurian Coli®. The resulting transformants were streaked out onto a fresh LB-agar plate with ampicillin and grown overnight at 37°C before being subjected to a more stringent screening process.

6.2.5 Further characterisation of improved mutants

Mutants identified from the initial screen as retaining activity after the heat inactivation step were subjected to a longer incubation at 85°C. The potentially improved mutants were streaked out onto fresh LB-agar plates, as described above, alongside cells containing the original pUC18.cd2 construct. The resulting colonies were incubated at 85°C for 45 minutes, before being chilled at -20°C and assayed for residual activity by the RBB-xylan agar overlay assay, as described in section 6.2.4. Plasmid was prepared from cultures of each mutant still retaining activity after this extended heat inactivation, as described in section 2.1.8, and the mutant xylA.cd2 insert was sequenced to identify any mutations in the coding sequence.

6.2.6 Expression and partial purification of mutant xylA.cd2 enzymes

The mutant xylA.cd2 proteins were expressed from 50ml cultures of LB supplemented with 100µg/ml ampicillin as described in section 2.2.5. Epicurian Coli® cells harbouring the mutant plasmid clones were harvested after approximately 16 hours of growth. The cells were disrupted by sonication and a cell extract was prepared as described in section 2.2.5.1.

6.2.7 Characterisation of mutant xylA.cd2 enzymes

The unfractionated preparations of mutant xylA.cd2 enzymes, along with a similar preparation of the original xylA.cd2 enzyme for comparison (transformed into Epicurian Coli® cells and prepared as described above), were characterised in the same way as the original xylA.cd2 protein (Chapter 3). Their specific activities were determined as outlined in section 3.2.5. Temperature optimum for activity was determined for all the enzymes as described in section 3.2.6, and their thermal stability at 60°C was determined by a thermal inactivation study as described in section 3.2.7.

6.3 RESULTS

6.3.1 Construction of the random mutant library

The *xylA.cd2* insert was amplified from pUC18.cd2 using primers designed to a region of the pUC18 vector flanking the poly-cloning site. The sequence of primers 5 and 6, which were a kind gift from Dr Simon Andrews, can be found in the Appendix.

6.3.1.1 Amplification of *xylA.cd2* by EP-PCR

The first round of EP-PCR resulted in a product with all of the template dilutions used (Figure 6.1a). The product from the 1/100,000 diluted template reaction was used as the template for the second round of EP-PCR. The second round reactions also resulted in a product being formed with all of the template dilutions used (Figure 6.1b). As for the second round reactions, the 1/100,000 diluted template reaction product was used as the template for the third round of EP-PCR. This time a significant product was formed only with the 1/1000 template dilution (Figure 6.1c). This third round product was purified by phenol/chloroform extraction, digested with HindIII and EcoRI and directionally cloned into similarly digested pUC18 plasmid vector. After transformation into electrocompetent Epicurian Coli® cells, successful transformants were selected for by growth on LB-agar plates containing 100µg/ml ampicillin.

6.3.1.2 Estimation of library size and number of active clones

Plating varying volumes of the transformed Epicurian Coli® cells onto LB-agar plates containing ampicillin, X-gal and RBB-xylan allowed an estimation of the size of the library and the proportion of xylanase-active clones. X-gal allows blue/white screening, indicating clones that do not/do contain an insertion in the poly-cloning region of the pUC18 plasmid, and RBB-xylan allows clones to be assessed for xylanase activity, with colonies expressing active mutant *xyl.cd2* displaying a clearing zone around them. These methods of assessment showed that of the white colonies, i.e. the ones with a *xylA.cd2* insert, in the random mutant library, approximately 50% were xylanase-active. The total size of the library, estimated by dividing the number of colonies on a plate by the

volume spread onto the plate, and multiplying by the total volume of the library, is approximately 60,000 clones.

6.3.2 Selection criteria for agar plate screen

The original xylA.cd2 enzyme was used to set selection criteria by which the random mutant enzymes could be assessed, using the method described in section 6.2.4. After determining that 85°C was a suitable temperature for the heat inactivation step, the original xylA.cd2, transformed into Epicurian Coli® cells, was subjected to inactivation at 85°C for 15, 30 and 45 minutes. After 30 minutes the majority of colonies did not show any remaining xylanase activity on the RBB-xylan agar. After 45 minutes all xylA.cd2 activity had been inactivated, as judged by the complete lack of clearing zones around colonies on the RBB-xylan agar. From these results it was decided to initially incubate the cells transformed with the random mutant library at 85°C for 30 minutes, then choose the colonies with a large visible halo around them and assay for remaining activity after 45 minutes at 85°C using the RBB-xylan agar overlay assay.

6.3.3 Identification of stable mutants

Using the initial agar plate screen (section 6.2.4) approximately 3500 colonies were screened and 24 mutants were identified as having large halos, indicating strong residual activity, after 30 minutes at 85°C. Plasmid was prepared from these 24 colonies, retransformed into Epicurian Coli® cells and subjected to a longer inactivation at 85°C. The original xylA.cd2 enzyme was incubated alongside the mutants for comparison. The results of this secondary heat inactivation step identified 4 mutants that still retained xylanase activity after 45 minutes, whereas the remaining 20 mutants, along with the original xylA.cd2, had no clearing zone around them, indicating no residual activity. These 4 mutants were identified as mutants 3, 4, 5 and 12, and were designated as such for further study.

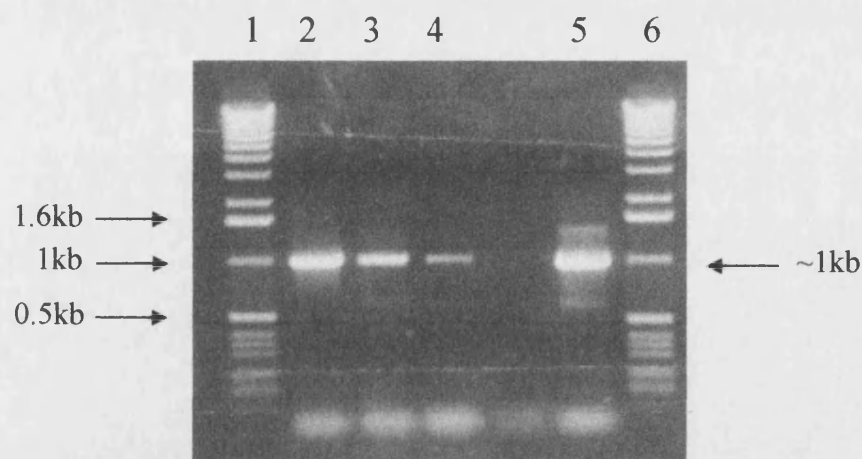


Figure 6.1a

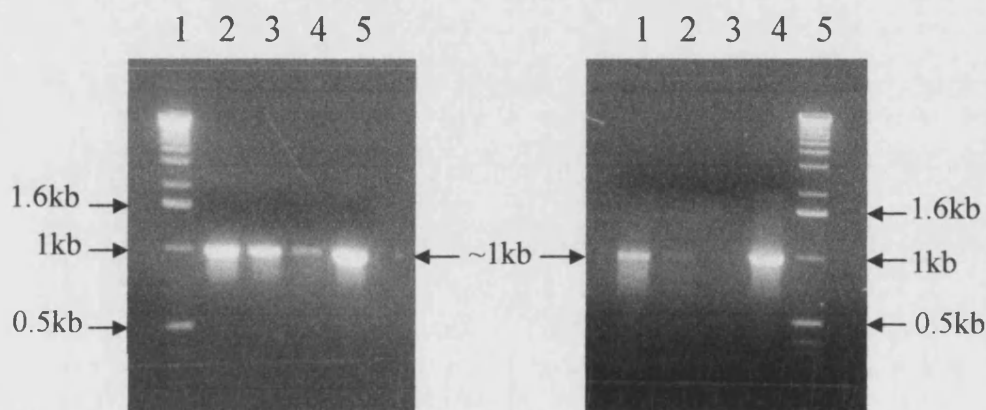


Figure 6.1b

Figure 6.1c

Figure 6.1 Identification of EP-PCR products by agarose gel electrophoresis

6.1a First round reaction products

Lane 1, 1kb DNA molecular weight markers; lane 2, 1/1000 diluted template product; lane 3, 1/10,000 diluted template product; lane 4, 1/100,000 diluted template product; lane 5, control reaction product (non-error inducing conditions); lane 6, 1kb DNA molecular weight markers.

6.1b Second round reaction products

Lanes as 6.1a lanes 1-5.

6.1c Third round reaction products

Lane 1, 1/1000 diluted template product; lane 2, 1/10,000 diluted template product; lane 3, 1/100,000 diluted template product; lane 4, control reaction product, lane 5, 1kb DNA molecular weight markers.

6.3.4 Sequencing of mutants 3, 4, 5 & 12

The inserts of the 4 mutant plasmid clones were sequenced using the M13 universal sequencing and reverse primers. One sequencing reaction from each direction allowed the full insert sequence to be obtained. Comparison of the mutant sequences to that of the original identified PCR-introduced mutations in the inserts for mutants 3, 4 and 12, and these are summarised in Table 6.2. No sequence mutations were identified in the xylA.cd2 coding region for mutant 5.

6.3.5 Characterisation of mutants 3, 4, 5 & 12

In order to further characterise the 4 isolated mutant enzymes, they were each expressed from a 50ml culture and partially purified by preparing a cell extract. A cell extract from a culture expressing the original xylA.cd2 was also prepared, and was assayed alongside the 4 mutants so that a comparison could be made between them.

6.3.5.1 *Specific activities*

The specific activities of the partially purified mutants and original xylA.cd2 were determined by carrying out a series of standard assays using dilutions of the cell extracts from 1/250 to 1/10,000. It was determined that a 1/4000 dilution of all the partially purified enzymes would be an appropriate dilution to use in order to ensure initial rates were being measured in further assays (data not shown). Table 6.3 summarises the specific activities.

6.3.5.2 *Temperature optima for activity*

The partially purified enzymes were assayed at various temperatures from 19°C to 80°C, and these results are shown in Figure 6.2. For ease of comparison the activity has been converted to specific activity, and the activity profiles for each of the 5 enzymes have been plotted on the same graph. Blank reactions (with 100µl PC buffer in place of the 100µl enzyme dilution) were carried out at each temperature to account for any degradation of the soluble xylan substrate at the higher temperatures, although no

significant increase in absorbance of the blank samples was observed. The maximum activity of the original xylA.cd2 and the mutant enzymes was observed at 55°C.

6.3.5.3 Thermal stability at 60 °C

Using the information already obtained about the thermal characteristics of the original xylA.cd2 (Chapter 3), 60°C was chosen as a suitable temperature at which to study the thermal stability of the partially purified mutants. Each mutant enzyme was heat inactivated over 15 minutes at 60°C, and Figure 6.3 graphically represents these results. Table 6.4 summarises the half-lives of each of the 4 mutant enzymes, in comparison to the half-life at 60°C of the original xylA.cd2.

MUTANT	LOCATION OF MUTATION*	ORIGINAL BASE	NEW BASE	ORIGINAL AMINO ACID	NEW AMINO ACID
3	136	A	G	Asn	Asp
4	652	A	G	Thr	Ala
12	88	A	G	Asn	Asp

Table 6.2 Summary of mutations identified in the xylA.cd2 coding region of the 4 random mutant clones

*The 'location of mutation' column refers to the base number of the mutation within the xylA.cd2 coding region, where the full region is 675 bases.

ENZYME	SPECIFIC ACTIVITY ($\mu\text{mol}/\text{min}/\text{mg}$ protein)
Original xylA.cd2	331
Mutant 3	306
Mutant 4	297
Mutant 5	229
Mutant 12	301

Table 6.3 Summary of original and mutant xylA.cd2 enzyme specific activities

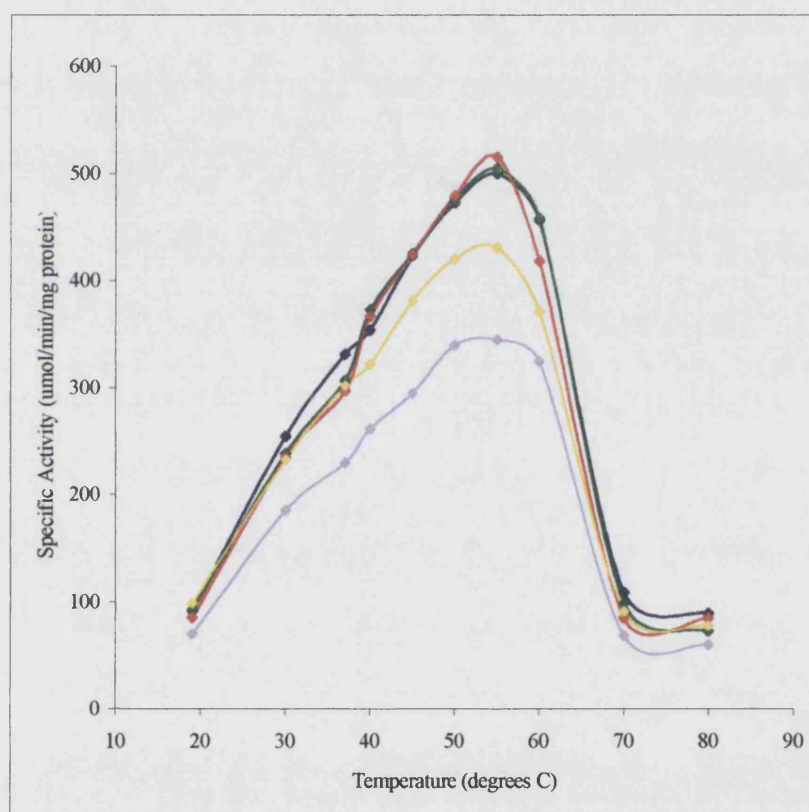


Figure 6.2 Temperature activity curves for original and 4 mutant xylA.cd2 enzymes

Activities are expressed as specific activity for each individual temperature. Each point represents the mean of duplicate assays. Blue line represents original xylA.cd2; green line represents mutant 3; red line represents mutant 4; purple line represents mutant 5; yellow line represents mutant 12.

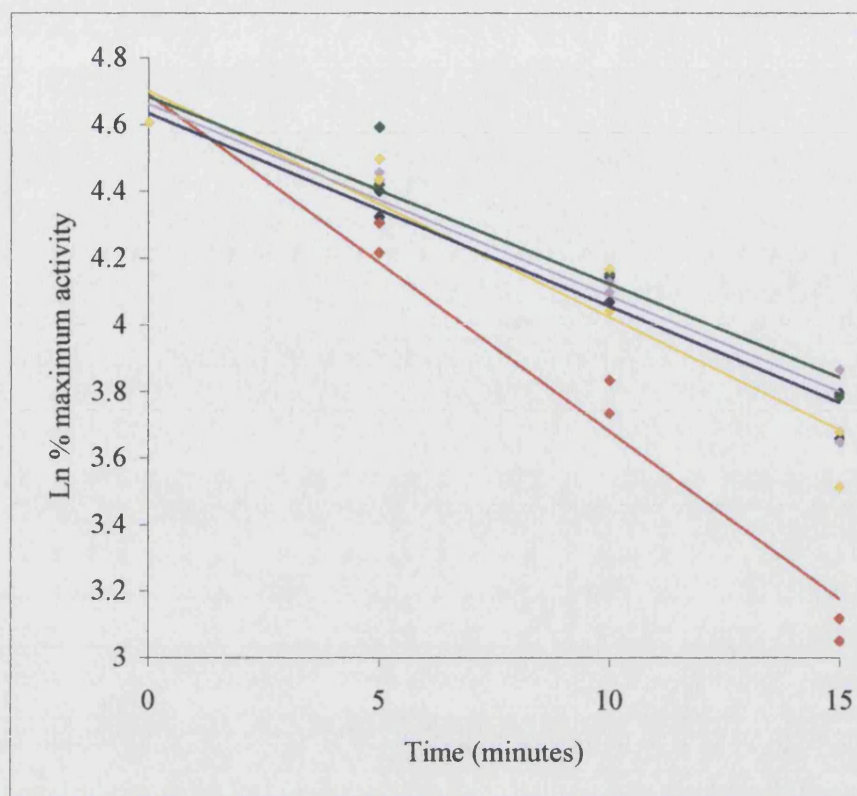


Figure 6.3 Thermal inactivation at 60°C of original and 4 mutant xylA.cd2 enzymes

Data are shown as ln (% activity) against incubation time (% activity being calculated as a percent of maximum activity, seen at time 0). Lines of best fit, calculated by linear regression, are shown. Blue line represents original xylA.cd2; green line represents mutant 3; red line represents mutant 4; purple line represents mutant 5; yellow line represents mutant 12.

ENZYME	$T_{1/2}$ AT 60°C (min)
Original xylA.cd2	12.5
Mutant 3	13.5
Mutant 4	8
Mutant 5	13
Mutant 12	11.5

Table 6.4 Comparison of half-lives at 60°C of original and mutant xylA.cd2 enzymes

6.4 DISCUSSION

6.4.1 Random mutant library construction

Error-prone PCR has been used to generate random mutants of the xylA.cd2 coding sequence, and these mutants have been cloned into pUC18 plasmid vector in order to produce a random mutant library where, in theory, each individual clone contains a slightly different xylA.cd2 insert. By using a DNA polymerase with reduced proof-reading ability along with ‘abnormal’ concentrations of MgCl₂ and deoxynucleoside triphosphates, and by diluting the template as much as possible to still achieve a product, it is possible to force the polymerase into making mistakes when it is copying the template DNA. As a result bases are misincorporated into the DNA product, and thus mutations are introduced into the coding sequence. Performing three rounds of EP-PCR, and using serial dilutions of the template, ensures that enough extension has been performed by the polymerase to be certain that mutations have been incorporated into the sequence. The conditions used in the production of this xylA.cd2 random mutant library, which were optimised by Dr Simon Andrews at the University of Newcastle, should result in the introduction of mutations that will equate to one or two amino acid substitutions per mutant enzyme.

6.4.2 Library screening and identification of improved mutants

Using the agar plate-based screen described in sections 6.2.4 and 6.2.5, 3500 random mutant clones were screened, and from these 24 were identified as having strong residual activity after the first heat inactivation step. These 24 were not the only mutants to display activity after the heat step, but the clearing zones around these colonies were clearly visible early after they had been overlaid with RBB-xylan. For ease of handling 24 mutants were chosen initially, and of these 24 four seemed to show improvements in stability after the second heat inactivation step.

Mutants 3, 4, 5 and 12 were identified from the secondary screen as being more stable than the original xylA.cd2. On sequencing the inserts of these four mutants it became apparent that while 3, 4 and 12 do have introduced errors in their sequence, mutant 5 does not. Mutants 3 and 12 share the same amino acid substitution, although not in the

same position within the enzyme; they both have a residue substituted from an asparagine to an aspartic acid. These substitutions could be considered 'thermostabilising' as the amide side chain of asparagine can undergo deamidation at higher temperatures, so changing it to a residue with a more stable side chain should help to improve the stability of the protein. Additionally, the peptide bond between asparagine and other amino acids is more prone to cleavage at elevated temps so removing this factor may also help to improve stability. Mutant 4 has a threonine to alanine substitution, and it is difficult to predict how, if at all, this substitution may lend itself to increasing thermostability. It is also difficult to suggest why mutant 5 appears more stable than the original xylA.cd2 when there are no apparent mutations in its sequence. One possible suggestion could be that a mutation outside the xylA.cd2 coding region, for example in the few lacZ residues expressed on the N-terminal of the xylA.cd2 protein, has lead to either an increase in stability, which would explain the results obtained, or an increase in expression of the enzyme. The latter may explain the observed results if an increase in expression meant that more enzyme was present inside the colonies containing the mutant 5 clone. More enzyme may mean that over the same heat incubation time as the other mutants not all the enzyme was inactivated. Or alternatively, the cells may lyse on heating and colonies expressing more enzyme may release it onto the agar, causing an artificially high clearing zone of activity when the plates are overlaid with RBB-xylan.

6.4.3 Expression and partial purification of improved mutants

In order to characterise mutants 3, 4, 5 and 12 in more detail these mutant enzymes were partially purified and their temperature activity profiles and thermal stability at 60°C were studied. As these are only partially purified enzymes, and the characterisation data available for the original xylA.cd2 is on pure protein, a cell extract was also prepared from a culture of the original enzyme, and this was studied in parallel to the mutants so that a true comparison between them could be made. As for the original xylA.cd2, these mutants are cloned in frame with the lacZ promoter of pUC18 and as a result the expressed protein has the extra few amino acids at the N-terminus. A mutation in these residues could be the reason for the apparent increase in stability seen in mutant 5, as

discussed above, although the sequence observed was only definite for the actual xylA.cd2 coding region so mutations in these residues could not be determined with certainty.

6.4.4 Comparison of improved mutants to original xylA.cd2

Before the EP-PCR library was screened for mutant xylA.cd2 enzymes displaying an improvement in thermostability, the agar plate-based screening method, outlined in section 6.2.4, was used to set selection criteria by which the mutants could be assessed. The original xylA.cd2 enzyme was put through the screen, and its characteristics were used to set the criteria that promising mutants must exceed in order to be considered improved in their thermal stability.

All four mutants demonstrate the same optimum temperature for activity as the original xylA.cd2 (55°C). In addition, the thermal stability data suggest that none of the mutants are any more stable than the original. They all have very similar half-lives at 60°C to the original xylA.cd2 (around 12 minutes), with the exception of mutant 4 which has a reduced half-life of 8 minutes. When the specific activities are compared mutants 3, 4 and 12 are all similar to each other and to the original enzyme while mutant 5 has an apparently decreased specific activity. These values are, however, only a rough guide. Specific activities calculated from cell extracts are subject to the influence of other factors, for example actual expression levels, and as such a true comparison of specific activities can only be made with values obtained from pure protein.

From these characterisation results it can be concluded that these four mutant xylA.cd2 enzymes do not demonstrate any improvements in stability in comparison to the original enzyme.

6.5 CONCLUSIONS

This chapter has described the use of directed evolution in attempts to develop a mutant xylA.cd2 enzyme that displays an improved thermal stability in comparison to the original enzyme. A random mutant library of xylA.cd2 clones has been produced, and an agar plate-based screening method has been used in an attempt to identify mutants demonstrating an increase in thermal stability. Four potentially improved mutants were isolated using this screen, but on further characterisation they did not actually appear to be any more stable than the original enzyme.

The results obtained in this chapter highlight the need for a much more reliable method of screening the random mutant library. It is often said that directed evolution experiments are only as successful as the screen used to isolate improved mutants from the random mutant library, and this has been demonstrated here. The agar plate screen used in this chapter has proved to be unsuccessful in isolating mutants demonstrating a true increase in stability, and confirms the need for a much more consistent and reproducible method of screening.

Chapter 7

DEVELOPMENT OF A SYSTEM FOR RANDOM MUTANT LIBRARY SCREENING

7.1 INTRODUCTION

Random mutagenesis experiments rely crucially on the accuracy of screening methods in order to identify variants from a random mutant library that show improvements in the desired properties. This has been demonstrated in Chapter 6, where the initial method of screening the *N. patriciarum* xylA.cd2 random mutant library has proved to be unreliable in identifying promising mutants demonstrating an increase in stability. The aim of this project is to increase the stability of xylA.cd2 whilst retaining its activity at physiological temperatures. This means that the directed evolution screening process needs to be capable of selecting for two individual properties: increased stability at elevated temperatures and maintenance of high activity at physiological temperatures. It has been shown that often the activities of thermophilic enzymes at lower temperatures are compromised with respect to their mesophilic or psychrophilic homologues (Meiering *et al.*, 1992; Shoichet *et al.*, 1995). This has lead to the suggestion that enzymes cannot be both highly thermostable and highly active at low temperatures. Rather than being due to a mutually exclusive relationship (stability and activity making mutually exclusive demands on enzyme flexibility), an explanation for this observed trade-off between stability and activity could be simply that natural selection has selected for one or the other, but not both properties (Schreiber *et al.*, 1994). This would suggest that it is possible for enzymes to be both thermostable and active at lower temperatures, providing that selective pressure is applied for both properties at the same time.

96-well plate based systems are commonly used in situations where many samples need to be screened quickly and efficiently. The availability of mechanical equipment such as automated colony-picking machines and reagent dispensers means that many more samples can be screened in a given time than would be physically possible by hand.

Even without robotic equipment microtitre plates allow efficient organisation of samples, and with basic equipment such as multi-channel pipettes many samples can be screened easily and proficiently. It is the aim of this section of work to design an efficient system that will facilitate the screening of a random mutant library of xylA.cd2 clones, and thereby permit the identification of variants demonstrating an increased stability whilst retaining high levels of activity at lower temperatures. In order to make the screen as efficient as possible, consideration has to be given not only to the effectiveness of each stage of the screening process, but also to the ease and convenience with which the screen may be performed. The basis for development of this screen comes from the thermostability screening method used by Giver *et al.* (1998). Their method of cell growth and thermostability screening in microtitre plates has been adapted for the xylA.cd2 enzyme. All the developmental work described in this chapter has been carried out on pUC18.xylA.cd2 clones transformed into *E. coli* JM109 cells. Due to the developmental nature of this section of work, this chapter will be in a slightly different format to previous ones, and will focus on each section of the screen individually.

7.2 MATERIALS AND EQUIPMENT

7.2.1 Materials

Lysozyme and Breath-Easy™ breathable membranes (catalogue number Z38,006-9) were purchased from Sigma, Poole, Dorset, UK. Thermofast® 96-well PCR plates and heatproof adhesive seals were purchased from Abgene, Surrey, UK. Gilson DistriTip repeat dispensing syringes were purchased from Anachem, Bedfordshire, UK. Deep-well plates and flat-bottomed microtitre plates were purchased from Thermo Life Sciences, Hampshire, UK. BugBuster™ protein extraction reagent was purchased from Novagen UK, Nottingham, UK (catalogue number 70584-3). All other materials not listed here can be found in sections 2.1.1 and 2.3.1.

7.2.2 Equipment

A Gilson Distriman repeat pipette and Finnpipette electronic multi-channel pipettes were used to dispense sample aliquots and manipulate micro-cultures. A Grant microplate heater, model QBTP, was used initially to heat the 96-well plates. The thermal cycler used in subsequent assays was an Eppendorf 96-well Mastercycler. Final absorbance values were measured on a SPECTRAmax® PLUS³⁸⁴ microplate reader and manipulated using SOFTmax® PRO software.

7.3 CELL GROWTH

7.3.1 Aim

To successfully grow JM109 pUC18.xylA.cd2 transformants in 96-well plate mini-cultures.

7.3.2 Method

Initial attempts to grow JM109 pUC18.xylA.cd2 clones in 96-well plate format were carried out in 1ml cultures in deep-well plates. This method proved unsuccessful due to excessive clumping of the cells during growth. Subsequent attempts to grow JM109 pUC18.xylA.cd2 clones were based on the method of Giver *et al.* (1998). 200µl of LB broth, supplemented with 100µg/ml ampicillin, was dispensed into all 96 wells of a flat-bottomed microtitre plate. Each individual well was inoculated with a single colony of JM109 containing the pUC18.xylA.cd2 plasmid using a sterile pipette tip. The plate was then covered with a breathable membrane and incubated at 30°C for 24 hours to allow cell growth. The breathable membrane is made from polyurethane and is permeable to oxygen, carbon dioxide and water vapour. The cultures were incubated with vigorous shaking at 320 rpm to ensure good aeration and gas exchange through the membrane. After 24 hours the mini-cultures were duplicated by transferring 5µl of each well into a new plate containing fresh medium and ampicillin. The original plates were stored at 4°C and the duplicate plates were again covered with a breathable membrane and grown for an additional 16 hours.

7.3.3 Results and discussion

The initial method proved unsuccessful very early on, with the cells clumping together during growth. The 1ml cultures were difficult to manipulate easily and rapidly due to their large size. The deep-well plates also proved difficult to seal with a membrane, and as such cross-contamination could not be ruled out.

The subsequent method was much more successful, both in terms of actual culture growth and ease of execution. Using standard 96-well microtitre plates and smaller volumes means that the cultures are easy to manipulate using multi-channel pipettes.

Growing the cultures at a slightly lower temperature eliminated the clumping problem, and sub-culturing for a second time seemed to even out the growth generally over all the wells so that the cell density (estimated by reading the absorbance of the cultures at 600nm) was fairly uniform over the entire plate. The breathable membranes were effective at sealing individual wells while still allowing the necessary gas exchange for cell growth. Cross contamination between wells was eliminated using the smaller culture volumes in standard microtitre plates. This was demonstrated by dispensing media to all wells of a plate but only inoculating a selection with single colonies. After incubation at 30°C for 24 hours there was only growth visible in the wells that had been inoculated with a single colony.

7.4 LYSIS OF CELL CULTURES

7.4.1 Aim

To develop a successful method of lysing the 200µl mini-cultures of JM109 cells containing the pUC18.xylA.cd2 plasmid, so that the xylA.cd2 enzyme can be released and subsequently assayed for activity.

A set of experiments was performed to determine which method, from a selection of commonly used cell lysis methods, would be most suited to lysing the mini-cultures *in situ* in the 96-well microtitre plates. In addition to the effectiveness of lysis, each method was assessed for ease and convenience of use. The effectiveness of each method was determined by assaying the culture lysate for xylanase activity using a scaled-down version of the standard DNS assay described in section 2.3.2.

7.4.2 Method

The methods of lysis studied were:

- a) Lysozyme
- b) Freeze-thawing
- c) BugBuster™
- d) Sonication

These methods were compared to cultures assayed for xylanase activity without any method of cell lysis. The protocol is outlined below:

4 plates containing replicas of the same twelve 200µl mini-cultures of JM109 harbouring the pUC18.xylA.cd2 plasmid were treated as follows: Plate 1 was treated with a 10mg/ml stock of lysozyme (isolated from chicken egg white)(1µl per 100µl of culture was added to each well to give a final concentration of 100µg/ml) and incubated at room temperature for 2 hours; plate 2 was stored at -20°C overnight to lyse the cell cultures by freeze-thawing; plate 3 was treated with 40µl of BugBuster™ (a commercially available detergent-based protein extraction reagent that perforates the *E. coli* cell wall to liberate the soluble protein) per well and incubated at room temperature for 15 minutes (according to manufacturer's instructions); plate 4 cultures were lysed by sonication (cultures subjected to 30s burst at 8-10 microns, peak to peak).

After lysis each culture was assayed for xylanase activity as follows. The standard DNS assay was scaled down 5-fold so that the whole assay could be performed in 96-well plates. 20µl of the lysed cell cultures were transferred to a 96-well plate and incubated with 80µl of 0.2% soluble xylan for 15 minutes at 37°C. The assay was terminated by the addition of 100µl of DNS reagent and the plates were incubated at 100°C for 20 minutes, followed by 10 minutes on ice. The absorbance of each sample was read in a microplate reader at 575nm.

7.4.3 Assessment of results

METHOD	% ACTIVITY (in comparison to no lysis)
No lysis	100 ± 5.5
Lysozyme	145 ± 5.6
Freeze-thawing	125 ± 4.4
BugBuster™	113 ± 8.1
Sonication	138 ± 10.1

Table 7.1 Comparison of xylanase activity after the various lysis methods tested

Activity is expressed as percent activity observed in the cultures assayed after no method of lysis (where 'no lysis' activity is 100%). Values given are mean ± standard error of 12 assays.

Table 7.1 summarises the lysis experiment results, and shows the mean and standard error of 12 samples assayed after the various lysis methods. It can be seen that the increase in activity seen after the various methods of lysis is not that large, with an average maximum increase of only 45% seen when lysozyme is used. The pUC18.xylA.cd2 clone expresses high levels of the highly active xylA.cd2 protein, which are detectable without actually lysing the cells. This is also visible when the Congo Red overlay assay is used to detect xylanase activity in *E. coli* cells streaked out on agar plates: these cells exhibit activity yet they are not broken open during the course of the assay. For the purpose of lysing random mutant xylA.cd2 cell cultures in the 96-well plate screen, the aim is to release as much of the enzyme as possible so that the

maximum amount of activity can be detected when the mutants are screened for activity and stability.

The above results suggest that using lysozyme has been the most effective way of lysing the cells, giving an increase in activity of just under 50%. In more detail, the method of lysis was as follows: 1µl of a 10mg/ml stock of lysozyme was added per 100µl of cell culture, giving a final concentration of 100µg/ml. After addition of lysozyme the wells were thoroughly mixed using a pipette to ensure even distribution of the lysozyme throughout the cell culture, and then the mixed cultures were incubated at room temperature for 2 hours with vigorous shaking at 320rpm, before being assayed for xylanase activity.

The other methods of lysis used varied in their success. Sonication showed an average increase in activity of 38%, only a few percent lower than lysozyme. Sonication, however, was the most difficult and time-consuming method to perform, with each well having to be sonicated individually, and it also had the largest error associated with it. There is a drop in increased activity seen between sonication and freeze-thawing, with freeze-thawing only showing a 25% average increase in activity over the 'no lysis' control. BugBuster™, the final method to be tested, was the least successful, showing an average increase in activity of only 13%. This method also had quite a large standard error associated with it.

The above results clearly suggest that lysozyme is the most effective method of lysing mini-cultures in 96-well plates. In addition to being effective at lysing the cells it was a simple method to employ, confirming that it would be ideal for the random mutant library screening system; the lysozyme was distributed into individual wells using a repeat dispenser, then the wells were mixed by pipetting the culture up and down with a multi-channel electronic pipette. The plates were then simply incubated with shaking at room temperature for 2 hours before being assayed.

7.4.4 Optimisation of lysis using lysozyme

Having determined that using lysozyme is the most effective way to lyse mini-cultures in 96-well plates, the method was optimised further in order to obtain as great an increase as possible in the activity seen in comparison to control cultures that have not been lysed.

Lysis of the mini-cultures was observed using a final lysozyme concentration of 100µg/ml, and with an increased concentration of 250µg/ml at both room temperature and 37°C for varying incubation times. After incubation the samples were assayed for xylanase activity as described above.

7.4.5 Assessment of results

	ROOM TEMPERATURE		37°C	
	100µg/ml lysozyme	250µg/ml lysozyme	100µg/ml lysozyme	250µg/ml lysozyme
No lysis	100	100	100	100
1hr incubation	108	145	101	111
2hr incubation	139	227	92	115
4hr incubation	161	196	79	101

Table 7.2 Comparison of xylanase activity after lysis of cell cultures with lysozyme for varying times and at varying temperatures

Activity is expressed as percent activity observed in the cultures assayed after no method of lysis (where 'no lysis' activity is 100%). Values given are the mean of duplicate assays.

Table 7.2 summarises the attempts to increase the amount of activity seen in cell cultures after lysis by varying the original lysozyme method conditions. It can be seen that increasing the concentration of lysozyme used from 100µg/ml to 250µg/ml made a significant difference at room temperature. After only a one hour incubation the activity had increased by almost 50%, equivalent to the increase seen after 2 hours incubation with 100µg/ml lysozyme. Another large increase was seen after 2 hours incubation, where over a 100% increase from the no lysis control was observed. After 4 hours

incubation with 100µg/ml lysozyme the activity was still increasing, and showed a 61% increase over the no lysis control. 4 hours incubation with 250µg/ml lysozyme showed a decrease in activity compared to the 2 hours value, but the activity remained significantly higher than after 4 hours with 100µg/ml.

Incubation at 37°C was not as successful as at room temperature, with both lysozyme concentrations used. The maximum amount of activity observed at 37°C was after 2 hours incubation with 250µg/ml lysozyme, but this only showed an increase of 15% above the no lysis control. A possible explanation for the decrease in activity seen after incubation at 37°C could be that the xylA.cd2 enzyme is being degraded by proteolysis. Intra-cellular proteases released as the cells are lysed could be responsible for breaking down some of the expressed xylA.cd2, and as a result a lower activity is observed. This would help to explain why less activity is seen at 37°C, as the proteases would be more active at this temperature.

7.4.6 Final culture lysis conditions

The results of these above experiments clearly demonstrate that in order to obtain the maximum amount of xylanase activity from random mutant xylA.cd2 mini-cultures the best way to lyse the cells is to use an increased concentration of 250µg/ml lysozyme, and to incubate the cultures at room temperature for 2 hours with vigorous shaking at 320 rpm.

7.5 OPTIMISATION OF XYLANASE ACTIVITY ASSAY

7.5.1 Aim

To optimise the conditions of the scaled down DNS assay in terms of lysate volume, amount of substrate and assay incubation time to ensure that the initial rate of reaction is measured.

Initially the 96-well plate assays were performed in flat-bottomed plates and the incubation steps were carried out on a micro-plate heater. As the assay optimisation progressed it became clear that this method was inaccurate and was compromising the precision essential for this screen. The improved method places samples to be assayed in 96-well PCR plates, and uses a 96-well thermal cycler for accurate incubation at any of the given temperatures. The problems associated with using the micro-plate heater will be discussed later.

7.5.2 Standard Curve

With each set of assays performed in 96-well plate format a standard curve was run in parallel. This was achieved using standard solutions of D(+)xylose in a scaled down version of the original method (section 2.3.2). Stock solutions ranging from 0.2 to 1mg/ml were made and 100µl of each of these were transferred to a 96-well plate along with 100µl of DNS reagent. The plate was sealed before being heated at 100°C for 20 minutes to develop the colour. 100µl of the standard solutions were transferred to a new plate to be read for absorbance at 575nm. Figure 7.1 shows a sample standard curve, with each point representing the mean of triplicate samples.

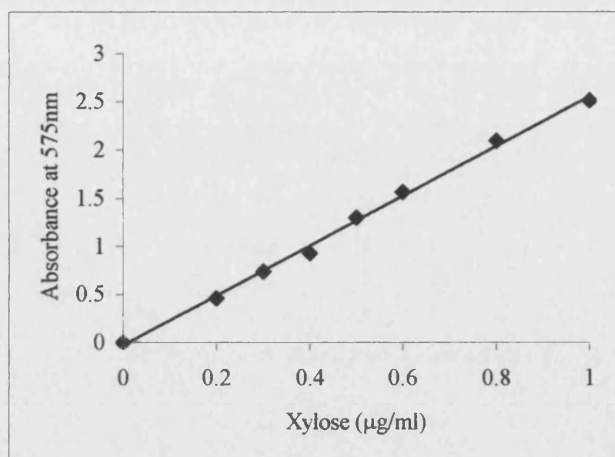


Figure 7.1 A typical standard curve obtained using 96-well plate assay format

7.5.3 Lysate volume, amount of substrate and assay incubation time

Previous studies on the original xylA.cd2 clone (Chapter 3) have shown that the expressed protein is highly active, and that it is necessary to make a large dilution in order to ensure measuring the initial rate of reaction when assaying the enzyme. It is necessary to make sure that the initial rate of reaction for the activity of random mutants is being measured in this 96-well plate screen, as this will ensure that any differences in activity before and after heat inactivation are as clear as possible to identify. Assays were performed with varying amounts of undiluted lysate, then with dilutions of lysate, for varying times to determine the best dilution and time combination that would ensure that the initial rate of reaction was being measured. The concentration of substrate was varied from the original 0.2% soluble xylan used in the standard assays in an attempt to increase the absorbance values obtained at 575nm after the 96-well plate assays; as large an absorbance as possible at 575nm will again help to make differences in activity as clear as possible to identify. The incubation time of the assays in 96-well plate format was also studied so that with the given conditions of lysate dilution and substrate amount it was certain that the initial rate of reaction was being measured. These studies and their results are reported below in chronological order.

7.5.3.1 Undiluted lysate

The culture lysates were assayed for activity as described in section 7.4.2: 20µl of lysate was incubated with 80µl of 0.2% soluble xylan for 15 minutes at 37°C, then 10µl DNS reagent was added and the samples heated for 20 minutes at 100°C to develop the colour. To initially determine the activity of xylA.cd2 in the culture lysates they were assayed undiluted. A comparison of the activity seen in 20µl of lysate and 5µl lysate (made up to 20µl with buffer) showed that the same amount of activity was visible in both, which suggested that both reactions were reaching completion over the 15 minutes of incubation at 37°C.

A time-course study using 5µl of the undiluted lysate showed that after 4 minutes the final absorbance seen at 575nm was the same as that seen after 15 minutes. These results all illustrated that, as expected, the expressed xylA.cd2 in the culture lysates was highly active, and in order to be sure of measuring the initial rate of the reaction the lysates would need to be diluted.

7.5.3.2 Diluted lysate

- Experiment 1

An assay was performed using varying volumes of a 20-fold dilution of culture lysate. The assay used the standard conditions of 15 minutes at 37°C and 0.2% soluble xylan substrate and is performed in a flat-bottomed 96-well plate on a micro-plate heater.

Figure 7.2 shows the results of this assay in graphical form. A linear relationship between observed activity and lysate volume, which is indicative of the measurement of initial rates, was observed only up to 10µl of added lysate. Therefore, if a 20-fold dilution of the culture lysate is to be used in the screen then a volume less than 10µl is necessary.

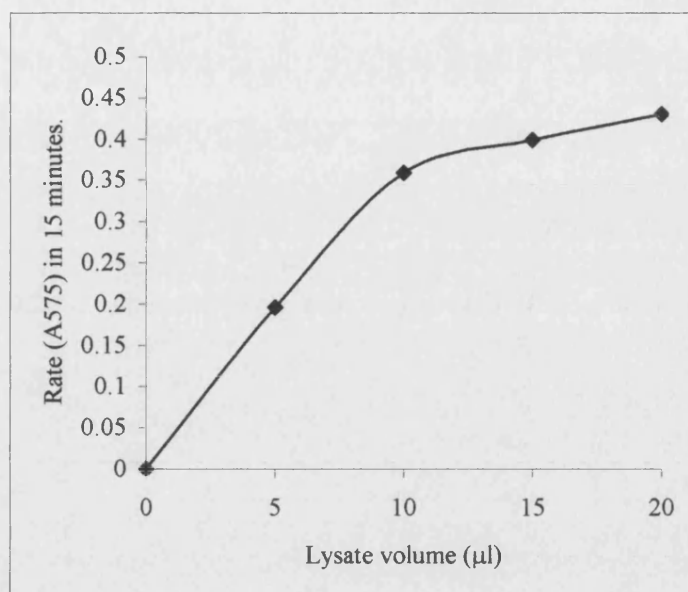


Figure 7.2 Study of xylA.cd2 activity against lysate volume for a 20-fold dilution of cell lysate

Each point represents the mean of 3 individual wells.

- Experiment 2

The above experiment was repeated using further dilutions of the cell lysates. In addition to a 20-fold dilution, 50-fold and 100-fold dilutions were also made and studied. Again the assays were performed using the standard conditions described above. Figure 7.3 graphically represents these assay results, and it can be clearly seen that the results using a 100-fold dilution most closely represent a straight line.

Final lysate conditions chosen from these results are 10μl of a 100-fold dilution of cell lysate.

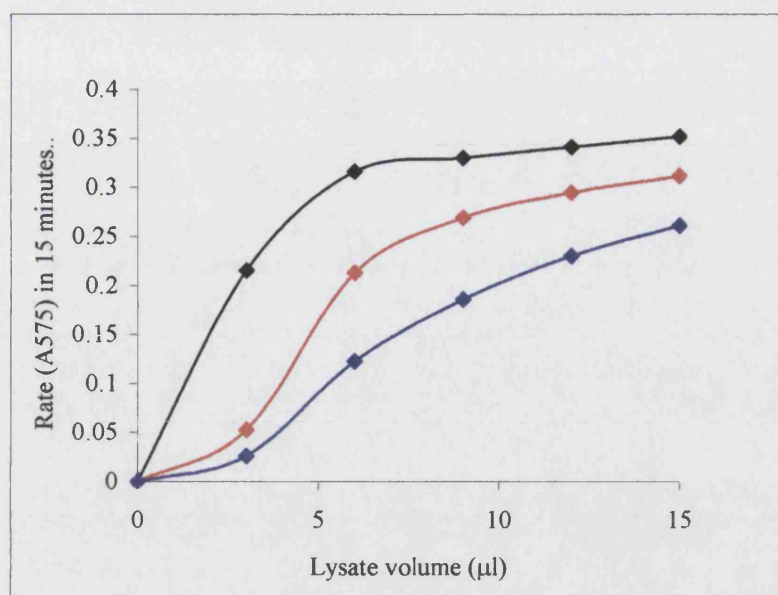


Figure 7.3 Study of xylA.cd2 activity against lysate volume for different cell lysate dilutions

Black line represents 20-fold dilution; red line represents 50-fold dilution; blue line represents 100-fold dilution. Each point represents the mean of 3 individual wells.

7.5.3.3 100-fold lysate dilution: assay incubation time study

Using the new dilution conditions for measuring activity in the cell lysates, a time-course study was carried out to determine the most appropriate incubation time for the assays to ensure initial rates are being measured. 100-fold dilutions of the cell lysates were made, and the assay was allowed to proceed for varying times up to 15 minutes. 0.2% soluble xylan was used as the substrate, and the assays were again performed in a 96-well flat-bottomed plate on a micro-plate heater.

The results of these assays, illustrated in Figure 7.4, clearly show that assaying for xylA.cd2 activity over 15 minutes using 10 μl of a 100-fold dilution of lysate does not measure the initial rate of the reaction. Figure 7.4 shows that the curve begins to level off after 5 minutes, indicating that if 10 μl of a 100-fold lysate dilution is used as the standard conditions for screening then the incubation time for the assays needs to be reduced.

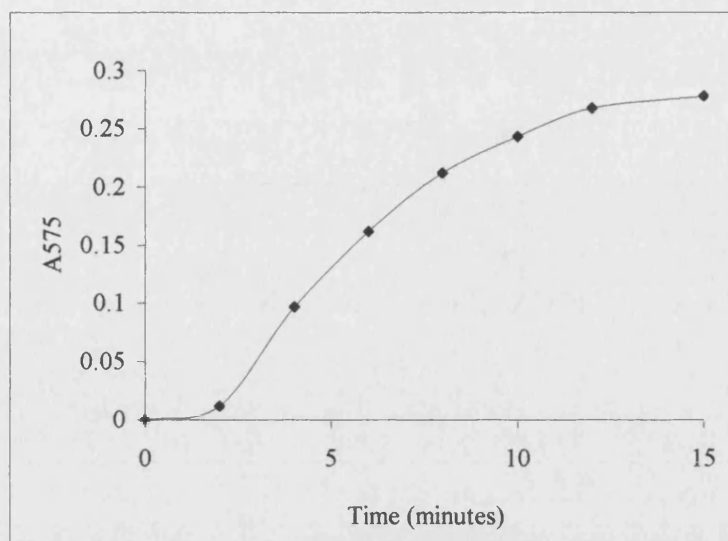


Figure 7.4 Study of xylA.cd2 activity against time for 10 μ l of a 100-fold dilution of culture lysate

Each point represents the mean of 2 individual wells.

It can be seen in Figure 7.4 that there is a visible lag in activity after the first minute of activity. This is most likely due to a delay in heating the reaction mixture to 37°C by the micro-plate reader. If the reaction only just reaches 37°C by the time it is terminated by the addition of DNS reagent then very little activity will be observed. This problem will be discussed in more detail later in this chapter.

Final assay incubation time chosen from these results is 8 minutes.

7.5.3.4 Varying substrate amount

Although the conditions of the assay are ensuring that the initial rate of reaction is being measured, the absorbance values measured at 575nm are quite low. Low absorbance values may make it more difficult to distinguish between variations seen in the random mutants, and to determine whether the variations are actual differences between the mutant and original xylA.cd2, or whether they are insignificant errors within the screening process. If the absorbance values can be increased this will help to eliminate

the possibility of overlooking promising mutants by amplifying the differences in their activity and stability.

Using the standard conditions so far of 10 μ l of a 100-fold dilution of lysate in an 8-minute assay, the percentage of soluble xylan used as substrate was varied and the activity was measured.

Figure 7.5 illustrates the effect of altering substrate concentration over the period of an 8-minute assay. It can be seen that increasing the percentage of soluble xylan used does increase the absorbance values obtained; a 3-fold increase from the 0.2% values is seen with 0.6% soluble xylan, but overall the increase in absorbance values is not that large.

This series of assays was repeated over 15 minutes. Although previously 15 minutes was shown to be outside the linear range of the assay with 0.2% soluble xylan substrate, if the overall absorbance can be increased using a higher percentage substrate over a longer assay then a step back can be taken and the amount of lysate can be altered such that the assay falls back into the linear range. Figure 7.6 represents these assay results, and demonstrates that a higher absorbance can be obtained using a longer assay and higher percentage substrate.

Final substrate percentage chosen from these results is 0.6%. Using this result the assay of activity against time needs to be repeated, using 0.6% soluble xylan to see if a 15-minute assay incubation time is outside the initial rate of reaction. If this is the case then altering the lysate volume may allow the assay to come back into the linear range while still retaining the higher absorbance values.

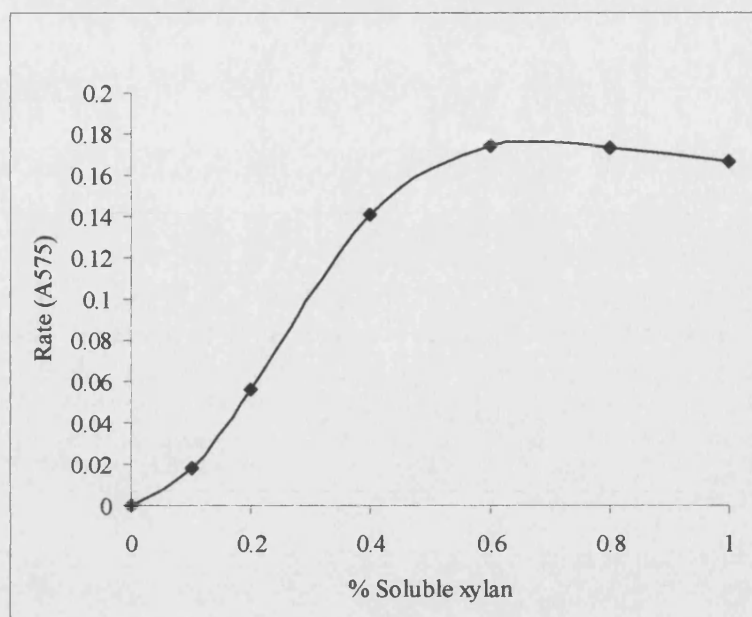


Figure 7.5 Study of xylA.cd2 activity against percentage of soluble xylan substrate for an 8-minute assay

Study used 10 μ l of a 100-fold dilution of culture lysate. Each point represents the mean of 3 individual wells.

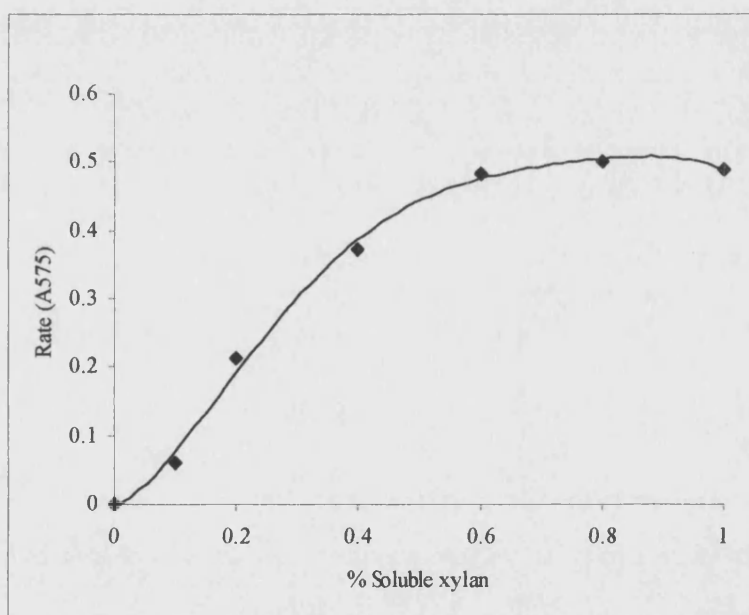


Figure 7.6 Study of xylA.cd2 activity against percentage of soluble xylan substrate for a 15-minute assay

Study used 10 μ l of a 100-fold dilution of culture lysate. Each point represents the mean of 3 individual wells.

7.5.3.5 Assay incubation time study: 0.6% soluble xylan, 100-fold lysate dilution

Using the new substrate amount of 0.6%, a time-course study was performed to determine the longest possible incubation time for the assay that would still allow the initial rate of reaction to be measured. The standard lysate conditions of 10 μ l of a 100-fold dilution were used in the time-course assays.

Figure 7.7 illustrates these results, and it can be seen that with the new percent substrate the assay is almost linear, with the curve beginning to level off after 15 minutes. There is a lag in activity visible after the first 2 minutes of the assay, and this is again most likely due to the samples not getting up to the correct temperature during the course of the assay.

Final assay incubation time based on these results is 10 minutes. There is now a need repeat the assays of activity against lysate volume to see whether decreasing the volume of diluted lysate will help to bring the final stages of this assay over 15 minutes into the linear range.

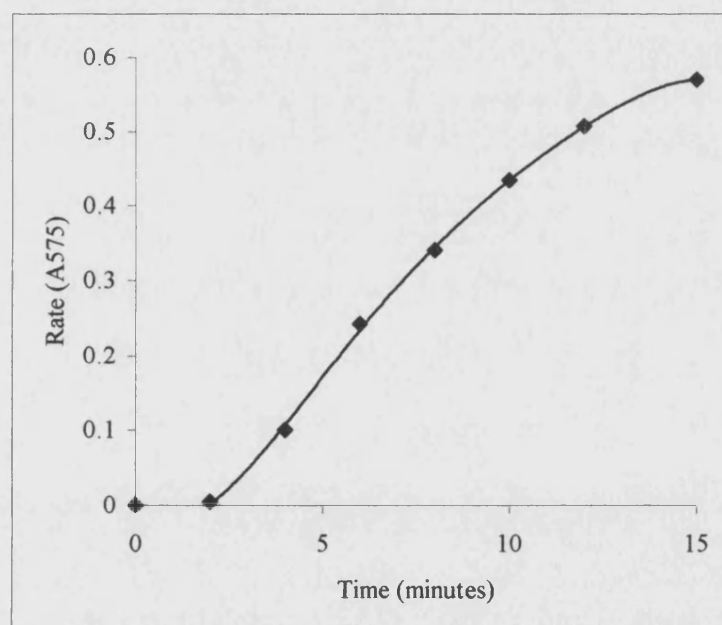


Figure 7.7 Study of xylA.cd2 activity against time

Study used 10 μ l of a 100-fold dilution of lysate and 0.6% soluble xylan substrate. Each point represents the mean of 3 individual wells.

7.5.3.6 Lysate volume study: 100-fold lysate dilution, 0.6% soluble xylan substrate, 15-minute assay

Using the now standard conditions of 0.6% soluble xylan substrate, 15-minute assay and 100-fold dilution of culture lysate, assays were performed that varied the volume of diluted lysate. The substrate and incubation time being used allow greater absorbance values to be observed, but as shown in the above section 15 minutes is outside the linear range of the assay. Reducing the volume of lysate slightly may help to ensure that the initial rate of reaction is being measured, while still allowing larger absorbance values to be measured.

Figure 7.8 represents the results of varying the 100-fold diluted lysate volume in the assay. It shows that if the lysate volume is reduced by just 2 μl , to 8 μl , then the assay comes into the linear range and the initial rate is being measured.

In order to reduce possible sources of error within this 96-well plate screen the number of steps requiring pipetting small volumes of liquid should really be kept to a minimum. Using 8 μl of a 100-fold dilution of culture lysate requires 3 different pipetting stages: one to dispense the buffer and lysate to make the 100-fold dilution; one to transfer 8 μl of the dilution to the assay plate; and one to add 12 μl of buffer to the 8 μl of lysate so that the final volume of the enzyme fraction of the assay is 20 μl . This can be reduced to only 2 stages by increasing the volume of lysate used, but using a more dilute lysate. 8 μl of a 100-fold dilution is equivalent to using 20 μl of a 250-fold dilution. This way, only 2 pipetting stages are required: one to make the dilution and one to transfer the 20 μl to the assay plate. Using this different lysate dilution will eliminate a step where error could be introduced into the screen, and so will help to keep the screen as accurate as possible. A final study needs to be performed using these new dilution amounts to be certain that the assay is still measuring the initial rate of the reaction.

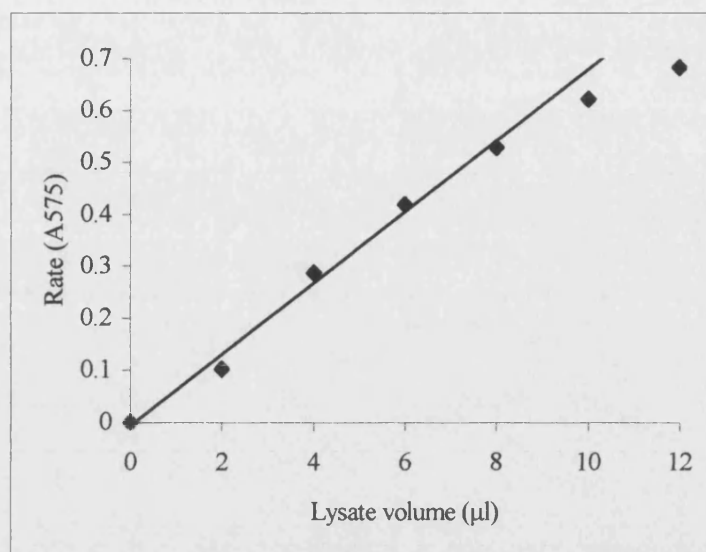


Figure 7.8 Study of xylA.cd2 activity (shown as absorbance at 575nm) against 100-fold diluted lysate volume

Study used 0.6% soluble xylan substrate over a 15-minute assay.

7.5.3.7 Final assay incubation time study: 250-fold lysate dilution, 0.6% soluble xylan substrate

A final time-course study was performed using the new lysate amount of 20μl of a 250-fold dilution, along with the standard 0.6% soluble xylan substrate, to confirm that 15 minutes is still within the linear range of the reaction.

Figure 7.9 represents these results and shows that 15 minutes is actually too long, as the straight-line portion of the graph has begun to level off after 12 minutes.

From these results the final assay conditions have been chosen as 20μl of a 250-fold dilution of culture lysate, with 80μl of 0.6% soluble xylan substrate over a 10-minute assay.

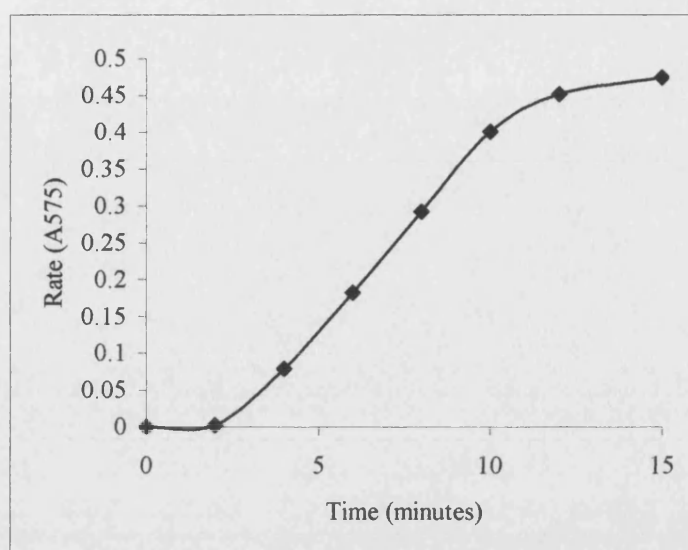


Figure 7.9 Study of xylA.cd2 activity (shown as absorbance at 575nm) against time
Study used 20 μ l of a 250-fold lysate dilution and 0.6% soluble xylan substrate.

7.6 ASSESSMENT OF THERMAL STABILITY

7.6.1 Aim

To develop a successful heat inactivation step that will allow the differentiation of random mutants showing an increase in stability and/or activity from those whose characteristics have remained the same as the original xylA.cd2.

The idea behind this section of the screening process is to determine the activity of individual xylA.cd2 random mutants both before and after a heat inactivation step. Using the method of Giver *et al.* (1998), the stability of each mutant will then be expressed as a ratio of residual (i.e. after heating) to initial (i.e. before heating) activity as follows:

$$S = A_r/A_i$$

Where,

S represents the stability of each mutant

A_r is the residual activity of each mutant, determined by activity assay at 37°C after heat inactivation, and is expressed as absorbance units at 575nm/10 minute assay

A_i is the initial activity of each mutant, determined by activity assay at 37°C, and is expressed as absorbance units at 575nm/10 minute assay

A method needs to be developed that incorporates the standard assay conditions determined in the above section with a heat incubation step so that sufficient loss of activity is seen. Again, all of the optimisation work described in this section has been carried out on pUC18.xylA.cd2 clones transformed into *E. coli* JM109 cells. It is intended to use the information obtained with the original xylA.cd2 enzyme to set selection criteria that will be applied to the randomly mutated enzymes.

It is known from studies of the original xylA.cd2 enzyme described in Chapter 3 that 60°C is a crucial temperature in terms of the stability of the enzyme. 60°C is just above the optimum temperature for activity of the enzyme, and beyond this temperature

inactivation is rapid. This would seem an ideal temperature around which to base the heat inactivation step, as any mutants with improved stability should be easily detectable at this temperature (as is shown with the site-directed mutant of xylA.cd2, described in Chapter 5).

7.6.2 Heat Inactivation: 65°C, micro-plate heater

Initial attempts to determine an appropriate temperature and incubation time for the heat inactivation step were performed in 96-well flat-bottomed plates on the micro-plate heater. Given the lag in activity already observed (thought to be due to the samples not immediately reaching the correct temperature), 65°C was chosen over 60°C for the initial heat inactivation studies. 250-fold dilutions of the culture lysates were made, and 20µl were transferred to a separate plate for the initial activity assay. The remaining 230µl of diluted lysate was heated at 65°C and 20µl samples were taken out at various time points and placed for 5 minutes in a second plate, which had been pre-chilled on ice to stop the inactivation, before being assayed for residual activity.

This method of heat inactivation proved to be somewhat unsuccessful. Figure 7.10 shows the results of this experiment, and it can be clearly seen that, while there is some sort of inactivation taking place, the method is not very accurate. It can be roughly estimated that approximately 50% of activity is lost over 15 minutes. Duplicate experiments were run in tandem, and the results of both are shown in Figure 7.10. It is expected that the results of this experiment should represent an inactivation curve when plotted as in Figure 7.10. The duplicate points are not as similar as would be hoped for two identical experiments on separate dilutions of the same culture lysate. These problems suggest that there has not been uniform heating across the plate during the heat inactivation step.

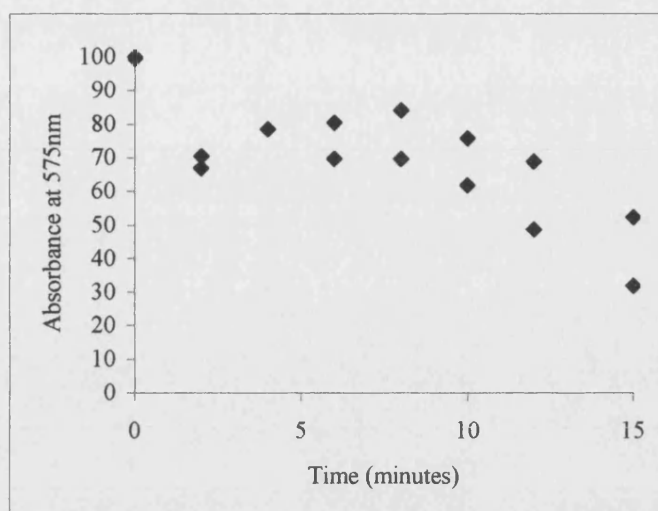


Figure 7.10 Heat inactivation study at 65°C using a micro-plate heater

Duplicate points are shown for each time point. The study used standard assay conditions of 250-fold lysate dilution, 0.6% soluble xylan substrate over 10 minutes. Activity is expressed as percent of maximum activity (observed at 0 minutes).

7.6.3 Problems with micro-plate heater

Throughout these optimisation experiments there have been noticeable problems with the incubation steps, both in the heat inactivation and the various assay steps. It has been apparent that the micro-plate heater has not been efficient at heating the samples being studied in the 96-well plates, and as a result the final absorbance values for the individual wells have not been as precise as they could have been. The most common problems observed are outlined below:

- Uneven heating seen across the whole plate. This is most noticeable after the heat inactivation step but presumably is occurring during all incubations. The effect is mainly due to the fact that the 96-well flat-bottomed plates do not actually sit flat on the heating block of the micro-plate heater.
- At the higher assay incubation temperature the flat-bottomed plates appear to warp over time, again leading to uneven heating across the whole plate.

- The seals used on the plates are not very effective, and at the higher incubation temperatures there is visible leakage and evaporation from individual wells.

It is essential for any screening process that all the individual stages of the screen are as uniform and reproducible as possible, and the introduction of possible sources of error is kept to a minimum. This is particularly important in a screen like this one, which relies on the measurement of small differences in activity to distinguish between random mutants that show an increased stability and/or activity, and those whose characteristics are the same as the original xylA.cd2. The equipment used to manipulate the culture lysates and transfer reagents to and from 96-well plates is all as precise as possible in terms of delivering accurate volumes: electronic multi-channel pipettes with volume handling tips ranging from 1µl to 500µl have been used. The only areas of the screen to be lacking in accuracy and precision are the heating steps.

So far these optimisation experiments have been carried out on cultures of original xylA.cd2, and the results obtained have been sufficient to draw conclusions about each separate optimisation experiment. Now that the assay conditions have been optimised, the real core of the screen needs to be developed; that is, determining the heat inactivation step such that random mutants with an increase in stability will stand out from those whose properties have remained the same as the original enzyme. For this part of the screen it is vital that the heating process is accurate and precise, and that each individual well within a 96-well plate receives the same treatment with regards to timed incubation at a given temperature. It was felt that the only way to achieve this with any degree of certainty was to change the apparatus used to heat the 96-well plates. Therefore, it was decided that the heat inactivation step, and all the assay steps, would now be performed on a 96-well thermal cycler. A thermal cycler is designed to deliver uniform heat, and 96-well PCR plates are designed for efficient heat transfer between the machine and the liquid within the individual wells. In addition, the thermal cycler has a 'hot-top' lid, which will serve to eliminate the evaporation problem seen with the original method.

7.6.4 Heat inactivation: 65°C, 96-well thermal cycler

The heat inactivation time-course experiment described above was repeated, the only difference being the equipment used to carry out the heat steps for both the inactivation and assay. As before, 250-fold dilutions of the culture lysates were made, 20µl were transferred out for the initial activity assay and the rest was heated at 65°C for varying times before being assayed for residual activity. The results of this experiment (not shown) clearly demonstrate that the heat inactivation step is now actually being carried out at the incorrect temperature; 65°C is much too high and all the activity is lost within 10 minutes.

7.6.5 Heat inactivation: 60°C, 96-well thermal cycler

The heat inactivation time-course experiment was repeated exactly as before, the only difference being that the inactivation was performed at 60°C rather than at 65°C. These results, illustrated in Figure 7.11, show clear inactivation and much improvement in the correlation between duplicate samples. This inactivation profile suggests that approximately 40% of activity is lost over 10 minutes.

Based on these results, the heat inactivation step has been chosen as 10 minutes at 60°C.

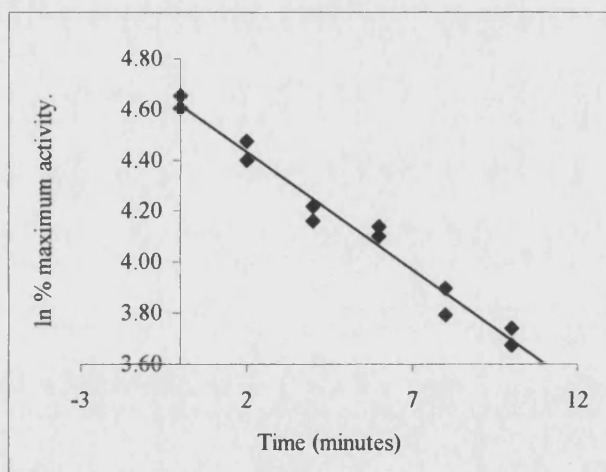


Figure 7.11 Heat inactivation study at 60°C using a 96-well thermal cycler

Duplicate points are shown for each time point. Study used standard assay conditions. Data are shown as ln (% activity) against incubation time (% activity being calculated as a percent of maximum activity, seen at time 0). Line of best fit shown is calculated by linear regression.

7.6.6 Heat inactivation: 60°C, 96-well thermal cycler, inactivating assay volume only

The aim of these optimisation experiments has been to determine the best way of screening random mutants of *xylA.cd2* in the most accurate and precise way possible. As discussed previously, reducing the number of stages within the screen will help to reduce the number of places where errors could be introduced. It was for this reason that it was decided to repeat the heat inactivation study using just the 20µl of diluted lysate required for the assay.

The new method was as follows: 250-fold dilutions of the culture lysates were made, then using a multi-channel pipette on repeat dispense mode 20µl of the dilutions were transferred to 2 new plates. The first plate was assayed for initial activity at 37°C, and the second plate was heated at 60°C for 10 minutes before being placed immediately in an ice/water bath for 5 minutes, and then assayed for residual activity at 37°C. This method was easier to perform in terms of lysate manipulation and ease of handling of the 96-well plates. It was possible to perform the inactivation step with such a small volume of lysate as the heated lid of the 96-well thermal cycler prevented any evaporation.

The results of this study however showed no activity in any of the wells after heating at 60°C. This was most likely due to the fact that the 20µl of diluted lysate reached 60°C almost immediately, and as a result 10 minutes completely inactivated the enzyme. This suggests that the earlier method of heating all the remaining diluted lysate (after 20µl had been removed for the initial activity assay) was not actually that effective at heating the lysate up to 60°C, and in actual fact the lysate dilutions were not up to 60°C for the full period of the assay. One final experiment now needs to be performed, and the heat inactivation time-course study repeated using only 20µl of the diluted lysates to determine an appropriate incubation time for heat inactivation.

7.6.7 Final heat inactivation study: 60°C time-course study with 20µl of diluted lysate only

The final heat inactivation study was a time-course study performed on only 20µl of the diluted lysates at 60°C. Figure 7.12 shows the results of this study. The inactivation profile shows that when heating only 20µl of lysate approximately 40% of activity is lost over only 3 minutes.

From these results the final heat inactivation conditions have been chosen as 3 minutes incubation at 60°C of 20µl of 250-fold diluted culture lysates, followed by immediate incubation in an ice/water bath for 5 minutes, then 5 minutes at room temperature before being assayed for residual activity at 37°C.

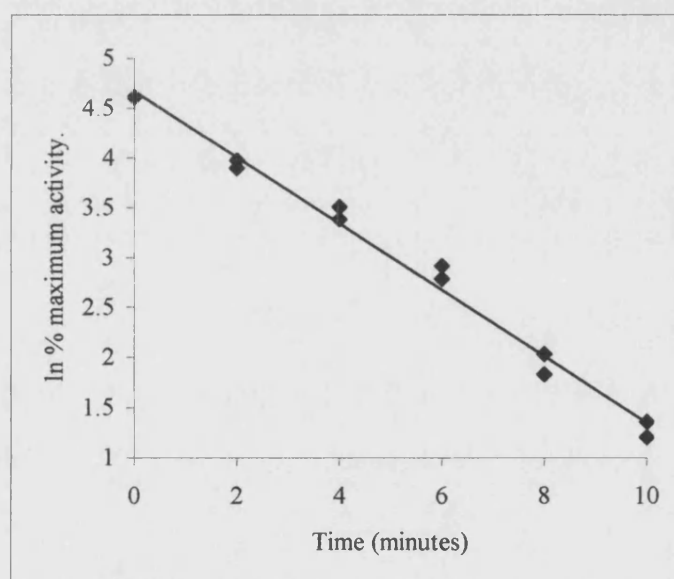


Figure 7.12 Heat inactivation study at 60°C using a 96-well thermal cycler and 20µl of diluted culture lysate only

Duplicate points are shown for each time point. The study used standard assay conditions. Data are shown as ln (% activity) against incubation time (% activity being calculated as a percent of maximum activity, seen at time 0). Line of best fit shown is calculated by linear regression.

7.7 FINAL TEST: USING OPTIMISED CONDITIONS IN AN ASSAY SITUATION

As a final confirmation that the developed 96-well plate screen is as consistent, reproducible and efficient as possible a final test assay was carried out using the original xylA.cd2 enzyme. A whole 96-well plate was inoculated with single colonies of *E. coli* containing the pUC18.cd2 plasmid construct, and the mini-cultures were grown and lysed using the now standard conditions, outlined in sections 7.3 and 7.4 above. The whole plate of lysates was then subjected to thermal stability screening and assay using the final conditions described in sections 7.5 and 7.6.

Figure 7.13 is a plot of stability, represented as A_r/A_i , against initial activity, A_i . This figure demonstrates the range over which values for the original xylA.cd2 can fall. Plotting the data obtained from the screening of true mutants on the same graph will help to visualise those that fall outside the 'normal' range of activities and stabilities for the original enzyme. This will aid the identification of mutants displaying improvements in stability and/or activity. Table 7.3 summarises the data obtained from this final study.

	MEAN VALUE ± STANDARD DEVIATION
Initial activity, A_i	0.835 ± 0.128
Residual activity, A_r	0.410 ± 0.130
Stability, A_r/A_i	0.479 ± 0.074

Table 7.3 Summary of the activity values obtained from the final test of the 96-well plate random mutant library screening system

Activity values shown are mean ± standard deviation obtained from 96 individual cell cultures.

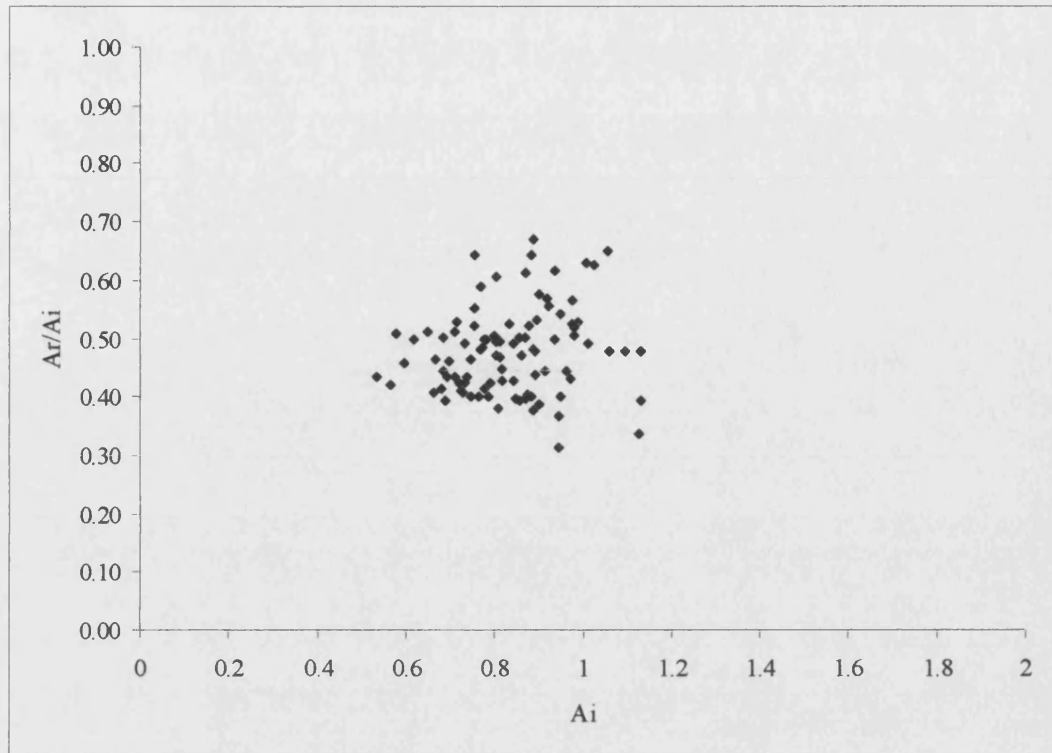


Figure 7.13 Graph showing stability against initial activity for 96 individual xylA.cd2 cultures

7.8 SUMMARY: OPTIMISED PROTOCOL AND SELECTION CRITERIA

The final optimised protocol for screening the xylA.cd2 random mutant library is as follows:

Growth of cell cultures

- Transformants demonstrating xylanase activity on RBB-xylan agar plates will be picked into individual wells of a 96-well plate, with each well containing 200µl of LB with 100µg/ml ampicillin.
- Cultures will be covered with a breathable membrane grown for 24 hours at 30°C with shaking at 320rpm.
- 5µl of each culture will be transferred to a new plate containing 200µl fresh LB with ampicillin and grown for a further 16 hours.

Lysis of cell cultures

- 5µl of a 10mg/ml stock of lysozyme will be dispensed into each well, and the wells mixed thoroughly with a multi-channel pipette.
- The cultures will be incubated at room temperature for 2 hours, with shaking at 320rpm.

Determination of xylanase activity and stability of mutants at 60°C

- Each lysate will be diluted 250-fold in PC buffer.
- 20µl aliquots will be transferred to 2 separate 96-well PCR plates: one plate will be assayed directly for activity at 37°C (initial activity, A_i); the other plate will be assayed for residual activity (A_r) after a heat inactivation step at 60°C.
- The heat inactivation step will be performed by covering the plate with a heat-proof seal and incubating at 60°C for 3 minutes in a 96-well thermal cycler, followed immediately by incubation on ice for 5 minutes, then incubation at room temperature for 5 minutes.

- Both plates will be assayed for activity (either initial or residual) by dispensing 80µl of a 0.6% soluble xylan solution into each well, covering with a heatproof seal and incubating the plates at 37°C in a 96-well thermal cycler.
- After 10 minutes the assay will be terminated by the addition of 100µl DNS reagent. The reagent colour will be developed by incubation at 100°C for 20 minutes in a 96-well thermal cycler, followed immediately by incubation on ice for 10 minutes, then 10 minutes at room temperature.
- 100µl of each sample will be transferred to a flat-bottomed 96-well plate and the absorbance of the plate read at 575nm.

Assessment of thermal stability of mutants

- The ratio of residual to initial activity (A_r/A_i) will be calculated for all the mutants and will be plotted on a graph of A_r/A_i against A_i . Mutant ratio values will be compared to the original xylA.cd2 characteristics.
- Mutants displaying less than 20% of the original xylA.cd2 activity will be discarded from further study.
- Mutants displaying residual activity greater than 60% (A_r/A_i value of greater than 0.6) will be put through a second screening process with a longer heat inactivation step of 5 minutes at 60°C.
- Promising mutants will be compared in more detail to the original xylA.cd2 with respect to their thermal stability and temperature activity profiles.

Chapter 8

RANDOM MUTANT LIBRARY SCREENING USING 96-WELL PLATE SYSTEM

8.1 INTRODUCTION

This chapter will bring together the random mutant library described in Chapter 6 and the 96-well plate screening system optimised in Chapter 7. It will describe the use of the screening system to study the random mutant library, and will describe the isolation of 12 mutant enzymes demonstrating an improvement in thermal stability over the original xylA.cd2. It will describe the characterisation of three of these 12 mutants, and the success of the 96-well plate system, judged by comparing the characteristics of the mutant and original enzymes, will be discussed.

8.2 MATERIALS AND METHODS

All methods used in this chapter not outlined below can be found in Chapters 2, 6 and 7.

8.2.1 Materials

All materials used in this section are as outlined in Chapter 2, sections 2.1.1, 2.2.1 and 2.3.1, Chapter 6, section 6.2.1 and Chapter 7, section 7.2.

8.2.2 Random mutant library screening

The random mutant library was transformed into Epicurian Coli® cells as described in section 6.2.3, and the transformants were spread onto LB-agar plates containing 500µg/ml RBB-xylan in addition to 100µg/ml ampicillin and 40µg/ml X-gal. Colonies with a clearing zone around them were picked into 200µl mini-cultures in 96-well plates and were grown as described in section 7.8. These mini-cultures were then lysed and assayed for activity before and after a heat inactivation step as described in section 7.8.

8.2.3 Further characterisation of improved mutants

Any random mutants displaying a residual activity greater than 60% were put through an extended heat inactivation step of 5 minutes at 60°C. Mutants still retaining at least 60% of activity after this step were chosen for more detailed studies, and of these any mutants showing only a slight decrease in activity between 3 and 5 minutes of inactivation were chosen for individual study. Plasmid was prepared from these mutant cultures as described in section 2.1.8, and the mutant xylA.cd2 inserts were sequenced to identify any mutations in the coding sequence.

8.2.4 Expression and partial purification of mutant xylA.cd2 enzymes

The mutant xylA.cd2 proteins were expressed from 50ml cultures of LB supplemented with 100µg/ml ampicillin as described in section 2.2.5. *E. coli* strain JM109 cells harbouring the mutant plasmid clones were harvested after approximately 16 hours of growth. The cells were disrupted by sonication and a crude cell extract was prepared as described in section 2.2.5.1.

8.2.5 Characterisation of mutant xylA.cd2 enzymes

The unfractionated preparations of mutant xylA.cd2 enzymes were characterised in the same way as the original xylA.cd2 protein (Chapter 3). Their specific activities were determined as outlined in section 3.2.5. Temperature optima for catalytic activity were determined for all the enzymes as described in section 3.2.6, and their thermal stabilities at 64°C were determined by a thermal inactivation study as described in section 3.2.7.

8.3 RESULTS

8.3.1 Initial random mutant selection

The random mutant library screened in this section of work is the one produced in Chapter 6, whose characteristics are described in section 6.3.1.2. Approximately 40,000 colonies were initially screened on RBB-xylan agar plates, and of these 960 (ten 96-well plates) xylanase-active colonies were picked into mini-cultures and assayed for activity and thermal stability.

8.3.2 Identification of stable mutants and further study

Of the 960 mutants picked into 96-well plate cultures and assayed for activity before and after a 3 minute heat inactivation step at 60°C, 135 displayed stability (A_r/A_i) greater than 60%. Figure 8.1 shows a stability versus initial activity plot for the 960 mutants screened, with the original xylA.cd2 data plotted on the same axes for comparison. The line on the graph at $A_r/A_i=0.6$ indicates the cut-off point below which mutants were deemed to have the same stability as the original enzyme. Of the 135 mutants above this line, 12 demonstrated a stability of at least 0.6 after the extended 5 minute heat inactivation step at 60°C. Figure 8.2 shows a stability versus initial activity plot for the 135 mutants put through the secondary heat inactivation step, with activities after both the 3 and 5 minute thermal inactivation steps plotted on the same axes. The data for the original enzyme after heat inactivation for 3 minutes is also included in Figure 8.2, to give an indication of the relative stability of the mutants in comparison to the original. From the calculated stabilities of the 12 mutants, 3 were seen to demonstrate almost the same activity after 3 and 5 minutes at 60°C (highlighted on figure 8.2). Based on these results these 3 mutants, known as 1-A10, 1-B6 and 2-C10, were selected for further individual study.

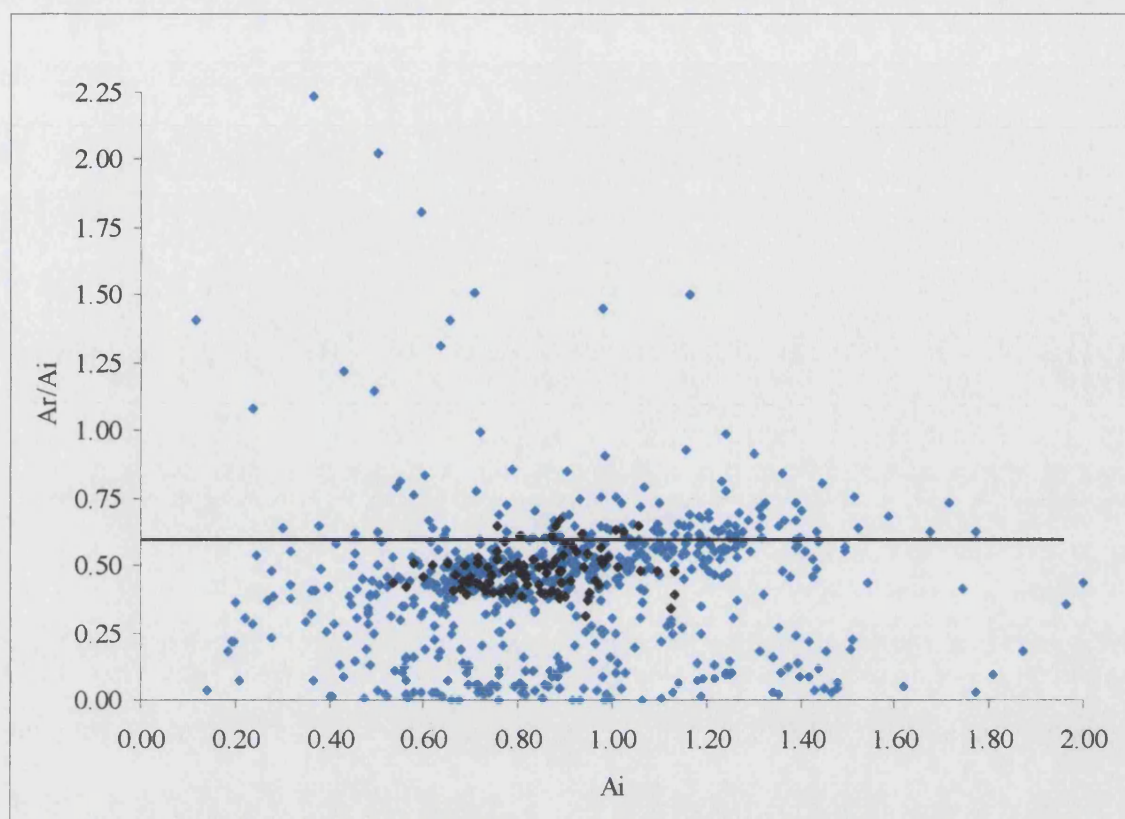


Figure 8.1 Stability versus initial activity plot for the 960 random mutants screened for activity after 3 minutes at 60°C

Black represents the original *xylA.cd2* samples; light blue represents the random mutant samples. A_i is the initial activity of each mutant, expressed as absorbance units at 575nm; A_r/A_i is the ratio of residual to initial activity of each mutant. The line represents the cut-off point for the selection criteria, and is positioned at $A_r/A_i=0.6$.

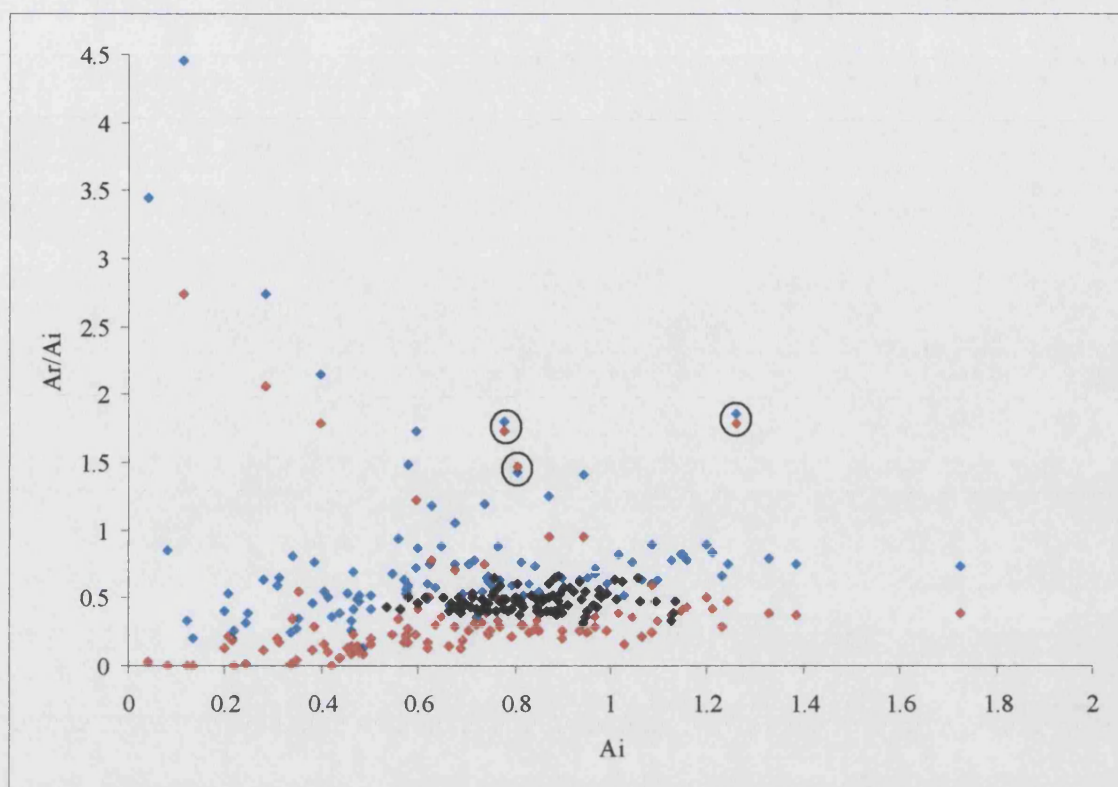


Figure 8.2 Stability versus initial activity plot for the 135 random mutants screened for activity after 3 and 5 minutes at 60°C

Black represents the original *xylA.cd2* samples after 3 minutes heat inactivation; light blue represents the 135 random mutant samples after 3 minutes heat inactivation; red represents the 135 random mutant samples after 5 minutes heat inactivation. Circles highlight mutants 1-A10, 1-B6 & 2-C10, all of which retain similar residual activity after both inactivation steps.

8.3.3 Sequencing of mutants 1-A10, 1-B6 & 2-C10

The inserts of the 3 mutant plasmid clones were sequenced using the M13 universal sequencing and reverse primers. One sequencing reaction from each direction allowed the full insert sequence to be obtained. Comparison of the mutant sequences to that of the original identified PCR-introduced mutations for all 3 mutants, and these are summarised in Table 8.1.

MUTANT	LOCATION OF MUTATION*	ORIGINAL BASE	NEW BASE	ORIGINAL AMINO ACID	NEW AMINO ACID
1-A10	-5**	A	G	Asp	Gly
1-B6	596	C	T	Ala	Val
2-C10	505	A	G	Thr	Ala
	596	C	T	Ala	Val

Table 8.1 Summary of mutations identified in the xylA.cd2 coding region of the 3 random mutant clones

*The 'location of mutation' column refers to the base number of the mutation within the xylA.cd2 coding region, where the full region is 675 bases. **negative number indicates that the mutation is upstream of the xylA.cd2 coding sequence, in the additional sequence from the lacZ gene that is expressed with the xylA.cd2 protein.

8.4.1 Characterisation of mutants 1-A10, 1-B6 & 2-C10

In order to further characterise the 3 isolated mutants, the genes were each expressed from a 50ml culture and a cell extract was prepared. A cell extract from a culture expressing the original xylA.cd2 was also prepared, and was assayed alongside the 3 mutants so that a comparison could be made between them.

8.4.1.1 Specific activities

The specific activities of the partially purified mutants and original xylA.cd2 were determined, using a 1/20,000 dilution of all the partially purified enzymes in order to ensure initial rates were being measured. Table 8.2 summarises the specific activities.

ENZYME	SPECIFIC ACTIVITY ($\mu\text{mol}/\text{min}/\text{mg}$ protein)
Original xylA.cd2	2210
1-A10	2155
1-B6	2390
2-C10	2510

Table 8.2 Summary of original and mutant xylA.cd2 enzyme specific activities

8.4.1.2 Temperature optima for activity

The partially purified enzymes were assayed at various temperatures from 18°C to 90°C. Figure 8.3 represents these results graphically, and shows the temperature activity profile for each of the 3 mutants alongside the original xylA.cd2 profile. As all 3 mutants demonstrate a similar specific activity to the original, these assay results have been represented as a percentage of the maximum activity observed. The maximum activity of mutants 1-A10 and 2-C10 was observed at 55°C, the same as the original xylA.cd2, but mutant 1-B6 shows a shift in its optimum temperature for activity to 60°C.

8.4.1.3 Thermal stability at 64 °C

Each mutant was heat inactivated over 5 minutes at 64°C, and Figure 8.4 graphically represents these results. Table 8.3 summarises the half-lives of each of the 3 mutant enzymes, in comparison to the half-life at 60°C of the original xylA.cd2.

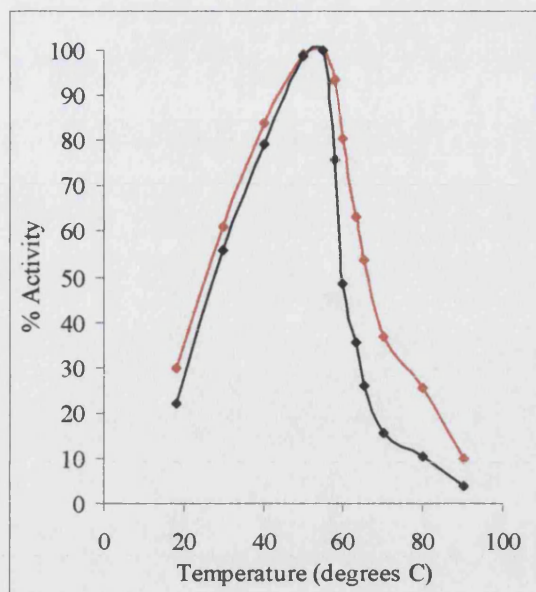


Figure 8.3a

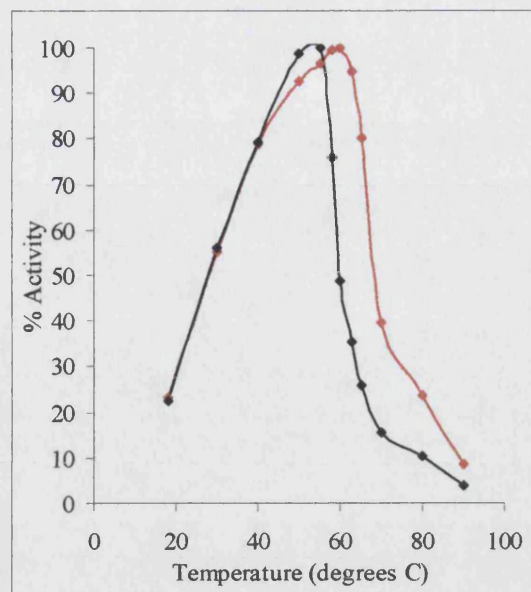


Figure 8.3b

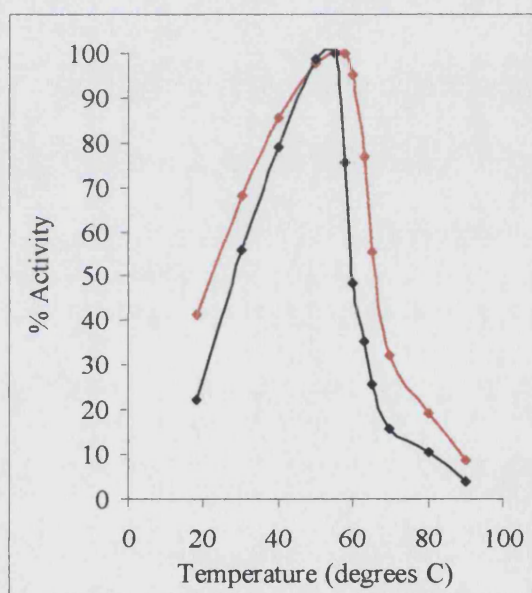


Figure 8.3c

Figure 8.3 Temperature activity curves for 3 mutant xylA.cd2 enzymes

Activities are expressed as a percentage of activity at the optimum (55°C for original, 1-A10 & 2-C10; 60°C for 1-B6). Each point represents the mean of duplicate assays. For all graphs black line represents original xylA.cd2; red line represents mutant enzyme.

Figure 8.3a Temperature activity curve for mutant 1-A10

Figure 8.3b Temperature activity curve for mutant 1-B6

Figure 8.3c Temperature activity curve for mutant 2-C10

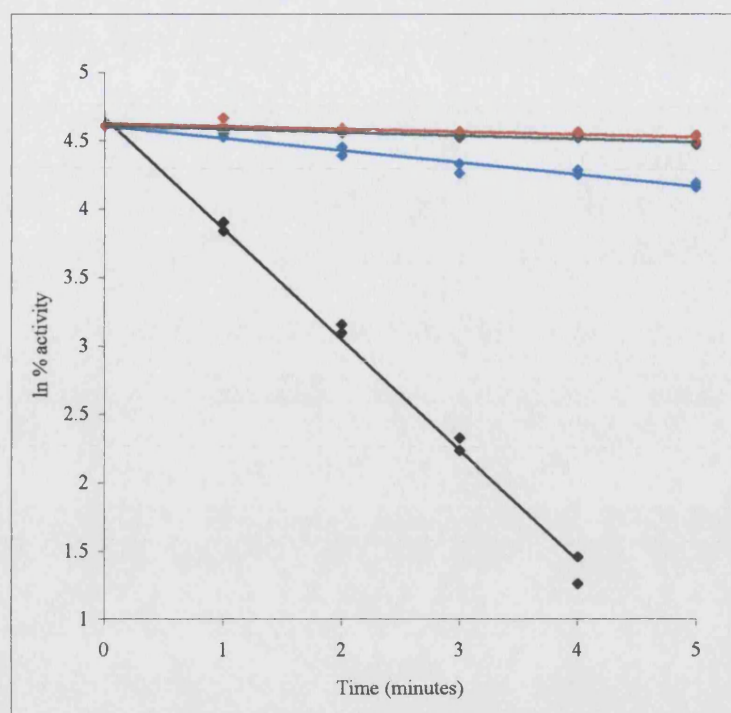


Figure 8.4 Thermal inactivation at 64°C of 3 mutant xylA.cd2 enzymes

Data are shown as ln (% activity) against incubation time (% activity being calculated as a percent of maximum activity, seen at time 0). Lines of best fit, calculated by linear regression, are shown. Black line represents original xylA.cd2; light blue line represents mutant 1-A10; green line represents mutant 1-B6; red line represents mutant 2-C10.

ENZYME	$T_{1/2}$ AT 64°C (minutes)
Original xylA.cd2	1
1-A10	8
1-B6	28.5
2-C10	36

Table 8.3 Comparison of half-lives at 64°C of original and mutant xylA.cd2 enzymes

8.4 DISCUSSION

8.4.1 Library screening and identification of improved mutants

Approximately 40,000 *E. coli* colonies, transformed with the random mutant library, were spread onto RBB-xylan agar plates, and of the xylanase-positive colonies enough to fill ten 96-well plates were picked into mini-cultures and screened using the 96-well plate system. Using the characteristics displayed by the original xylA.cd2 within the plate system (described in detail in Chapter 7), the selection criteria for identifying potentially improved mutants were that any mutant demonstrating activity after the heat inactivation step of at least 60% of its initial activity would be chosen for further study. The screening system identified 135 mutants after the 3-minute heat inactivation that retained 60% or more of their initial activity. These 135 were condensed into two new plates and subjected to a 5-minute heat inactivation, and of these 135, twelve retained 60% or more of their initial activity after this 5-minute incubation. Of these 12 there were three mutants that did not appear to lose significant activity between the 3 and 5-minute inactivation steps. In comparison to the original xylA.cd2, which loses approximately 75% of its activity over 5 minutes at 60°C, the data for these 3 mutants suggest that they are substantially more stable at 60°C than the original. It is for this reason that these 3 were chosen from the 12 for further individual study.

8.4.2 Characterisation of improved mutants

8.4.2.1 Sequence comparison

Sequencing the inserts of the 3 mutants identified mutations in the xylA.cd2 coding sequence of 1-B6 and 2-C10, but not in 1-A10. The only obvious change in the sequence of 1-A10 is actually 5 bases upstream of the xylA.cd2 coding sequence, in the sequence that codes for the extra 12 residues expressed at the N-terminus of the xylA.cd2 protein. These residues are from the lacZ protein, and are expressed upstream of the xylA.cd2 protein due to the way in which it is cloned into the pUC18 vector (described fully in section 3.4.1). It was suggested in Chapter 3 that these additional 12 N-terminal residues may influence both the activity and stability properties of the xylA.cd2 enzyme, but without expressing xylA.cd2 without them it would be difficult to predict with any degree of certainty. It would be possible to express the xylA.cd2 protein without the

additional N-terminal residues by cloning the coding sequence into a different plasmid vector, for example pET-3a. There is, however, limited information available on the expression of xylA.cd2 without any additional N-terminal residues, and it suggests that without these additional residues xylA.cd2 expression is very poor (Hazlewood, unpublished data). The sequence results for mutant 1-A10, particularly when viewed with the stability data for this enzyme, suggest that these additional residues do have an effect on the stabilisation of xylA.cd2 at elevated temperatures.

The sequence mutations identified in the other 2 mutants are within the xylA.cd2 coding region. Mutant 1-B6 has a mutation that equates to an alanine to valine substitution in the expressed protein (A199V). Mutant 2-C10 has two amino acid substitutions: a threonine to alanine (T169A) and an alanine to valine (A199V). Interestingly, the A199V substitution is at the same location in both these mutant enzymes, which may suggest that this residue plays an important role in stabilising the enzyme, particularly when it has been isolated in two individual mutants. The modelled structure of xylA.cd2 described in Chapter 4 has been used to suggest possible stabilising mechanisms for these amino acid substitutions. The location of the T169A substitution is on a loop in the xylA.cd2 structure that was introduced to accommodate an insertion in its sequence in comparison to the template enzyme. This makes it more difficult to predict how the substitution may be affecting the overall structure, as the location of the loop is not well defined. However, if the residues are situated on a loop structure as in the model, it is likely that the threonine is on the surface of the protein with its side-chain pointing into the hydrophobic core; the same position adopted by the alanine in the model. The A199V substitution is situated in a β -strand. The residue is in the active site cleft but the side-chain points into the core of the protein, between a β -sheet, rather than into the active site cleft. It has been suggested that perhaps the larger side-chain of valine protrudes into a cavity within the core of the enzyme, and this is how it helps to stabilise the enzyme at elevated temperatures (a cavity would cause destabilisation at higher temperatures, and filling it with a more bulky side-chain may help to stabilise). In addition, sequence comparison of xylA.cd2 with the other family 11 xylanases shows that most others have either a valine or threonine in this position. These suggestions are

predictions based on the modelled structure of xylA.cd2, and can only be confirmed if the actual crystal structure is solved. Another interesting consideration is that both the T169A and A199V substitutions are substitutions for a more hydrophobic residue. The structural basis of thermostability in proteins has been extensively reviewed, and increased numbers of hydrophobic interactions are frequently cited as factors involved in increasing thermostability (Vieille and Zeikus, 2001; Sterner and Liebl, 2001). For example, a comparative study of ten different triosephosphate isomerase structures identified an increased number of buried hydrophobic residues as one of the major factors contributing to the increased thermostability (Maes *et al.*, 1999). It could be considered that these substitutions seen in the mutant xylA.cd2 proteins are contributing to an increase in stability by increasing the number of hydrophobic interactions within the protein, particularly when comparison to the modelled structure suggests that the orientation of these residues is into the core of the enzyme.

8.4.2.2 Thermoactivity and thermostability

The purpose of individually studying apparently improved mutants was to confirm that the characteristics they displayed in the screen were indeed true characteristics, and not artefacts of some stage of the screen itself. The individual studies of thermoactivity and thermostability at 64°C were performed on cell extracts prepared for each enzyme, and as previously a cell extract of the original xylA.cd2 was also prepared and assayed in parallel for comparison.

All 3 mutants show an increase in stability over the original enzyme at 64°C. XylA.cd2 inactivates very rapidly at this temperature, with the partially pure preparation having a half-life of just less than 1 minute. In contrast, 1-A10, the least stable of the 3 mutants, has a half-life of 8 minutes, 1-B6 has a half-life of 28.5 minutes at 64°C, and 2-C10, the most stable of the mutants, has a half-life of 36 minutes. These are quite considerable increases in stability, and when the amino acid substitutions are considered it may seem sensible that 1-A10 demonstrates the smallest increase in stability and 1-C10 the largest. 1-A10 has a substitution just outside the core xylA.cd2 residues that may be influencing the structure of the actual xylA.cd2 protein from an external position. 1-B6 has one

internal substitution that is in some way stabilising the enzyme. 2-C10 has two substitutions, one potentially on the surface of the protein, and the other buried within the core of the enzyme, in the same position as the mutation in 1-B6. The fact that 2-C10 has two mutations, and is displaying the greatest increase in stability supports the theory that stability can be achieved accumulatively by a combination of effects, rather than by a single change within the protein.

Although the specific activities calculated in this chapter do give the impression that there is very little difference between the 3 mutants and the original enzyme, these specific activities are calculated from activity measurements in a cell extract, rather than from purified protein. While these specific activity values do reflect to a certain degree the activities of the proteins, there are other factors, such as differences in expression levels, which may have some bearing on the actual activity. It is for this reason that a true comparison of the specific activities of these mutant proteins with the original xylA.cd2 can only be made when the mutants have been purified.

Despite the fact that the specific activity values cannot be relied on 100% to indicate true differences between the mutant and original xylA.cd2 proteins, the results of these characterisation experiments do indicate that the stability of xylA.cd2 has been substantially improved without compromising its catalytic activity.

8.5 CONCLUSIONS

This chapter has described the identification of three mutants of xylA.cd2 from the random mutant library generated in Chapter 6 that demonstrate a considerable improvement in thermal stability over the original xylA.cd2 enzyme.

The results of this chapter confirm that the 96-well plate screen developed in Chapter 7 is a much more reliable and consistent method of screening the random mutant library than the original agar plate-based screen used in Chapter 6. It has allowed the rapid screening of a large number of random mutant library clones, demonstrating that it possesses the properties necessary of a screen that is to study the large numbers of random mutants generated in a directed evolution experiment. The screen has been used to identify twelve random mutants that display an increase in thermal stability. Of these twelve, three show consistent increases in stability when analysed using standard methods, verifying that the screen is not only reliable but also accurate enough to screen the products of a directed evolution experiment and successfully identify mutants demonstrating improvements in the desired property, i.e. thermal stability.

The three mutants characterised in detail demonstrate considerable increases in thermostability; the most improved demonstrating a 35-fold increase in stability over the original xylA.cd2 at 64°C. Despite the improvements in stability none of the three mutants appear to have compromised activity at lower temperatures, an important consideration in achieving the aims of this project as a whole. The results of this chapter suggest that it is possible for enzymes to be both thermostable and active at lower temperatures, providing that selective pressure is applied for both properties at the same time.

Chapter 9

FINAL CONCLUSIONS AND FUTURE WORK

9.1 FINAL CONCLUSIONS

The aim of this project was to increase the thermal stability of xylanase A from the mesophilic anaerobic fungus *Neocallimastix patriciarum*, whilst retaining its high levels of activity at lower temperatures. Two separate mutagenesis techniques have been utilised in attempts to achieve this goal: site-directed mutagenesis and directed evolution, or random mutagenesis. Both approaches were applied to the second catalytic domain of xylanase A (xylA.cd2) only. The site-directed approach involved the development of a model three-dimensional structure of xylA.cd2, followed by the design and introduction of mutations predicted to increase its thermal stability. In this case a disulphide bond was introduced into xylA.cd2. The directed evolution approach involved construction of a library of random mutants of xylA.cd2 by subjecting the gene encoding xylA.cd2 to a series of error-prone PCR steps in order to introduce random mutations. A reliable, consistent and reproducible screen was then developed and used to screen this random mutant library in order to identify those mutants displaying an improved thermal stability while still retaining high levels of activity at lower temperatures.

Chapter 5 describes the introduction into xylA.cd2 of two mutations identified from the model structure as being possible targets for increased thermal stability. The mutations were designed to introduce a disulphide bond into the enzyme. Characterisation of the mutant enzyme with respect to the original xylA.cd2 shows that it is more stable, having a greater activation energy for the inactivation process and a half-life at least 2.5 times greater than the original enzyme at the temperatures studied (58-64°C). These results demonstrate the effectiveness of structure-based design as a tool for making improvements in a given enzyme. Given that the mutations were based on a modelled structure rather than the actual three-dimensional crystal structure of xylA.cd2, the results described in chapter 5 are satisfying: often modelled structures do not accurately

reflect the detailed structure of a protein and mutations predicted from a modelled structure can cause major disruption to the overall stability of an enzyme, and as a result dramatically reduce its catalytic efficiency. However, while the introduction of a disulphide bond does appear to have contributed to an increase in stability of the xylA.cd2 enzyme, the improvement is not that large, particularly in comparison to the results obtained using the directed evolution approach. Given that the site-directed mutant is still as active as the original enzyme (indicating that its folded, native structure has not been affected by the introduction of a disulphide bond) greater improvements to its thermal stability could be made by introducing further site-specific mutations. Other improvements based on the structural model suggested in Chapter 4 include the introduction of a surface aromatic cluster, and the introduction of a greater number of ionic interactions. Another option for improving the thermostability of the site-directed mutant is to use it as a template for directed evolution. The process of directed evolution is accumulative, with the small changes in a given property identified at each round of mutagenesis contributing to the overall improvement seen in the final mutant. With its already improved thermal stability, the site-directed mutant represents a good base for further improvements.

The results of Chapter 6 demonstrate the need for an accurate, reproducible screening system with which to analyse the products of a directed evolution experiment. The library of random mutants produced by error-prone PCR contains the coding sequence for many thousands of enzymes that could potentially possess improvements in the characteristic of interest. The three mutants isolated from the 96-well plate screen described in Chapter 7 all demonstrate true improvements in thermal stability over the original xylA.cd2 enzyme when characterised individually. This validates the reliability of the screening system, and supports the theory that directed evolution experiments are only as successful as the system by which the random mutant library is screened. The three mutants characterised in Chapter 8 would all be good candidates for further rounds of directed evolution. Considering that most directed evolution experiments are performed over several rounds of mutagenesis and screening, the fact that quite considerable improvements have been made in just one round of mutagenesis bodes well

for further rounds, and suggests that it should be possible using this method to identify a final xylA.cd2 mutant demonstrating a substantial increase in stability.

9.2 FUTURE WORK

In addition to improving the site-directed mutant xylA.cd2 and subjecting the three improved random mutants to further rounds of directed evolution, as proposed above, there are other suggestions for further work that emerge from the results of this project. One area where further investigation is required is in the characterisation of the remaining nine mutants identified from the random mutant library screen. Chapter 8 describes the identification of 12 mutants displaying increased thermal stabilities after a 5 minute incubation at 60°C, but time constraints allowed the individual characterisation of only three of these 12. Given the improvements in thermal stability demonstrated by the three characterised mutants, it is reasonable to project that the remaining nine mutants will also demonstrate increased thermostability.

All 12 improved mutants could be used as templates for further rounds of error-prone PCR and screening. A sensible suggestion may also be to use DNA shuffling technology to recombine these improved mutants, with the aim of identifying a single mutant containing combinations of mutations that impart an even greater thermostability. This single mutant could then be used as a template for more rounds of random mutagenesis, recombination and screening.

The aim of this project was to increase the thermal stability of xylA.cd2 whilst retaining its high levels of activity at lower temperatures. The mutants obtained in this study, particularly those identified by the directed evolution approach, are notably more stable than the original xylA.cd2 enzyme yet still retain good activity at lower temperatures. Their thermal stability, however, is not yet appropriate enough for use in the intended industrial application. The results of this study more than demonstrate the effectiveness of the methods employed at increasing thermal stability, and it is my opinion that further rounds of mutagenesis and/or recombination and screening would fulfil the aims of

developing an enzyme with significantly improved thermal stability that retains its high activity at lower temperatures.

APPENDIX

Summary of primers used throughout the project.

PRIMER	FORWARD /REVERSE	REFERENCE	SEQUENCE (5' – 3')
Primer 1 ^a	Forward	Section 3.2.2	<div style="text-align: center;">→</div> CAA GGA TCC AAA GTT TAC TGT CGG TAA T
Primer 2 ^b	Reverse	Section 3.2.2	ACG GGA TCC GGC AGA <i>CTA</i> GGC TGG ACT AGA ACC CTT TGG
Primer 3 ^c	Forward	Section 5.2.2	CAT ATT ACT GTC TCA TGT CAC TTT AAG GAA TG
Primer 4 ^c	Forward	Section 5.2.2	GA AAA ATG GTA ACC TGT GAT GGA GCT CAA
Primer 5	Forward	Section 6.2.2	CCT CTT CGC TAT TAC GCC AGC TGG
Primer 6	Reverse	Section 6.2.2	CGA CAG GTT TCC CGA CTG GAA AGC

^a Bold type indicates the position of a BamHI restriction site; arrow indicates the start of the cd2 coding region

^b Bold type indicates the position of a BamHI restriction site; bold italic type indicates the introduced stop codon

^c Bold type indicates the introduced mutations

REFERENCES

- Affholter, J. & Arnold, F.H. (1999). Engineering a revolution. *Chem. In Britain* 35: 48-51
- Arase, A., Yomo, T., Urabe, I., Hata, Y., Katsube, Y. & Okada, H. (1993). Stabilization of xylanase by random mutagenesis. *FEBS Letters*. 316: 123-127
- Arnold, F.H. (1996). Directed evolution: Creating biocatalysts for the future. *Chem. Eng. Sci.* 51: 5091-5102
- Arnold, F.H. (1998). Enzyme engineering reaches the boiling point. *Proc. Natl. Acad. Sci. USA*. 95: 2035-2036
- Arnold, F.H., Wintrode, P.L., Miyazaki, K. & Gershenon, A. (2001). How enzymes adapt: Lessons from directed evolution. *Trends Biochem.Sci.* 26: 100-106
- Arnott, M.A., Michael, R.A., Thompson, C.R., Hough, D.W. & Danson, M.J. (2000). Thermostability and thermoactivity of citrate synthases from the thermophilic and hyperthermophilic archaea, *Thermoplasma acidophilum* and *Pyrococcus furiosus*. *J. Mol. Biol.* 304:657-668
- Bailey, M.J., Biely, P. & Poutanen, K. (1992). Interlaboratory testing of methods for assay of xylanase activity. *J. Biotechnol.* 23: 257-270
- Bayer, E.A., Setter, E. & Lamed, R. (1985). Organisation and distribution of the cellulosome in *Clostridium thermocellum*. *J. Bacteriol.* 163: 552-559
- Bedford, M.R. & Morgan A. J. (1996). The use of enzymes in canola-based diets. 2nd *European Symposium on Feed Enzymes*. 125-131
- Biely, P. (1985). Microbial xylanolytic systems. *Trends Biotech.* 3: 286-290
- Black, G.W., Hazlewood, G.P., Millward-Sadler, S.J., Laurie, J.I. & Gilbert, H.J. (1995). A modular xylanase containing a novel non-catalytic xylan-specific binding domain. *Biochemical J.* 307: 191-195
- Bradford, M. (1976). A rapid and sensitive method for the quantitation of microgram quantities of protein utilising the principle of protein-dye binding. *Analyt. Biochem.* 72: 248-254
- Bray, M.R. & Clarke, A.J. (1992). Action pattern of xylo-oligosaccharide hydrolysis by *Schizophyllum commune* xylanase A. *Eur. J. Biochem.* 204: 191-196

- Charnock, S.J., Bolam, D.N., Turkenburg, J.P., Gilbert, H.J., Ferreira, L.M.A., Davies, G.J. & Fontes, C.M.G.A. (2000). The X6 "Thermostabilizing" domains of xylanases are carbohydrate-binding modules: Structure and biochemistry of the *Clostridium thermocellum* X6b domain. *Biochemistry*.39: 5013-5021
- Chauvt, J.M., Comtat, J. & Noe, P. (1987). Assistance in bleaching of never-dried pulps by the use of xylanases: consequences on pulp properties. *Proceedings of the 4th International Congress on Wood and Pulping Industry*, 325-327
- Chen, R. (2001). Enzyme engineering: Rational design versus directed evolution. *Trends Biotech.* 19: 13-14
- Chen, R., Greer, A. & Dean, A.M. (1996). Redesigning secondary structure to invert coenzyme specificity in isopropylmalate dehydrogenase. *Proc. Natl. Acad. Sci. USA.* 93: 12171-12176
- Chen, Y-L., Tang, T-Y. & Cheng, K-J. (2001). Directed evolution to produce an alkalophilic variant from a *Neocallimastix patriciarum* xylanase. *Can. J. Microbiol.* 47: 1088-1094
- Clarke, J.H., Davidson, K., Gilbert, H.J., Fontes, C.M.G.A. & Hazlewood, G.P. (1996). A modular xylanase from mesophilic *Cellulomonas fimi* contains the same cellulose-binding and thermostabilizing domains as xylanases from thermophilic bacteria. *FEMS Microbiol. Letters.* 139: 27-35
- Classen, H.L. (1995). Enzymes in action, feed mix enzymes special issue. Misset pp. 3-8
- Coughlan, M.P. & Hazlewood, G.P. (1993). B-1,4-D-Xylan-dgrading enzyme systems: biochemistry, molecular biology and applications. *Biotechnol. Appl. Biochem.* 17: 259-289
- Couthino, P.M. & Henrissat, B. (1999). Carbohydrate-Active Enzymes server at URL: <http://afmb.cnrs-mrs.fr/~cazy/CAZY/index.html>
- Danson, M.J. & Hough, D.W. (1998). Structure, function and stability of enzymes from the archaea. *Trends Microbiol.* 6: 307-314
- Danson, M.J. & Hough, D.W. (2002). Thermostabilty and activity of extremozymes. *Encyclopaedia of Life Support Systems* (knowledge foundations area: Extremophiles). In press
- Davies, G. & Henrissat, B. (1995). Structures and mechanisms of glycosyl hydrolases. *Structure.* 3: 853-859
- Dekker, R.F.H. & Richards, G.N. (1976). Hemicellulases: Their occurrence, purification properties and mode of action. *Adv. Carbohydr. Chem. Biochem.* 32: 277-352

- Dill, K.A. (1990). Dominant forces in protein folding. *Biochemistry*. 29: 7133-7155
- Ellis, P.R., Rayment, P. & Wang, Q. (1996). Physioc-chemical perspective of plant polysaccharides in relation to glucose absorption, insulin secretion and the entero-insular axis. *Proc. Nutritional Soc.* 55: 881-898
- Fanutti, C., Ponyi, T., Black, G.W., Hazlewood, G.P. & Gilbert, H.J. (1995). The conserved noncatalytic 20-residue sequence in cellulases and hemicellulases from anaerobic fungi functions as a protein docking domain. *J. Biol. Chem.* 49: 29314-29322
- Ferreira, L.M.A., Durrant, A.J., Hall, J., Hazlewood, G.P. & Gilbert, H.J. (1990). Spatial separation of protein domains is not necessary for catalytic activity or substrate binding in a xylanase. *Biochemical J.* 269: 261-264
- Fontes, C.M.G.A., Hazlewood, G.P., Morag, E., Hall, J., Hurst, B.H. & Gilbert, H.J. (1995). Evidence for a general role for non-catalytic thermostabilizing domains in xylanases from thermophilic bacteria. *Biochemical J.* 307: 151-158
- Fromant, M., Blanquet, S. & Plateau, P. (1995). Direct random mutagenesis of gene-sized DNA fragments using polymerase chain reaction. *Analyt. Biochem.* 224: 347-353
- Georgiou, G. & DeWitt, N. (1999). Enzyme beauty. *Nature Biotech.* 17: 1161-1162
- Georis, J., Lemos Esteves, F. De, Lamotte-Brasseur, J., Bougnet, V., Devreese, B., Giannotta, F., Granica, B. & Frere, J-M. (2000). An additional aromatic interaction improves the thermostability and thermophilicity of mesophilic family 11 xylanase: Structural basis and molecular study. *Protein Sci.* 9: 466-475
- Gerngross, U.T., Romanic, M.P.M, Kobayashi, T., Huskisson, N.S. & Demain, A.L. (1993). Sequencing of a *Clostridium thermocellum* gene (CIPA) encoding the cellulosomal SL-protein reveals an unusual degree of internal homology. *Mol. Microbiol.* 8: 325-334
- Gibbs, M.D., Reeves, R.A. & Bergquist, P.L. (1995). Cloning, sequencing and expression of a xylanase gene from the extreme thermophile *Dictoglomus thermophilum* Rt46B.1 and activity of the enzyme on fibre-bound substrate. *Appl. Environ. Microbiol.* 61: 4403-4408
- Gilbert, H.J. & Hazlewood, G.P. (1993). Bacterial Cellulases and xylanases. *J. Gen. Microbiol.* 139: 187-194
- Gilbert, H.J., Hazlewood, G.P., Laurie, J.I., Orpin, C.G. & Xue, G.P. (1992). Homologous catalytic domains in a ruminal fungal xylanase: evidence for gene duplication and prokaryotic origin. *Mol. Microbiol.* 6: 2065-2072

- Gilkes, N.R., Henrissat, B., Kilburn, D.G., Miller, R.C., Jr. & Warren, R.A.J. (1991). Domains in microbial β -1,4-Glycanases: Sequence conservation, function and enzyme families. *Microbiol. Rev.* pp. 303-315
- Giver, L., Gershenson, A., Freskgard, P-O. & Arnold, F.H. (1998). Directed evolution of a thermostable esterase. *Proc. Natl. Acad. Sci. USA.* 95: 12809-12813
- Gonzalez-Blasco, G., Sanz-Aparicio, J., Gonzalez, B., Hermoso, J.A. & Polaina, J. (2000). Directed evolution of β -glucosidase A from *Paenibacillus polymyxa* to thermal resistance. *J. Biol. Chem.* 275: 13708-13712
- Gruber, K., Klintschar, G. Hayen, M., Schlacher, A., Steiner, W. & Kratky, C. (1998). Thermophilic xylanase from *Thermomyces lanuginosus*: High-resolution X-ray structure and modelling studies. *Biochemistry* 37: 13475-13485
- Haney, P., Konisky, J. Koretke, K.K., Luthey-Schulten, Z. & Wolynes, P.G. (1997). Structural basis for thermostability and identification of potential active site residues for adenylate kinases from the archaeal genus *Methanococcus*. *Proteins: Struct. Funct. Genet.* 28: 117-130
- Harris, G.W., Pickersgill, R.W., Connerton, I., Debeire, P., Touzel, J.P., Breton, C. & Perez, S. (1997). Structural basis of the properties of an industrially relevant thermophilic xylanase. *Proteins: Struct. Funct. Genet.* 29: 77-86
- Havukainen, R., Torronen, A., Laitinen, T. & Rouvinen, J. (1996). Covalent binding of 3 epoxyalkyl xylosides to the active site of endo-1,4-xylanase II from *T. reesei*. *Biochemistry.* 35: 9617-9624
- Hazlewood, G.P., Romaniec, M.P.M., Davidson, K., Grepinet, O., Beguin, P., Millet, J., Raynaud, O. & Aubert, J-P (1988). A catalog of clostridium-thermocellum endoglucanase, beta-glucosidase and xylanase genes cloned in escherichia-coli. *FEMS Microbiol. Letters.* 51: 231-236
- Henrissat, B. (1991). A classification of glycosyl hydrolases based on amino acid sequence similarities. *Biochemistry. J.* 280: 309-316
- Henrissat, B. & Bairoch, A. (1993). New families in the classification of glycosyl hydrolases based on amino acid sequence similarities. *Biochemical J.* 293: 781-788
- Hugenholtz, P. & Pace, N.R. (1996). Identifying microbial diversity in the natural environment: A molecular phylogenetic approach. *Trends Biotechnol.* 14: 190-197
- Inbarr, J. & Bedford, M.R. (1994). Stability of feed enzymes to steam pelleting during feed processing. *Animal Feed Sci. Technol.* 46: 179-196

- Ito, S., Kobayashi, T., Ara, K., Ozaki, K., Kawai, S. & Hatada, Y. (1998). Alkaline detergent enzymes from alkaliphiles: Enzymatic properties, genetics and structure. *Extremophiles* 2: 185-190
- Joo, H., Lin, Z.L. & Arnold, F.H. (1999). Laboratory evolution of peroxide-mediated cytochrome P₄₅₀ hydroxylation. *Nature* 399: 670-673
- Kantelinen, A., Hortling, B., Sundquist, J., Linko, M. & Viikari, L. (1993). Proposed mechanism of the enzymatic bleaching of kraft pulp with xylanases. *Holtzforschung*. 47: 318-324
- Koshland, D.E. (1953). Stereochemistry and the mechanism of enzymatic reactions. *Biol. Rev. Camb. Philos. Soc.* 28: 416-436
- Kuchner, O. & Arnold, F.H. (1997). Directed evolution of enzyme catalysts. *Trends Biotech.* 15: 523-530
- Kumar, P.R., Eswaramoorthy, S., Vithayathil, P.J. & Viswamitra, M.A. (2000a). The tertiary structure at 1.59 Å resolution and the proposed amino acid sequence of a family 11 xylanase from the thermophilic fungus *Paecilomyces varioti* Bainier. *J. Mol. Biol.* 295: 581-593
- Kumar, S., Tsai, C.J. & Nussinov, R. (2000b). Factors enhancing protein thermostability. *Protein Eng.* 13: 179-191
- Laemmli, U.K. (1970). Cleavage of structural proteins during the assembly of the head of bacteriophage T4. *Nature* 227: 680-685
- Lamed, R., Setter, E., Kenig, R. & Bayer, E.A. (1983). The cellulosome-a discrete cell surface organelle of *Clostridium thermocellum* which exhibits separate antigenic, cellulose-binding and various cellulolytic activities. *Biotechnol. Bioeng. Symp.* 13: 163-181
- Laskowski, R.A., MacArthur, M.W., Moss, D.S. & Thornton, M.J. (1993). PROCHECK: A program to check the stereochemical quality of protein structures. *J. Appl. Cryst.* 26: 283-291
- Lee, Y.E., Lowe, S.E., Henrissat, B. & Zeikus, J.G. (1993). Characterization of the active-site and thermostability regions of endoxylanase from thermoanaerobacterium-saccharolyticum B6A-RI. *J. Bacteriol.* 175: 5890-5898
- Liebeton, K., Zonta, A., Schimossek, K., Nardini, M., Lang, D., Dijkstra, B.W., Peetz, M.T. & Jager, K. (2000). Directed evolution of an enantioselective lipase. *Chem. Biol.* 7: 709-718

- Liu, J-H., Selinger, B.L., Tsai, C-F. & Cheng, K-J. (1999). Characterization of a *Neocallimastix patriciarum* xylanase gene and its product. *Can. J. Microbiol.* 45: 970-974
- Luthy, R., Bowie, J.Y. & Eisenberg, D. (1992). Assessment of protein models with three-dimensional profiles. *Nature.* 356: 283-291
- Lytle, B.L., Myers, C., Kruss, K. & Wu, J.H.D. (1996). Interactions of the CelS binding ligand with various receptor domains of the *Clostridium thermocellum* cellulosomal scaffolding protein, CipA. *J. Bacteriol.* 178: 1200-1203
- Maat, J., Roza, M., Verbakel, J., Stam, H., Santos de Silva, M.J., Bosse, M., Egmond, M.R., Hagemans, M.L.D., Gorcom, R.F.M. van & Hessing, J.G.M. (1992). Xylanases and their application in bakery. In *Progress in Biotechnology.* 7: 349-360. In the series: Xylans and Xylanases (Visser, J. & Beldman, G. Eds.) Elsevier Science Publishers, Amsterdam
- Maes, D., Zeelen, J.P., Thanki, N., Beaucamp, N., Alvarez, M., Thi, M.H.D., Backmann, J., Martial, J.A., Wyns, L., Jaenicke, R. & Wierenga, R.K. (1999). The crystal structure of triosephosphate isomerase (TIM) from *Thermotoga maritima*: A comparative thermostability structural analysis of 10 different TIM structures. *Proteins: Struct. Funct. Genet.* 37: 441-453
- McCarter, J. & Withers, S.G. (1994). Mechanisms of enzymatic glycoside hydrolases. *Structure.* 4: 885-892
- McCarthy, A.A., Morris, D.D., Bergquist, P.L & Baker, E.N (2000). Structure of XynB, a highly thermostable β -1,4-xylanase from *Dictoglomus thermophilum* Rt46B.1, at 1.8Å resolution. *Acta Cryst.* D56: 1367-1375
- McDonough, T.J. (1992). A survey of mechanical pulp bleaching in Canada: single-stage hydrosulphite lines are the rule. *Pulp & Paper Can.* 93: 57-62
- Meiering, E.M., Serrano, L. & Fersht, A.R. (1992). Effect of active-site residues in barnase on activity and stability. *J. Mol. Biol.* 225: 585-589
- Miao, S., Ziser, L., Aebersold, R. & Withers, S.G. (1994). Identification of glutamic acid 78 as the active site nucleophile in *B. subtilis* xylanase using electrospray tandem mass spectrometry. *Biochemistry.* 33: 7027-7032
- Miller, G.L. (1959). Use of dinitrosalicylic acid reagent for determination of reducing sugars. *Analyt. Chem.* 31: 426-428
- Moreau, A., Shareck, F., Kluephel, D. & Morosoli, R. (1994). Increase in catalytic activity and thermostability of the xylanase A of *Streptomyces lividans* 1326 by site-specific mutagenesis. *Enzyme Microb. Technol.* 16: 420-424

Mueller-Harvey, I., Hartley, R.D., Harris, P.J. & Curzon, E.H. (1996). Linkage of para-coumaroyl and feruloyl groups to cell wall polysaccharides of barley straw. *Carbohydr. Res.* 148: 71-85

Orpin, C.G. & Munn, E.A. (1986). *Neocallimastix patriciarum* sp. nov., a new member of the Neocallimasticaceae inhabiting the rumen of sheep. *Trans. Br. Mycol. Soc.* 86: 178-181

Puls, J. & Schuseil, J. (1993). Chemistry of hemicelluloses: Relationship between hemicellulose structure and enzymes required for hydrolysis. In *Hemicellulose and Hemicellulases* (Coughlan, M.P. & Hazlewood, G.P. eds.), pp. 1-28. Portland Press, London

Russell, R.J.M., Ferguson, M.C., Hough, D.W., Danson, M.J. & Taylor, G.L. (1997). The crystal structure of citrate synthase from the hyperthermophilic archaeon *Pyrococcus furiosus* at 1.9 Å resolution. *Biochemistry*. 36: 9983-9994

Saul, D.J., Williams, L.C., Reeves, R.A., Gibbs, M.D. & Bergquist, P.L. (1995). Sequencing and expression of a xylanase gene from the hyperthermophile *Thermotoga* sp. Strain FjSS3-B.1 and characterisation of the recombinant enzyme and its activity on kraft pulp. *Appl. Environ. Microbiol.* 61: 4110-4113

Schreiber, G., Buckle, A.M. & Fersht, A.R. (1994). Stability and function: Two constraints in the evolution of barstar and other proteins. *Structure* 2: 945-951

Shibuya, H., Kaneko, S. & Hayashi, K. (2000). Enhancement of the thermostability and hydrolytic activity of xylanase by random gene shuffling. *Biochemical J.* 349: 651-656

Shoichet, B.K., Baas, W.A., Kuroki, R. & Matthews, B.W. (1995). A relationship between protein stability and protein function. *Proc. Natl. Acad. Sci. USA.* 92: 452-456

Simpson, P.J., Bolam, D.N., Cooper, A., Ciruela, A., Hazlewood, G.P., Gilbert, H.J. & Williamson, M.P. (1999). A family IIb xylan-binding domain has a similar secondary structure to a homologous family IIa cellulose-binding domain but different ligand specificity. *Structure*. 7: 853-864

Sinnott, M.L. (1990). Catalytic mechanisms of enzymic glycosyl transfer. *Chem. Rev.* 90: 1171-1202

Stemmer, W.P.C. (1994a). Rapid evolution of a protein *in vitro* by DNA shuffling. *Nature* 370: 389-391

Stemmer, W.P.C. (1994b). DNA shuffling by random fragmentation and reassembly: *In vitro* recombination for molecular evolution. *Proc. Natl. Acad. Sci. USA.* 91: 10747-10751

- Sterner, R. & Liebl, W. (2001). Thermophilic adaptation of proteins. *Crit. Rev. Biochem. Mol. Biol.* 36: 39-106
- Sudendey, C. & Kamphues, J. (1995). Effect of enzyme addition (amylase, xylanase and β -glucanase) on digestive processes in the intestinal tract of force fed weaner piglets. *Proc. Soc. Nutritional Phys.* 3: 145-171
- Sunna, A., Gibbs, M.D. & Bergquist, P.L. (2000a). A novel thermostable multidomain 1,4- β -xylanase from '*Caldibacillus cellulovorans*' and effect of its xylan-binding domain on enzyme activity. *Microbiol.* 146: 2947-2955
- Sunna, A., Gibbs, M.D. & Bergquist, P.L. (2000b). The thermostabilizing domain, XynA, of *Caldibacillus cellulovorans* xylanase is a xylan binding domain. *Biochemical J.* 346: 583-586
- Teather, R.M. & Wood, P.J. (1982). Use of congo red-polysaccharide interactions in enumeration and characterisation of cellulolytic bacteria from the bovine rumen. *Appl. Environ. Microbiol.* 43 (4): 777-780
- Timell, T.E. (1967). Recent progress in the chemistry of wood hemicelluloses. *Wood Sci. Technol.* 49: 499-521
- Tobin, M.B., Gustafsson, C. & Huisman, G.W. (2000). Directed evolution: The 'rational' basis for 'irrational' design. *Curr. Opin. Struct. Biol.* 10: 421-427
- Tomme, P., Warren, R.A.J., Miller, R.C., Jr, Kilburn, D.G. & Gilkes, N.R. (1995). In *Enzymatic Degradation of Insoluble Carbohydrates* (Saddler, J.N. & Penner, M.H., eds.), pp. 142-163, American Chemical Society, Washington DC
- Torronen, A., Harkki, A. & Rouvinen, J. (1994). 3-D structure of endo-1,4- β -xylanase II from *Trichoderma reesei*: 2 conformational states in the active site. *EMBO J.* 13: 2493-2501
- Torronen, A. & Rouvinen, J. (1995). Structural comparison of 2 major endo-1,4- β -xylanases from *Trichoderma reesei*. *Biochemistry.* 34: 847-856
- Van den Burg, B., Vriend, G., Veltman, O.R., Venema, G. & Eijssink, V.G.H. (1998). Engineering an enzyme to resist boiling. *Proc. Natl. Acad. Sci. USA.* 95: 2056-2060
- Van der Klis, J.D., van Voorst, A. & van Cruyningen, C. (1993). Effects of a soluble polysaccharide (carboxymethyl cellulose) on the rate of marker excretion from the G. I. tract of broilers. *Poultry Science.* 72:503-512

- Vetriani, C., Maeder, D.L., Tolliday, N., Yip, K.S.P., Stillman, T.J., Britton, K.L., Rice, D.W., Klump, H.H. & Robb, F.T. (1998). Protein thermostability above 100°C: A key role for ionic interactions. *Proc. Natl. Acad. Sci. USA*. 95: 12300-12305
- Vieille, C. & Zeikus, G.J. (2001). Hyperthermophilic enzymes: Sources, uses, and molecular mechanisms for thermostability. *Microbiol. Mol. Biol. Rev.* 65: 1-44
- Viikari, L., Kantelinen, A., Sundquist, J. & Linko, M. (1994). Xylanases in bleaching. From an idea to industry. *FEMS Microbiol. Letters*. 13: 335-350
- Villafranca, J.E., Howell, E.E., Voet, D.H., Strobell, M.S., Ogden, R.C., Abelson, J.N. & Kraut, J. (1983). Directed mutagenesis of dihydrofolate-reductase. *Science* 222: 782-788
- Wakarchuk, W.W., Campbell, R.L., Sung, W.L., Davodi, J. & Yaguchi, M. (1994). Mutational and crystallographic analysis of the active site residues of the *B. circulans* xylanase. *Protein Sci.* 3: 467-475
- Whistler, R.L. & Richards, E.L. (1970). Hemicelluloses. In *The Carbohydrates-Chemistry and Biochemistry* (Pigman, W. & Horton, D. eds.), 2nd edition, vol. 2A, pp. 447-469. Academic Press, Inc., New York
- Williams, A.G. & Orpin, C.G. (1987). Polysaccharide-degrading enzymes formed by three species of anaerobic fungi grown on a range of carbohydrates substrates. *Can. J. Microbiol.* 33: 418-426
- Winterhalten, C., Heinrich, P., Candussio, A., Wich, G. & Liebl, W. (1995). Identification of a novel cellulose-binding domain within the multidomain 120kDa xylanase Xylanase A of the hyperthermophilic bacterium *Thermotoga maritima*. *Mol. Microbiol.* 15: 431-444
- Yaron, S., Morag, E., Bayer, E.A., Lamed, R. & Shoham, Y. (1995). Expression, purification and subunit-binding properties of cohesion-2 and cohesion-3 of the clostridium-thermocellum cellulosome. *FEBS Letters*. 360: 121-124
- Yip, K.S.P., Stillman, T.J., Britton, K.L., Artymiuk, P.J., Baker, P.J., Sedelnikova, S.E., Engel, P.C., Pasquo, A., Chiaraluce, R., Consalvi, V., Scandurra, R. & Rice, D.W. (1995). The structure of *Pyrococcus furiosus* glutamate dehydrogenase reveals a key role for ion-pair networks in maintaining enzyme stability at extreme temperatures. *Structure* 3: 1147-1158
- Yip, K.S.P., Britton, K.L., Stillman, T.J., Lebbink, J., De Vos, W.M., Robb, F.T., Vetriani, C., Maeder, D. & Rice, D.W. (1998). Insights into the molecular basis of thermal stability from the analysis of ion-pair networks in the glutamate dehydrogenase family. *Eur. J. Biochem.* 255: 336-346

You, L. & Arnold, F.H. (1996). Directed evolution of subtilisin E in *Bacillus subtilis* to enhance total activity in aqueous dimethylformamide. *Protein Eng.* 9: 77-83

Zhang, J-H, Dawes, G. & Stemmer, W.P.C. (1997). Directed evolution of a fucosidase from a galactosidase by DNA shuffling and screening. *Proc. Natl. Acad. Sci. USA.* 94: 4504-4509

Zhao, H. & Arnold, F.H. (1999). Directed evolution converts subtilisin E into a functional equivalent of thermitase. *Protein Eng.* 12: 47-53